Binding to an unusual inactive kinase conformation by highly selective inhibitors of inositol-requiring enzyme 1α kinase-endoribonuclease

Giampiero Colombano[1], John J. Caldwell[1], Thomas P. Matthews[1], Chitra Bhatia[3], Amar Joshi[3], Tatiana McHardy[1], Ngai Yi Mok[1], Yvette Newbatt[1], Lisa Pickard[1], Jade Strover[2], Somaieh Hedayat[1], Michael I. Walton[1], Stephanie M. Myers[1], Alan M. Jones[1], Harry Saville[1], Craig McAndrew[1], Rosemary Burke[1], Suzanne A. Eccles[1], Faith E. Davies[2,†], Richard Bayliss[3,4], Ian Collins[1,]*

1. Cancer Research UK Cancer Therapeutics Unit and 2. Division of Molecular Pathology, The Institute of Cancer Research, London, SW7 3RP, U.K.

3. Department of Molecular and Cell Biology, University of Leicester, LE1 7RH, U.K.

4. School of Molecular and Cellular Biology, Faculty of Biological Sciences, University of Leeds, LS2 9JT, U.K.

Supporting Information

Contents:

1. Supplementary Figure S1

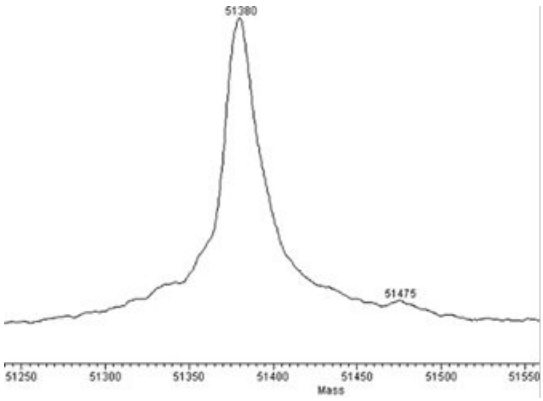

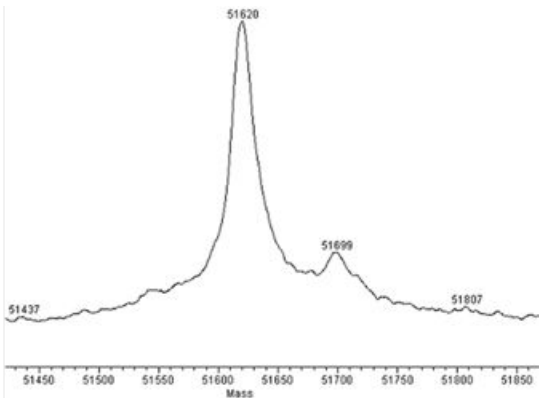

G547 IRE1α (λ-phosphatase treated)

M= 51380

G547 IRE1α (incubated with ATP)

M= 51620

Supplementary Figure S1: Mass spectrometry characterisation of dephosphorylated and phosphorylated recombinant G547 IRE1α proteins.

2. Supplementary Figure S2

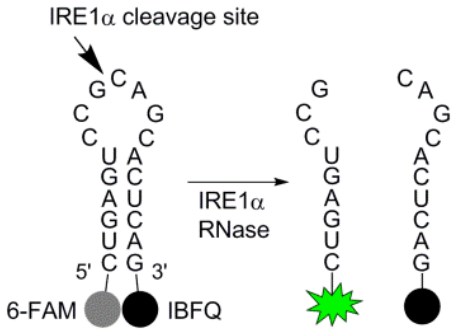

Supplementary Figure S2: Schematic of the cleavage of a fluorescence-labelled stem-loop RNA used to measure inhibition of IRE1α RNase activity *in vitro*.

3. Supplementary Figure S3

A

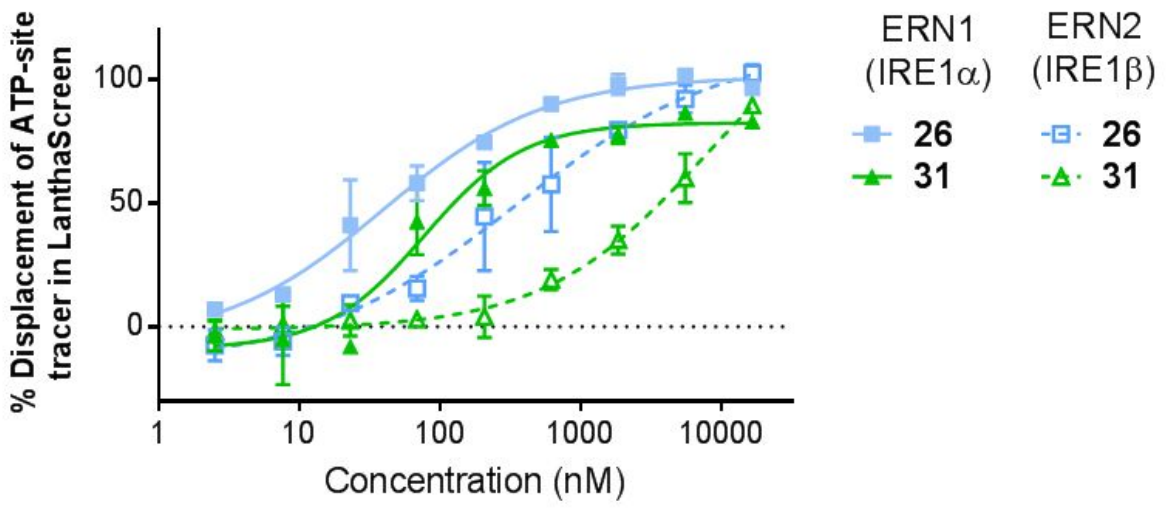

26 IRE1α IC_{50} = 39 nM; IRE1β IC_{50} = 345 nM

31 IRE1α IC_{50} = 77 nM; IRE1β IC_{50} = 7682 nM

B

IRE1α	**IRE1β**	**IRE1α**	**IRE1β**	**IRE1α**	**IRE1β**
Leu577	Leu	Ile642	Leu	Glu651	Glu
Val586	Val	Glu643	Glu	Phe712	Phe
Ala597	Ala	Leu644	Leu	His723	Cys
Lys599	Lys	Cys645	Cys	Phe725	Phe
Ile626	Leu	Ala646	Arg		
Tyr628	Tyr	Ala647	Ala		

Supplementary Figure S3: **A)** Compounds **26** and **31** have selectivity for IRE1α over IRE1β in parallel kinase binding assays (LanthaScreen format, SelectScreen profiling service conducted at Life Technologies (now Thermo Fisher) https://www.thermofisher.com/uk/en/home/products-and-services/services/custom-services/screening-and-profiling-services/selectscreen-profiling-service.html); **B)** Amino acid residues of the binding site of **2** to IRE1α, and the corresponding residues in the sequence of IRE1β.[34]

4. Supplementary Figure S4

A

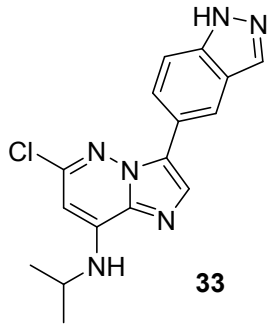

33

IRE1α S726 autophosphorylation IC_{50} = 276 (±108) nM

IRE1α ATP site binding IC_{50} = 736 (±491) nM

B

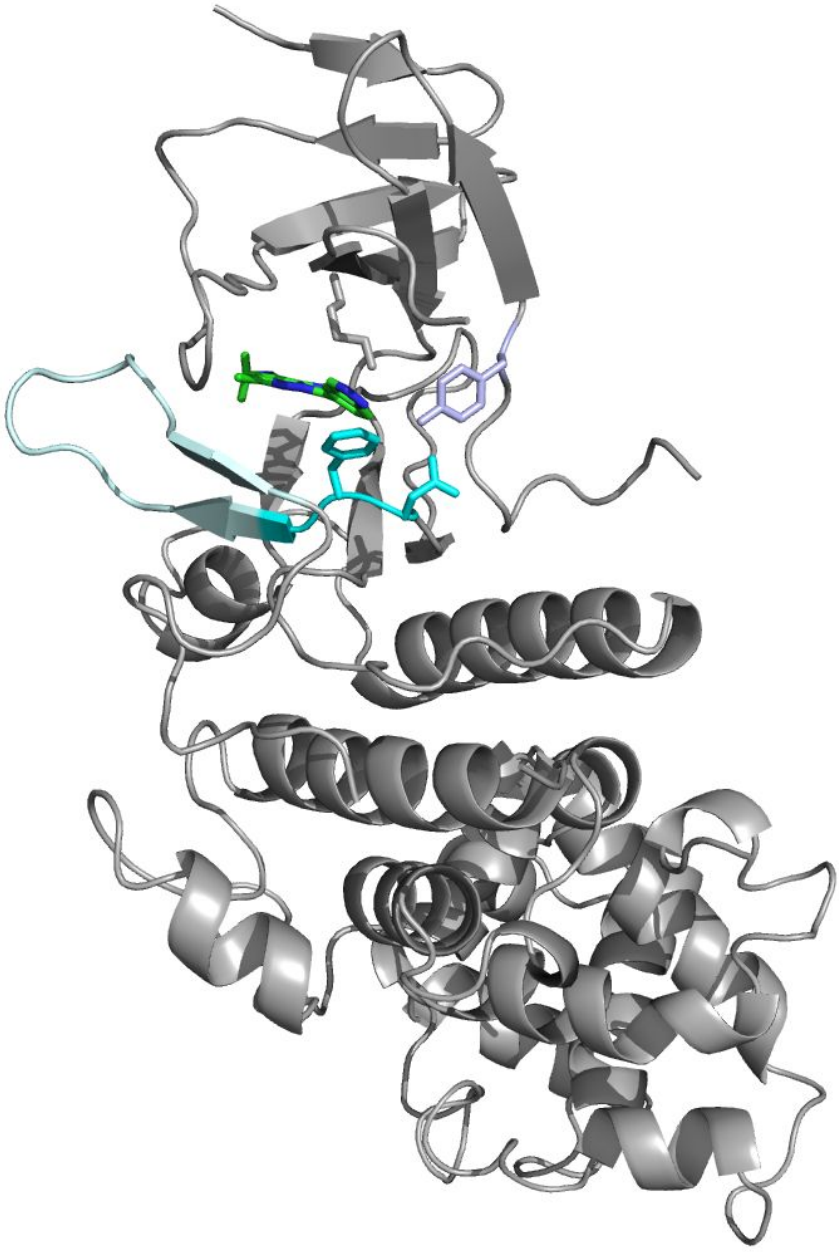

Supplementary Figure S4: A) Structure and IRE1α inhibition of compound **33**; **B)** Crystal structure (PDB 6hv0) of **33** (green sticks) bound to IRE1α KEN domain (grey cartoon) showing the conformations of the DFG motif (cyan), activation loop segment (pale cyan), Y628 (blue) and K599 (grey).

5. Supplementary Figure S5

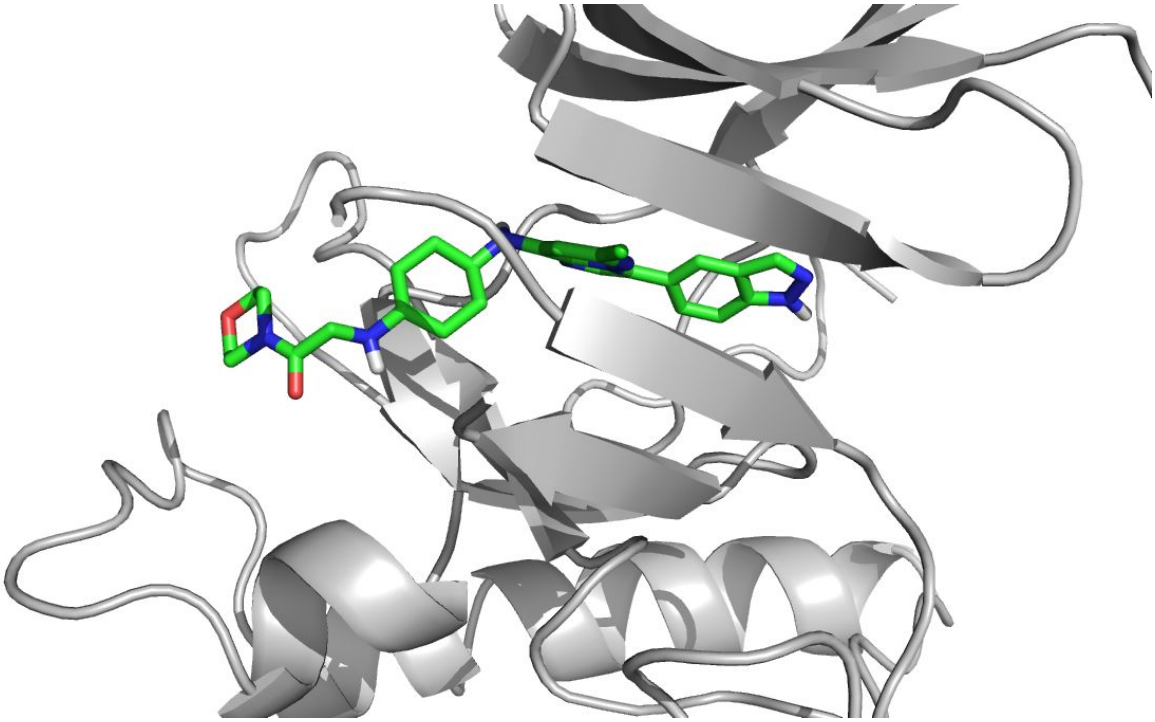

Supplementary Figure S5: Model of the binding of **26** (green sticks) to IRE1α (grey cartoon) using the kinase conformation observed for **2**-IRE1α (PDB 6hx1). Detail of the ATP-binding site shown.

6. Supplementary Figure S6

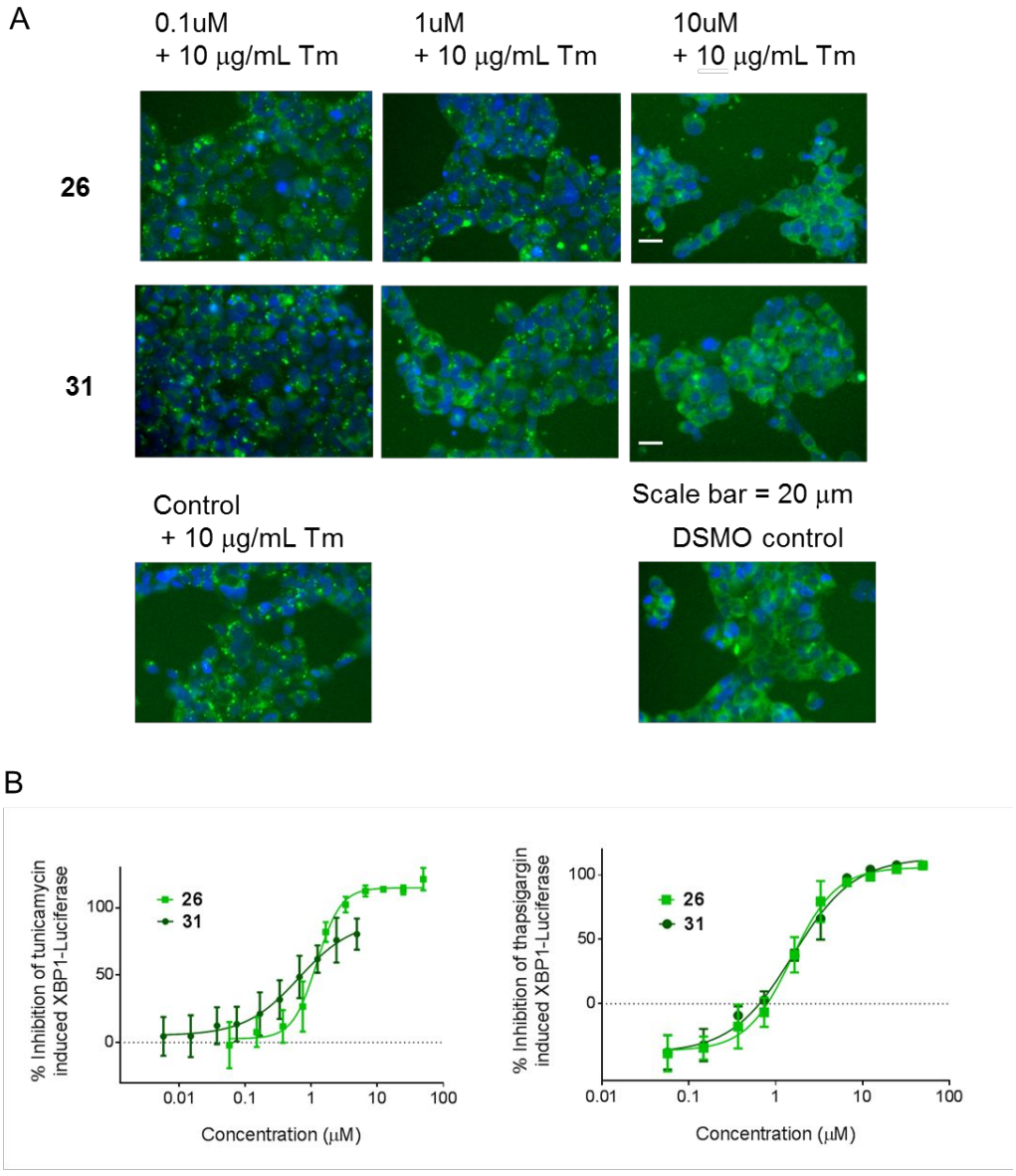

C

	Inhibition of tunicamycin-induced GFP-IRE1α foci in HEK293 cells		Inhibition of XBP1-Luc mRNA splicing in HEK293 cells			
			tunicamycin-induced		thapsigargin-induced	
	IC_{50} (μM) (mean ±SD)	*n*	IC_{50} (μM) (mean ±SD)	*n*	IC_{50} (μM) (mean ±SD)	*n*
26	1.88 ±0.09	2	1.18 ±0.17	5	1.52 ±0.21	2
31	0.74 ±0.03	2	0.68 ±0.22	5	1.63 ±0.34	2

Supplementary Figure 6: Compounds **26** and **31** inhibit IRE1α oligomerisation and RNase activity in HEK293 cells. (**A**) Inhibition of tunicamycin-induced oligomerization of GFP-IRE1α in HEK293 cells. Representative microscopic images from compound dilution series used to quantify IRE1α foci formation. (**B**) Inhibition of tunicamycin- and thapsigargin-induced splicing of XBP1-Luc reporter mRNA in HEK293 cells. (**C**) Summary of inhibition of IRE1α oligomerization and RNA splicing activity in HEK293 cells.

7. Supplementary Figure S7

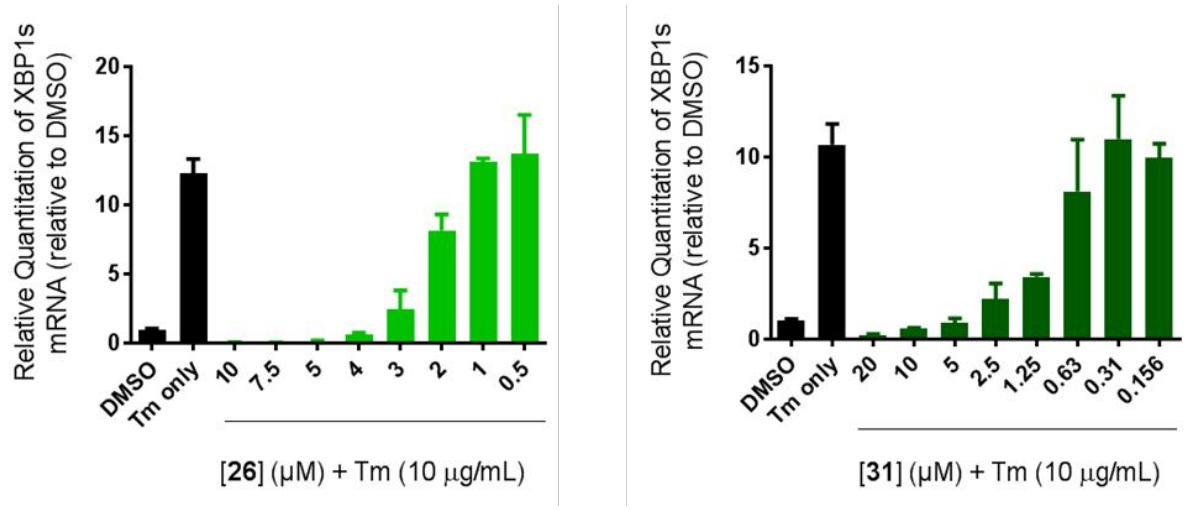

Supplementary Figure S7: Compounds **26** and **31** inhibit IRE1α-dependent XBP1s mRNA expression in H929 cells. Inhibition of tunicamycin-induced XBP1s mRNA expression as measured by RT-qPCR. Data shown for a single experiment representative of n=3.

8. Supplementary Figure S8

A

Compound 31

pS724 IRE1α

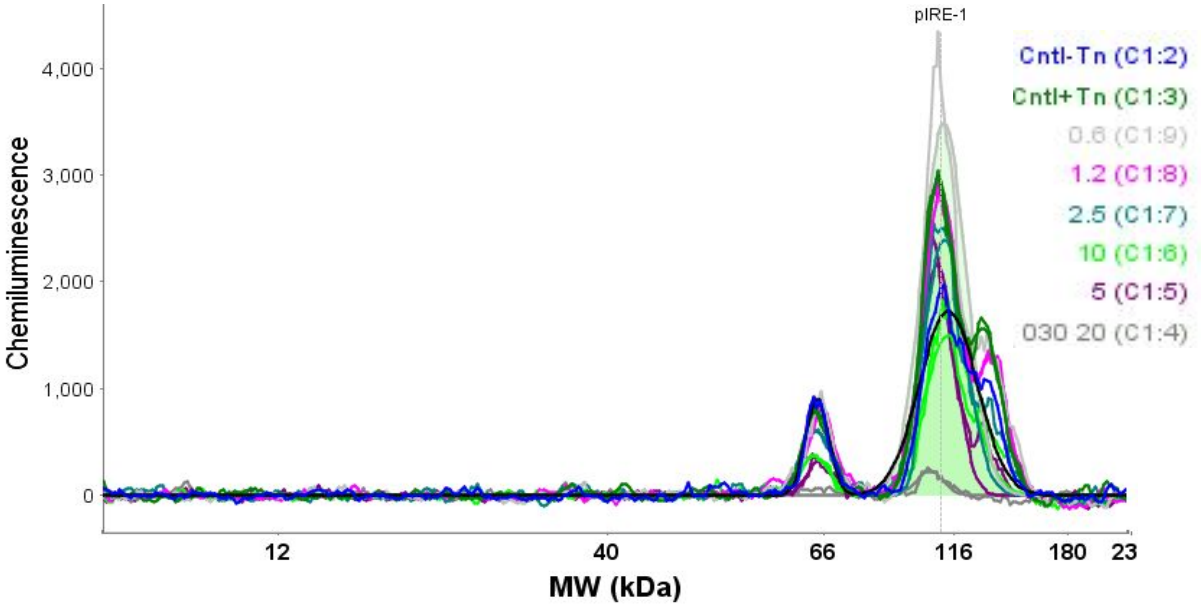

Total IRE1α

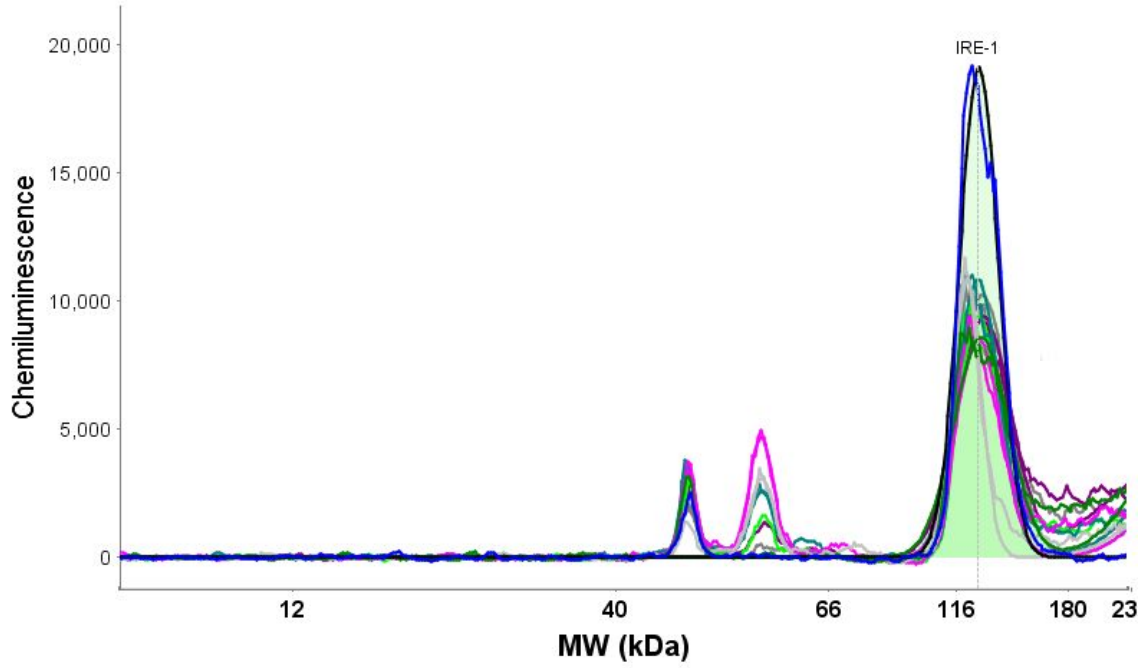

B

Compound 26

pS724 IRE1α

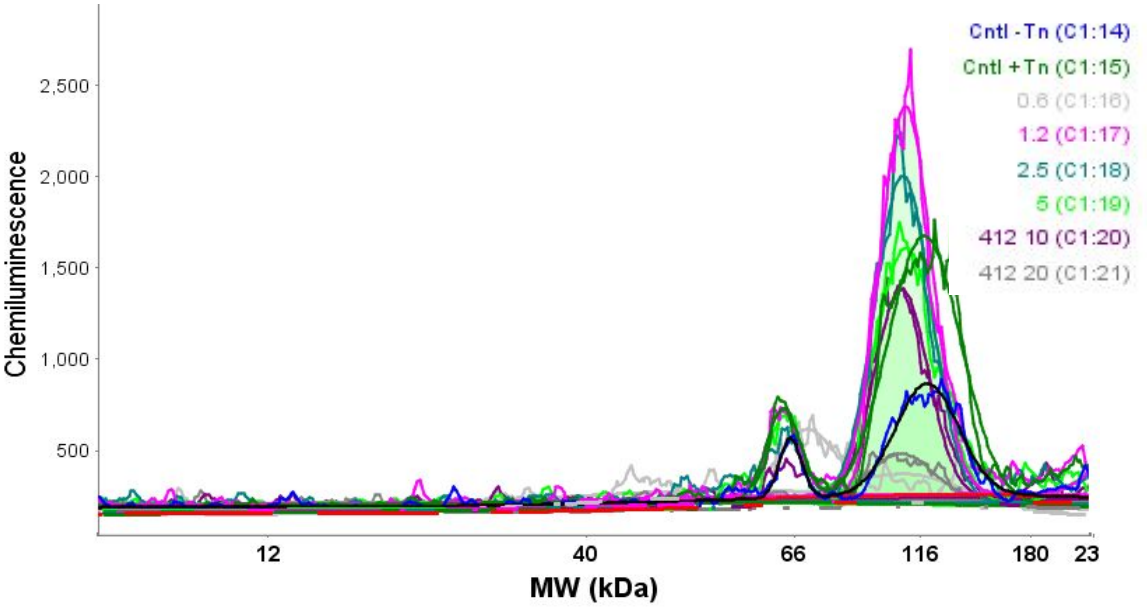

Total IRE1α

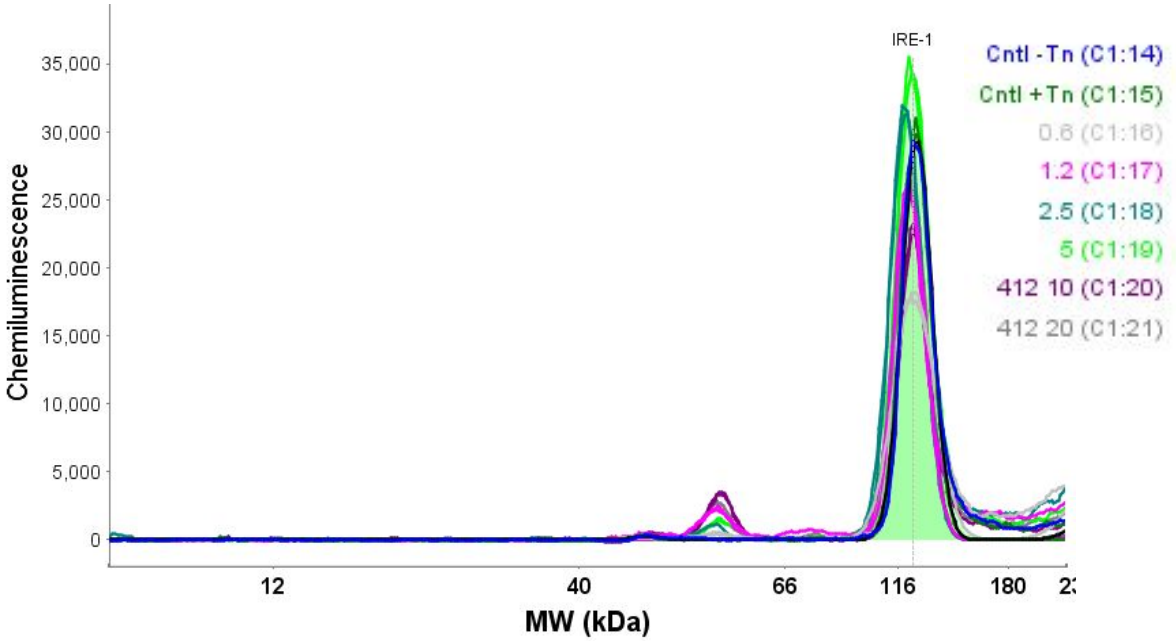

Supplementary Figure S8: Compounds (**A**) **31** and (**B**) **26** dose-dependently inhibit tunicamycin-induced expression of pS724 IRE1α in H929 cells. Quantification of pS724 IRE1α using capillary electrophoresis immunoassay relative to total IRE1α (Simple Western™).

9. Supplementary Figure S9

A

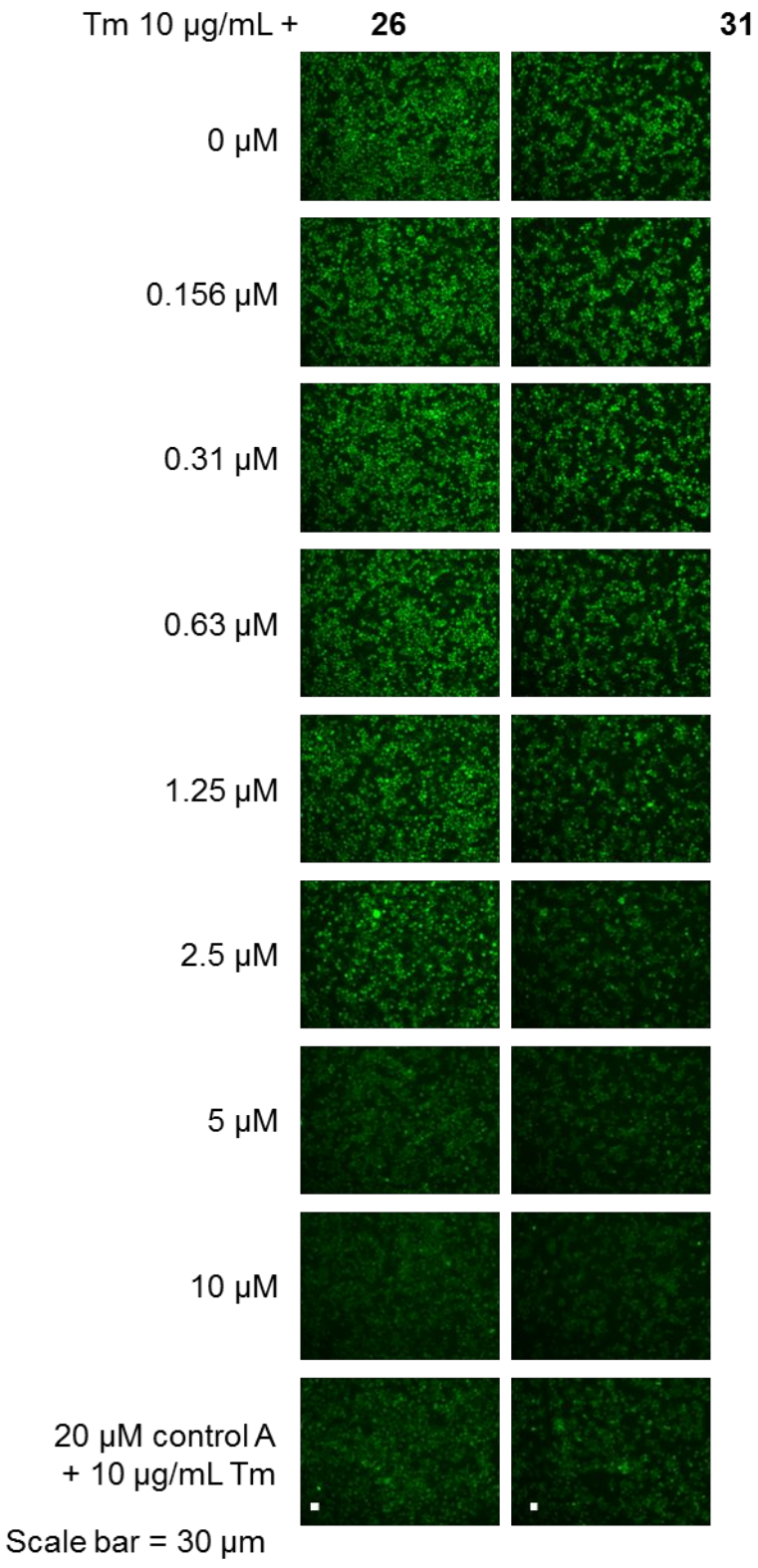

B

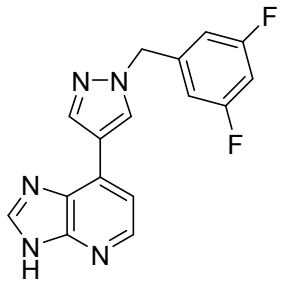

7-(1-(3,5-difluorobenzyl)-1*H*-pyrazol-4-yl)-3*H*-imidazo[4,5-*b*]pyridine

IRE1α autophosphoarylation DELFIA	IC_{50} = 3111 (±1821) nM
IRE1a ATP-site binding assay	IC_{50} = 3276 (±320) nM
XBP1 reporter cleavage in HEK293TN	IC_{50} = 6203 (±1683) nM
HEK293 cytotoxicity (CellTitreBlue)	IC_{50} > 50 000 nM

Supplementary Figure S9: **A)** Compounds **26** and **31** dose-dependently inhibit tunicamycin-induced expression of XBP1s in NCI-H929 cells. Representative microscopic images from compound dilution series. Quantification of XBP1s expression by immunofluorescence; **B)** Structure and activities of 7-(1-(3,5-difluorobenzyl)-1*H*-pyrazol-4-yl)-3*H*-imidazo[4,5-*b*]pyridine (Control A) used at high concentration (20-50 μM) as a normalization control for quantifying inhibition of XBP1s protein expression in NCI-H929 cells or inhibition of cleavage of an XBP1-luciferase fusion mRNA reporter expressed in HEK293TN cells.

10. **Supplementary Figure S10**: In vitro autophosphorylation, ATP-site binding and RNase assay titrations for compounds **2**, **26** and **31**.

A

IRE1α DELFIA titrations, Compound **2**, n=8

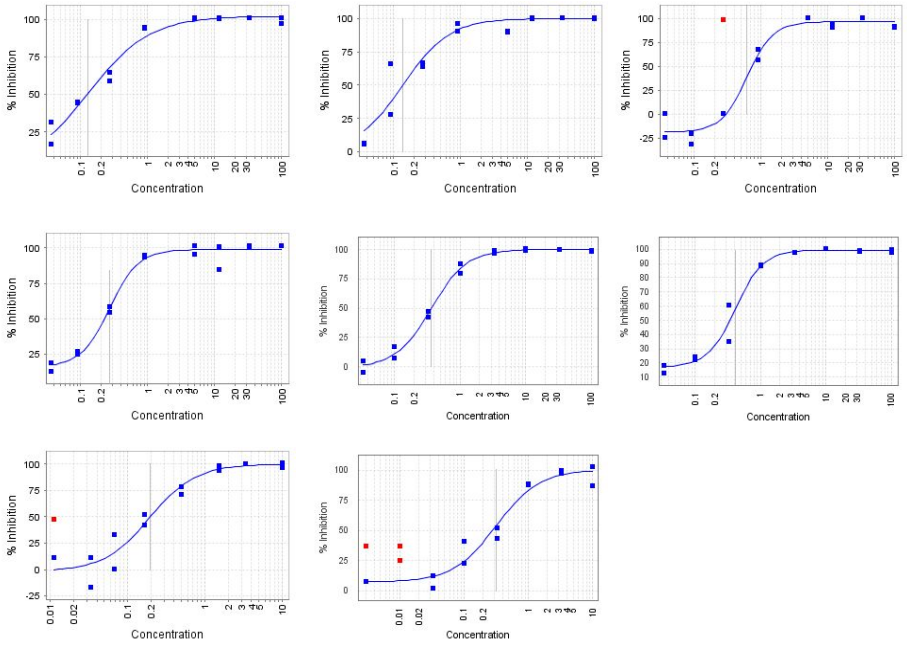

IRE1α DELFIA titrations, Compound **26**, n=3

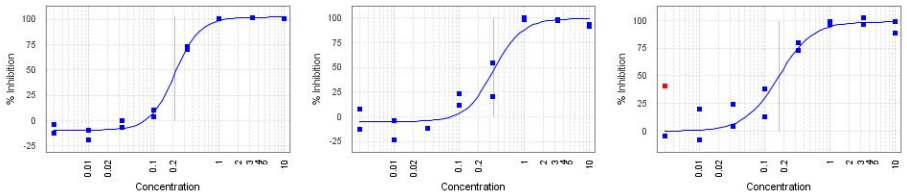

IRE1α DELFIA titrations, Compound **31**, n=8

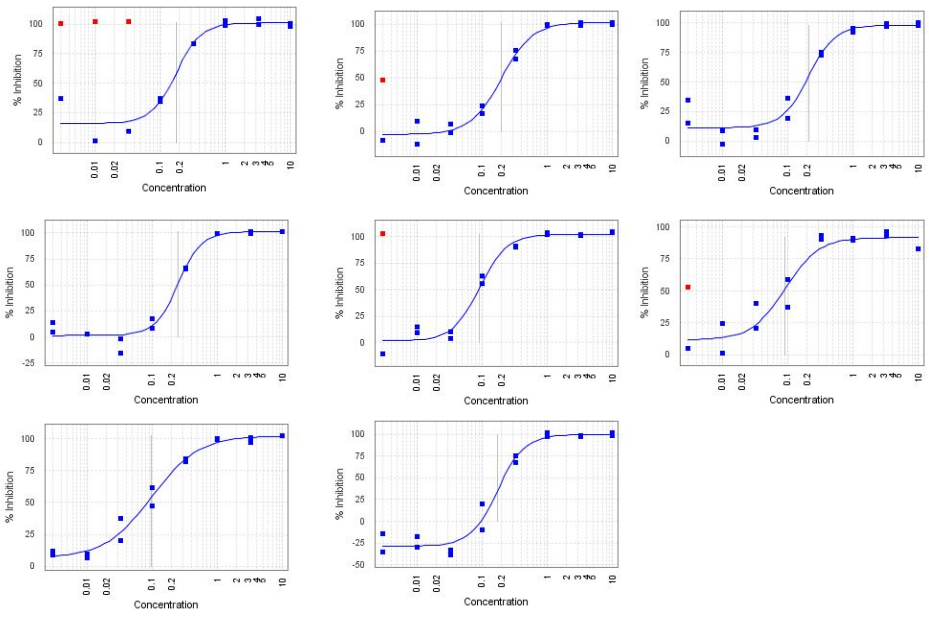

B

IRE1α LanthaScreen titrations, Compound **2**, n=13

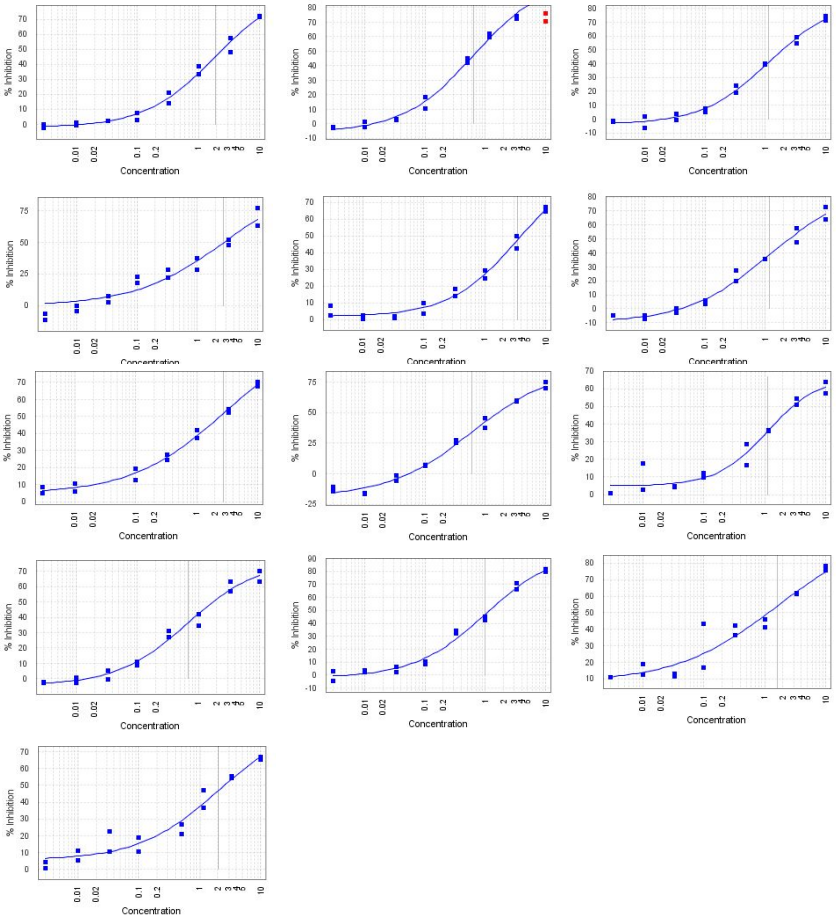

IRE1α LanthaScreen titrations, Compound **26**, n=5

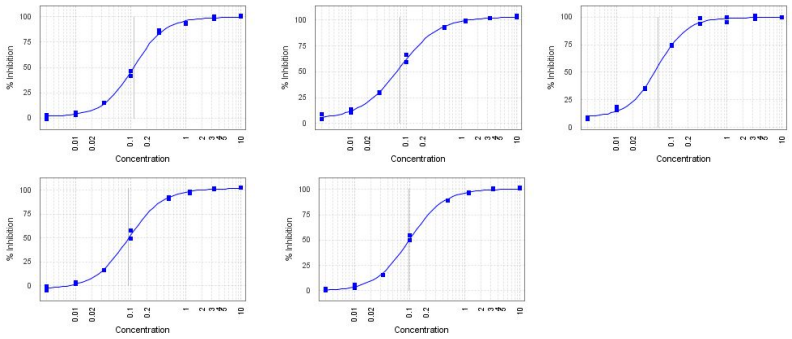

IRE1α LanthaScreen titrations, Compound **31**, n=3

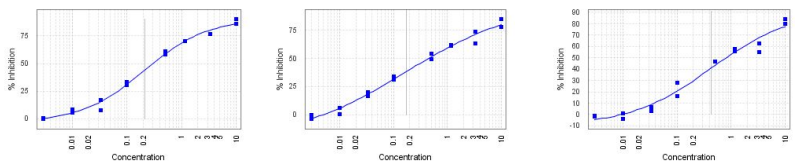

C

IRE1α RNase FRET derepression titrations, Compound **2**, n=2

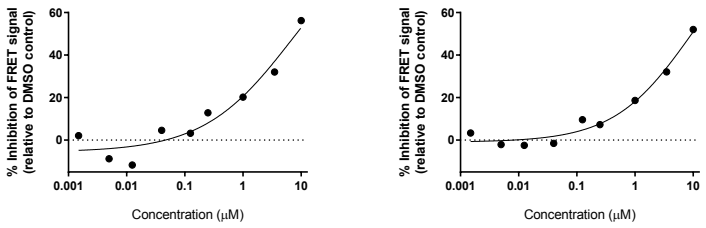

D

IRE1α RNase FRET derepression titrations, Compound **26**, n=13

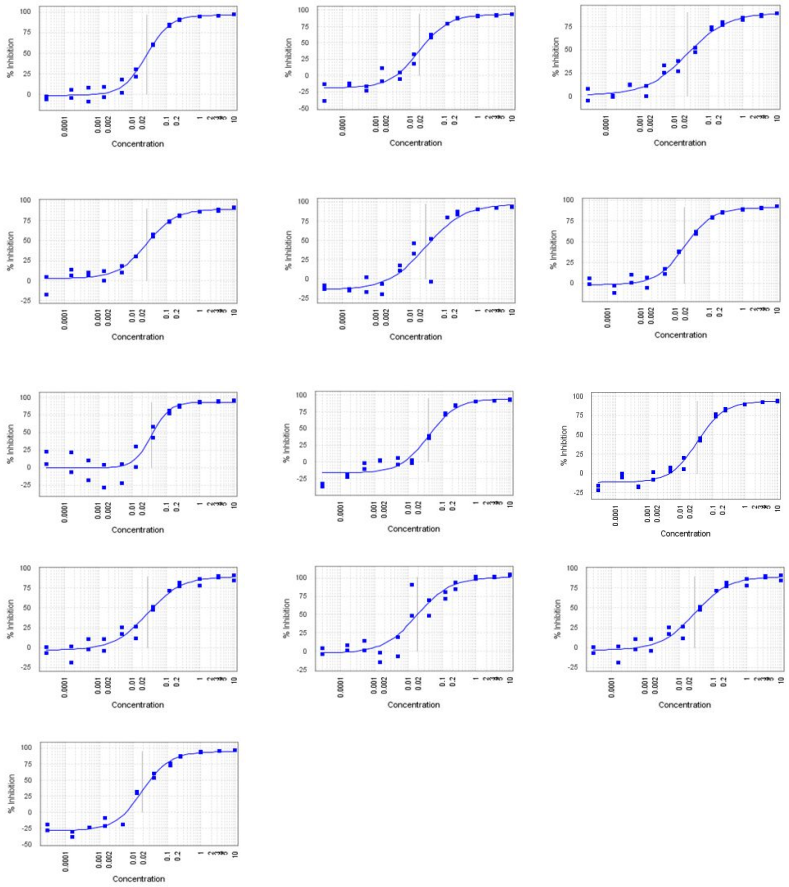

IRE1α RNase FRET derepression titrations, Compound **31**, n=6

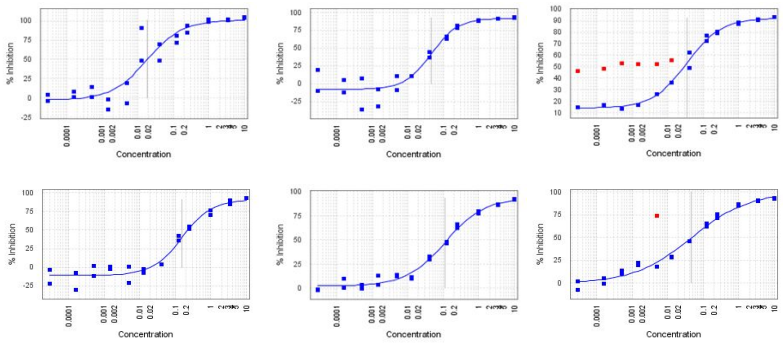

Supplementary Figure S10: **A)** IRE1α in vitro autophosphorylation assay (DELFIA) titrations for compounds **2**, **26** and **31**. Individual determinations with technical duplicates. Red squares indicate duplicate points excluded from the assay curve analysis. **B)** IRE1α in vitro ATP-site binding assay (LanthaScreen) titrations for compounds **2**, **26** and **31**. Individual determinations with technical duplicates. Red squares indicate duplicate points excluded from the assay curve analysis. **C)** IRE1α in vitro RNase assay (FRET derepression) titrations for compound **2**. Individual determinations in singlicate. **D)** IRE1α in vitro RNase assay (FRET derepression) titrations for compounds **26** and **31**. Individual determinations with technical duplicates. Red squares indicate duplicate points excluded from the assay curve analysis.

11. **Supplementary Table S1**: Selectivity profile of compounds **2**, **26** and **31** tested against 455 human kinases at 1000 nM.

	% control activity remaining at a test concentration of 1000 nM[a]		
Compound	**2**	**26**	**31**
Kinase[b]			
AAK1	39	28	100
ABL1(E255K)-phosphorylated	100	56	86
ABL1(F317I)-nonphosphorylated	71	28	63
ABL1(F317I)-phosphorylated	93	8.1	76
ABL1(F317L)-nonphosphorylated	68	26	76
ABL1(F317L)-phosphorylated	60	6.2	73
ABL1(H396P)-nonphosphorylated	74	16	42
ABL1(H396P)-phosphorylated	73	46	67
ABL1(M351T)-phosphorylated	91	57	78
ABL1(Q252H)-nonphosphorylated	93	48	64
ABL1(Q252H)-phosphorylated	78	46	79
ABL1(T315I)-nonphosphorylated	76	38	71
ABL1(T315I)-phosphorylated	94	50	87
ABL1(Y253F)-phosphorylated	71	55	75
ABL1-nonphosphorylated	76	44	58
ABL1-phosphorylated	94	54	81
ABL2	100	56	92
ACVR1	90	95	99
ACVR1B	89	91	100
ACVR2A	100	100	97
ACVR2B	100	99	100
ACVRL1	98	100	100
ADCK3	79	88	85
ADCK4	93	84	77
AKT1	98	100	100
AKT2	99	99	80
AKT3	100	100	90
ALK	92	94	70
ALK(C1156Y)	88	64	91
ALK(L1196M)	77	90	94
AMPK-alpha1	96	85	94
AMPK-alpha2	94	92	99
ANKK1	75	48	100
ARK5	99	100	100
ASK1	70	100	100
ASK2	83	96	100
AURKA	90	98	75
AURKB	90	55	83
AURKC	92	58	92
AXL	84	88	99

BIKE	34	13	91
BLK	53	95	79
BMPR1A	95	86	100
BMPR1B	100	100	67
BMPR2	96	100	91
BMX	96	92	100
BRAF	98	98	96
BRAF(V600E)	99	89	98
BRK	87	85	93
BRSK1	96	86	100
BRSK2	100	98	84
BTK	98	100	70
BUB1	83	58	59
CAMK1	100	77	84
CAMK1B	n.d.	75	100
CAMK1D	100	71	85
CAMK1G	76	51	100
CAMK2A	100	47	99
CAMK2B	90	69	100
CAMK2D	97	62	100
CAMK2G	100	52	100
CAMK4	100	100	100
CAMKK1	94	52	98
CAMKK2	99	42	100
CASK	87	59	100
CDC2L1	100	100	92
CDC2L2	100	99	90
CDC2L5	92	84	96
CDK11	97	98	91
CDK2	88	95	98
CDK3	95	90	97
CDK4	n.d.	100	100
CDK4-cyclinD1	88	93	87
CDK4-cyclinD3	78	100	97
CDK5	100	92	99
CDK7	68	16	61
CDK8	82	97	70
CDK9	98	43	95
CDKL1	74	90	67
CDKL2	83	88	81
CDKL3	100	88	90
CDKL5	100	46	96
CHEK1	88	100	100
CHEK2	88	61	100
CIT	73	74	85
CLK1	4	1.2	16
CLK2	9.6	4.2	79
CLK3	70	52	100

CLK4	1.5	2.1	20
CSF1R	79	21	60
CSF1R-autoinhibited	98	91	100
CSK	100	94	98
CSNK1A1	100	58	97
CSNK1A1L	100	88	100
CSNK1D	64	61	100
CSNK1E	71	44	100
CSNK1G1	100	95	100
CSNK1G2	100	95	96
CSNK1G3	100	100	100
CSNK2A1	85	75	99
CSNK2A2	94	100	100
CTK	91	95	69
DAPK1	98	66	99
DAPK2	91	69	98
DAPK3	85	34	84
DCAMKL1	99	100	81
DCAMKL2	95	92	96
DCAMKL3	100	100	100
DDR1	22	100	96
DDR2	86	98	100
DLK	89	83	100
DMPK	84	99	89
DMPK2	62	81	100
DRAK1	18	20	91
DRAK2	93	61	92
DYRK1A	5.1	0.35	71
DYRK1B	1	0.85	63
DYRK2	28	8	99
EGFR	71	80	100
EGFR(E746-A750del)	84	91	100
EGFR(G719C)	91	93	71
EGFR(G719S)	85	97	71
EGFR(L747-E749del, A750P)	87	83	81
EGFR(L747-S752del, P753S)	89	81	100
EGFR(L747-T751del,Sins)	88	96	92
EGFR(L858R)	68	83	100
EGFR(L858R,T790M)	82	90	100
EGFR(L861Q)	82	100	100
EGFR(S752-I759del)	94	95	97
EGFR(T790M)	92	100	100
EIF2AK1	100	78	78
EPHA1	80	84	99
EPHA2	94	99	94
EPHA3	78	88	100
EPHA4	84	99	100
EPHA5	99	93	99

EPHA6	79	93	82
EPHA7	94	97	94
EPHA8	90	90	92
EPHB1	100	89	84
EPHB2	83	94	96
EPHB3	82	88	92
EPHB4	79	95	100
EPHB6	68	89	83
ERBB2	100	97	84
ERBB3	96	99	71
ERBB4	99	100	100
ERK1	95	100	92
ERK2	92	93	99
ERK3	96	68	94
ERK4	100	99	93
ERK5	100	98	87
ERK8	87	81	100
ERN1	69	41	33
FAK	91	100	97
FER	98	100	82
FES	87	88	96
FGFR1	99	94	87
FGFR2	85	91	84
FGFR3	90	94	91
FGFR3(G697C)	78	85	91
FGFR4	94	99	98
FGR	75	93	100
FLT1	90	11	45
FLT3	2.5	3	83
FLT3(D835H)	13	5.5	90
FLT3(D835V)	n.d.	0	69
FLT3(D835Y)	10	17	100
FLT3(ITD)	5.6	0.25	91
FLT3(ITD,D835V)	n.d.[a]	0.7	76
FLT3(ITD,D835Y)	n.d.	25	77
FLT3(K663Q)	3.8	13	83
FLT3(N841I)	7.5	0	96
FLT3(R834Q)	94	0.7	100
FLT3-autoinhibited	42	0.65	90
FLT4	95	83	100
FRK	90	96	92
FYN	95	96	98
GAK	8.8	10	33
GCN2(Kin.Dom.2,S808G)	93	97	77
GRK1	100	80	82
GRK2	n.d.	84	100
GRK3	n.d.	74	91
GRK4	42	79	100

GRK7	97	63	77
GSK3A	93	100	84
GSK3B	99	92	96
HASPIN	21	22	66
HCK	80	93	87
HIPK1	42	0.45	74
HIPK2	62	0.7	85
HIPK3	63	2.4	89
HIPK4	8.6	5.1	71
HPK1	75	88	97
HUNK	90	100	92
ICK	80	74	97
IGF1R	100	100	95
IKK-alpha	76	100	90
IKK-beta	83	94	90
IKK-epsilon	94	100	78
INSR	99	91	97
INSRR	96	85	100
IRAK1	95	45	89
IRAK3	100	49	95
IRAK4	92	85	91
ITK	92	84	91
JAK1(JH1domain-catalytic)	100	100	100
JAK1(JH2domain-pseudokinase)	93	100	82
JAK2(JH1domain-catalytic)	91	99	100
JAK3(JH1domain-catalytic)	100	100	82
JNK1	91	83	67
JNK2	91	80	75
JNK3	89	79	99
KIT	1.6	0	68
KIT(A829P)	75	45	94
KIT(D816H)	100	63	96
KIT(D816V)	78	29	81
KIT(L576P)	1.2	0	61
KIT(V559D)	0.45	0.05	67
KIT(V559D,T670I)	20	0.85	97
KIT(V559D,V654A)	7.8	0.7	27
KIT-autoinhibited	82	34	98
LATS1	82	82	86
LATS2	58	73	94
LCK	100	87	82
LIMK1	100	97	98
LIMK2	94	85	100
LKB1	52	98	77
LOK	100	100	91
LRRK2	94	90	100
LRRK2(G2019S)	91	76	88
LTK	100	88	88

LYN	92	96	95
LZK	100	100	98
MAK	82	61	69
MAP3K1	99	92	89
MAP3K15	83	98	100
MAP3K2	74	100	62
MAP3K3	88	89	73
MAP3K4	74	86	86
MAP4K2	99	76	85
MAP4K3	71	92	99
MAP4K4	92	75	100
MAP4K5	98	87	100
MAPKAPK2	92	100	100
MAPKAPK5	91	98	82
MARK1	86	94	94
MARK2	96	88	100
MARK3	100	99	60
MARK4	92	95	93
MAST1	91	73	63
MEK1	95	93	80
MEK2	92	89	80
MEK3	87	100	88
MEK4	75	100	100
MEK5	85	95	71
MEK6	98	93	929
MELK	35	16	96
MERTK	100	70	82
MET	90	100	97
MET(M1250T)	89	82	98
MET(Y1235D)	100	97	99
MINK	72	57	87
MKK7	92	100	93
MKNK1	82	88	83
MKNK2	80	67	74
MLCK	80	6.6	89
MLK1	85	100	93
MLK2	100	92	88
MLK3	100	100	81
MRCKA	90	82	97
MRCKB	64	97	100
MST1	100	100	95
MST1R	99	64	77
MST2	85	92	100
MST3	100	91	92
MST4	88	84	100
MTOR	98	100	89
MUSK	72	42	40
MYLK	79	42	81

MYLK2	82	52	89
MYLK4	67	24	91
MYO3A	96	96	97
MYO3B	82	92	73
NDR1	75	96	86
NDR2	94	94	100
NEK1	84	92	96
NEK10	92	72	100
NEK11	88	100	92
NEK2	100	92	92
NEK3	93	88	100
NEK4	99	100	95
NEK5	93	86	96
NEK6	99	100	96
NEK7	97	99	94
NEK9	100	91	100
NIK	90	78	92
NIM1	97	91	77
NLK	70	100	100
OSR1	79	99	100
p38-alpha	100	99	95
p38-beta	94	94	99
p38-delta	89	60	72
p38-gamma	73	91	83
PAK1	98	99	89
PAK2	71	76	91
PAK3	63	81	100
PAK4	79	93	86
PAK6	100	98	97
PAK7	98	93	95
PCTK1	97	87	37
PCTK2	98	66	2.7
PCTK3	79	80	88
PDGFRA	12	0.3	94
PDGFRB	1.3	0.05	56
PDPK1	88	100	100
PFTAIRE2	100	40	91
PFTK1	87	99	96
PHKG1	91	17	92
PHKG2	85	29	98
PIK3C2B	86	97	100
PIK3C2G	91	80	82
PIK3CA	72	97	90
PIK3CA(C420R)	88	89	85
PIK3CA(E542K	72	93	65
PIK3CA(E545A)	88	100	78
PIK3CA(E545K)	75	80	68
PIK3CA(H1047L)	95	98	70

PIK3CA(H1047Y)	89	82	100
PIK3CA(I800L)	83	88	58
PIK3CA(M1043I)	59	81	78
PIK3CA(Q546K)	88	100	81
PIK3CB	82	93	97
PIK3CD	92	90	75
PIK3CG	78	100	100
PIK4CB	3.3	21	73
PKFYVE	n.d.	87	26
PIM1	100	68	95
PIM2	100	100	100
PIM3	95	71	92
PIP5K1A	100	80	91
PIP5K1C	85	91	84
PIP5K2B	78	87	81
PIP5K2C	67	93	100
PKAC-alpha	68	100	94
PKAC-beta	86	99	90
PKMYT1	81	94	100
PKN1	100	71	91
PKN2	100	100	98
PLK1	97	90	96
PLK2	66	100	90
PLK3	90	89	90
PLK4	87	100	99
PRKCD	93	90	62
PRKCE	100	96	86
PRKCH	96	100	100
PRKCI	88	100	89
PRKCQ	94	85	100
PRKD1	100	98	99
PRKD2	100	100	93
PRKD3	98	94	100
PRKG1	84	32	83
PRKG2	84	64	64
PRKR	97	97	81
PRKX	91	80	100
PRP4	60	97	93
PYK2	84	86	99
QSK	78	82	100
RAF1	99	100	100
RET	100	100	96
RET(M918T)	100	92	80
RET(V804L)	100	88	92
RET(V804M)	97	82	100
RIOK1	35	33	88
RIOK2	70	67	61
RIOK3	31	32	94

RIPK1	91	74	94
RIPK2	88	61	100
RIPK4	96	95	98
RIPK5	98	91	79
ROCK1	36	22	76
ROCK2	31	21	100
ROS1	100	100	96
RPS6KA4(Kin.Dom.1-N-terminal)	100	99	91
RPS6KA4(Kin.Dom.2-C-terminal)	87	81	86
RPS6KA5(Kin.Dom.1-N-terminal)	100	99	100
RPS6KA5(Kin.Dom.2-C-terminal)	93	80	99
RSK1(Kin.Dom.1-N-terminal)	72	54	100
RSK1(Kin.Dom.2-C-terminal)	83	59	96
RSK2(Kin.Dom.1-N-terminal)	37	19	100
RSK2(Kin.Dom.2-C-terminal)	89	100	73
RSK3(Kin.Dom.1-N-terminal)	82	52	78
RSK3(Kin.Dom.2-C-terminal)	100	94	80
RSK4(Kin.Dom.1-N-terminal)	27	13	97
RSK4(Kin.Dom.2-C-terminal)	92	56	88
S6K1	90	88	95
SBK1	87	89	77
SGK	91	94	76
SgK110	100	100	100
SGK2	89	100	83
SGK3	91	65	93
SIK	98	89	91
SIK2	73	97	100
SLK	100	98	80
SNARK	99	73	88
SNRK	99	100	79
SRC	100	100	100
SRMS	91	86	95
SRPK1	100	79	84
SRPK2	73	79	93
SRPK3	49	66	100
STK16	100	83	96
STK33	47	25	100
STK35	77	97	100
STK36	91	95	93
STK39	88	89	98
SYK	97	100	92
TAK1	91	47	65
TAOK1	93	85	75
TAOK2	87	100	98
TAOK3	92	91	77
TBK1	71	90	76
TEC	100	97	88
TESK1	92	91	100

TGFBR1	100	100	92
TGFBR2	100	100	100
TIE1	99	67	84
TIE2	78	89	91
TLK1	96	87	93
TLK2	98	95	89
TNIK	80	47	97
TNK1	69	100	100
TNK2	86	93	100
TNNI3K	97	100	100
TRKA	89	19	96
TRKB	89	69	91
TRKC	87	100	100
TRPM6	100	92	85
TSSK1B	100	92	88
TSSK3	n.d.	100	91
TTK	77	54	90
TXK	85	88	93
TYK2(JH1domain-catalytic)	87	100	74
TYK2(JH2domain-pseudokinase)	91	99	73
TYRO3	69	86	99
ULK1	78	97	79
ULK2	98	94	83
ULK3	78	95	68
VEGFR2	79	35	71
VRK2	867	98	82
VPS34	n.d.	94	97
WEE1	100	100	100
WEE2	94	87	97
WNK1	89	100	76
WNK2	n.d.	34	100
WNK3	96	100	82
WNK4	n.d.	100	83
YANK1	95	98	73
YANK2	94	100	100
YANK3	100	99	73
YES	91	93	96
YSK1	92	100	99
YSK4	45	23	77
ZAK	86	87	93
ZAP70	84	100	83

[a] n.d. = not determined; [b] blue highlight = mutant kinase, pink highlight = wild type lipid kinase.

12. **Supplementary Table S2**: HPLC purities of test compounds **2**, **5** – **12**, **19** – **33**.

No.	Purity[a] (%)	No.	Purity[a] (%)	No.	Purity[a] (%)
2	99.7	**12**	99.2	**26**	99.4
5	96.0	**19**	98.3	**27**	100.0
6	98.7	**20**	100.0	**28**	100.0
7	100.0	**21**	100.0	**29**	100.0
8	100.0	**22**	100.0	**30**	98.8
9	100.0	**23**	100.0	**31**	100.0
10	100.0	**24**	98.3	**32**	100.0
11	99.1	**25**	97.7	**33**	99.2

[a] Determined by HPLC (AUC, UV-Vis) as described in the Experimental Methods.

13. Generation of an HEK293TN XBP1 luciferase reporter cell line

A lentiviral plasmid reporter for IRE1α RNase activity was constructed from the FLAG-XBP1ΔDBD coding region (nucleotides 410-633 of XBP1), which lacks the DNA binding domain but contains a 26 nucleotide intron cleaved by IRE1α (obtained from Dr Chris Bakal, ICR), as a blunt/XbaI fragment. This was linked to the N-terminus of the PEST-destabilised firefly luciferase (luc2P) from pGL4.24 (E8421; Promega) as a blunt/BamHI fragment. These units were combined in the pCMV promoter vector pCDF1-MCS2-EF1-Puro (CD110B-1; System Biosciences), opened with XbaI/BamHI, in a three-fragment ligation giving the construct pCDF1-FLAG-XBP1ΔDBD-luc2P. The luciferase domain was arranged to be in frame with the upstream XBP ORF only when the 26 nucleotide intron was spliced out by IRE1α activity. Conversely, when IRE1α is inactive or inhibited and the 26 nucleotide intron of XBP1 is present, the luciferase domain is out of frame resulting in a minimal luciferase signal.

HEK293TN (LV900A-1; System Biosciences) packaging cells were seeded in a 6 well plate at a density of 5 $x10^5$/well in DMEM (41966; Life Technologies) supplemented with 10% foetal bovine serum (FBS) (F7524; Sigma-Aldrich) and incubated at 37ºC/5% CO_2 overnight. The pPACKF1™ Packaging Plasmid mix (LV100A-1; System Biosciences) and lentiviral plasmid were pre-mixed in the presence of Opti-MEM® reduced serum medium (31985047; Life Technologies). The Arrest-In Transfection Reagent (ATR1740; Open Biosystems) was also pre-mixed in the presence of Opti-MEM®. The 2 mixtures were combined and incubated at r.t. for 20 min. The DMEM/10% FBS cell medium was replaced with Opti-MEM® and the

transfection mix added to the cells. The cells were subsequently incubated at 37°C/5% CO_2 for 6 h. The medium was replaced with DMEM/5% FBS and the cells incubated for a further 72 h at 37°C/5% CO_2. The supernatant containing the virus was harvested and concentrated using the Lenti-X ^{TM} Concentrator (631231; Clontech).

HEK293TN cells were seeded in a 6 well plate at a density of 1 x10^{5}/well and incubated at 37°C/5% CO_2 overnight. The medium was removed and replaced with a dilution of either 0, 1:10 or 1:50 virus in DMEM/10% FBS/5 µg/mL polybrene (1 mL volume). The plate was centrifuged at 800 rpm (37°C) for 1 h. 1 mL/well of additional DMEM/10% FBS was added and the plate incubated for 72 h (37°C/5% CO_2). The transduced cells were subsequently passaged into fresh medium DMEM/10% FBS/1 µg/mL puromycin (in T75 flasks) for 7 d. Following growth of stable transformants, 6 colonies were selected at random to be individually cultured in DMEM/10% FBS and assayed for luciferase activity. The remaining cells were cultured as a heterogeneous population.

14. Methods to determine inhibition of an XBP1 luciferase reporter in HEK293TN cells and assess compound cytotoxicity to HEK293TN cells

Reporter XBP1s HEK293TN cells were seeded at 2000 cells/well (30 µL) in DMEM/10% in 384 well white polystyrene plates (164610; Thermo Fisher Scientific) and incubated at 37°C/5% CO_2 overnight. Compounds were diluted to a stock concentration of 10 mM in 100% DMSO and dispensed into the assay plate in a concentration response curve (CRC) format using an Echo 550® acoustic dispenser (Labcyte). Compound CRCs ranged from 57 nM to 49 µM in 1% DMSO (final assay

concentration). The compounds and cells were incubated at 37°C/5% CO_2 for 1 h. To induce the stress response the stress agent tunicamycin was added. A concentration of tunicamycin was chosen to reflect a 70%-80% stimulation of activity. Tunicamycin was diluted to a stock concentration of 10 mg/mL in 100% DMSO. This was further diluted to 909 µg/mL, was then added into a Labcyte plate and dispensed into all assay wells using the using the Echo 550® (final concentration 0.68 µg/mL). Control wells contained either 50 µM 7-(1-(3,5-difluorobenzyl)-1*H*-pyrazol-4-yl)-3*H*-imidazo[4,5-*b*]pyridine (Supplementary Figure S9) in 1% DMSO (maximum inhibition) or tunicamycin (maximal response) (0.68µg/mL) (The plates were incubated at 37°C/5% CO_2 for 5 h prior to addition of 15 µL/well Steady-Glo Luciferase Assay System reagent (E2520; Promega). The plates were incubated at r.t. for 30 min and the luminescent signal was detected using an EnVision Multimode Plate Reader (Perkin Elmer Lifesciences). In addition, to monitor cytotoxic effects caused by test compounds, compounds +/- tunicamycin were added as previously described. Then, 5 µL CellTitreBlue® reagent (Promega) was added for 3 h at 37°C/5% CO_2 and plates were read on the EnVision Multimode Plate Reader. Compound IRE1α agonist activity, leading to enhanced cleavage of the reporter XBP1-luciferase fusion mRNA, was addressed by testing compounds in the absence of tunicamycin. In this case the tunicamycin was added to the high controls at a higher concentration of 50 µM.

15. Quantification of XBP1s expression in NCI-H929 cells by immunofluorescence

NCI-H929 (ATCC) suspension cells were maintained in RPMI (72400-054) supplemented with 5% SeraPlus FBS (Pan BioTech) and 5% Hyclone tetracycline-free FBS (GE Healthcare) and maintained at 37°C, 5% CO_2. To aid the attachment of the cells for immunofluorescence, the plates (6005182, Packard Viewplate) were coated with 50 µL poly-L-lysine (0.01%, P4707 Sigma). NCI-H929 cells were then plated at $4x10^5$ cells/mL in 80 µL of media and left overnight at 5%CO_2/37°C. Dilution series to construct a concentration response curve for each of the compounds were established using the Echo®550 acoustic dispenser (Labcyte). Compounds and DMSO (1 µL final volume) were first added to a dry 96 well plate (Greiner). An intermediate dilution (10x final concentration) was achieved by the addition of 49 µL RPMI/10% FBS. 10 µL of this solution was added to the cells (1:500 final dilution). In addition, difluorobenzyl)-1H-pyrazol-4-yl)-3H-imidazo[4,5-b]pyridine (Supplementary Figure S9) (20 µM final) was added in the same way to control wells to give the low control for normalization. The range of concentrations for these experiments was from 20 µM-0.0156 µM final concentration. Tunicamycin (10 µg/mL final, 10 µL) was then added to each of the wells and incubated at 5%CO_2/37°C for 4 h.

The cells were then fixed with formaldehyde (3.7% final in PBS, F8775, Sigma) for 15 min at r.t., permeabilised with ice cold methanol (15 min at -20°C) and followed by a blocking step with 5% BSA (w/v) (A2153, Sigma)/1% triton X-100 (v/v) (A984, Sigma) in PBS for 1 h at room temperature. The primary antibody incubation for XBP1s (619502, Biolegend 0.13 µg/mL) was then carried out overnight at 4°C in 1% BSA (w/v), 0.5% TritonX-100(v/v). Following a wash step, a secondary goat anti-rabbit Alexa Fluor®488 antibody (A11034, 4 µg/mL) was added for detection of XBP1s (1 h incubation at r.t.) and finally the nuclear dye Hoechst 33342 (H3570, 2

μg/mL final) was added for 15 min at r.t. Images were captured on an IN Cell Analyzer 1000 (GE Healthcare) using the 360_40x excitation and HQ460_40M and HQ480_40X HQ535_50M emission filters (10x objective, >4000 cells analysed per well, 8 fields/well) and analysed using the IN Cell Analyzer Workstation software 3.7.2. Nuclei were detected and segmented using the 360_40x - HQ460_40M channel (minimum area 35 μm^2). Apoptotic/mitotic nuclei were removed from the quantification by detecting DNA fragmentation of the nuclei in the Hoechst channel. Cells with fragmented nuclei were eliminated from the quantification so that only XBP1s nuclear intensity from 'healthy' cells was measured. Cells were separated into 'Healthy', 'Mitotic', and 'Apoptotic' cells by using 'Decision tree' in WorkStation software. Briefly, small condensed bright nuclei in the 360_40X – HQ460_40M channel were detected by plotting a threshold graph of nucleus/cytoplasmic (nuc/cyt) intensity and total area of fragmented DNA (organelle). Nuclei with a nuc/cyt intensity >2.2 and a total area >9 were mitotic and excluded. To remove nuclei that were fragmented or apoptotic the remaining population was then further subdivided and those with a nuc/cyt intensity <0.7 and a total area <0.7 were also excluded. The residual healthy cell population thus had larger and brighter Hoechst stained nuclei. As XBP1s showed a nuclear localisation the same minimum area criteria was used to measure the intensity in the 480_40X – HQ535_50M green channel. The mean well background intensity was then subtracted from the mean XBP1 nuclear intensity to determine the IC_{50} relative to the 7-(1-(3,5-difluorobenzyl)-1*H*-pyrazol-4-yl)-3*H*-imidazo[4,5-*b*]pyridine + tunicamycin and the tunicamycin only controls using Dotmatics Studies (Dotmatics, UK).

16. Quantification of XBP1s and DNAJB9 mRNA expression in NCI-H929 cells by qPCR

Unless otherwise stated all reagents were purchased from ThermoFisher Scientific. NCI-H929 (ATCC) suspension cells were maintained in RPMI supplemented with 5% SeraPlus FBS (Pan BioTech) and 5% Hyclone tetracycline free FBS (GE Healthcare) and maintained at 37°C, 5% CO_2. Cells were plated at $5x10^5$ cells/mL in a 24 well plate and left to equilibrate at 37°C, 5% CO_2 for 2 h. Compounds (+/- tunicamycin (Sigma T7765; Sigma) were then diluted in DMSO (1:2 fold) and added to the cell culture media to give final concentrations ranging from 20 µM to 0.078 µM (0.3% DMSO, 10 µg/mL tunicamycin final concentration). The cells were treated with compound for 4 h at 5% CO_2 and 37°C, harvested, centrifuged and the cell pellet resuspended in nucleic acid purification buffer (200 µL). The lysates were then transferred in to a MagNa Pure 96 (Roche) well processing plate and the RNA extracted using an automated protocol on the MagNa Pure 96 instrument (Roche). This methodology uses a DNAase step to inactivate genomic DNA.

Following extraction, the RNA was quantified using the Quanti-iTRNA broad range kit (Q10213) and read using the monochromator (ex/em wavelengths 644/673 nm) on an EnVision Multimode Plate Reader (Perkin Elmer Lifesciences). All samples were then normalised with DNase/RNase free water (Ambion) to give the same quantity of RNA (typically 500-1000 ng/µL) in each sample. Normalisation was carried out on the Janus® Automated workstation (Perkin Elmer Lifesciences) and the samples collected in a 96 well PCR plate (ABI microamp plate). To carry out the Reverse Transcription of the normalised RNA to cDNA, the cDNA synthesis kit iScript™ (Bio-Rad) was used and carried out on a Tetrad PTC-225 thermal cycler (MJ research; reaction protocol - 5 min at 25ºC, 30 min at 42ºC, 5 min at 85ºC, hold

at 4ºC). The resulting cDNA was then diluted in DNase/RNase free water to a concentration of 100 ng/µL.

For quantification of XBP1s mRNA, real time PCR – TaqMan, was carried out in a multiplex reaction with the human RPLPO (large ribosomal protein) endogenous control gene. For each sample, a reaction mixture containing the following components was made: 5 µL 2X TaqMan universal master mix (4304437); XBP1s (20x) (Hs03929085_g1, XBP1s FAM-MGB) 0.5 µL; human RPLPO VIC™ MGB (20x, 4326314E) (0.5 µL); nuclease free water (2 µL); cDNA template (2 µL). Final reaction volume was 10 µL. Each sample was run in triplicate in a 384 well plate (Applied Biosystems).

For quantification of DNAJB9 mRNA, real time PCR – TaqMan, was carried out in a singleplex reactions with the RPLPO endogenous control gene run in separate wells. For each sample, two reaction mixtures containing the following components were made: 1.5 µL 2XTaqMan universal master mix; DNAJB9 (20x) (Hs01052402_m1, DNAJB9 FAM-MGB) 0.5 µL; nuclease-free water (2.5 µL); cDNA template (2 µL). 2.5 µL 2 X TaqMan universal master mix; human RPLPO VIC™ MGB (20x) (0.5 µL); nuclease-free water (2.5 µL); cDNA template (2 µL). Final reaction volumes were 10 µL. Each sample was run in triplicate in a 384 well plate (Applied Biosystems). All the TaqMan reactions were carried out on the ViiA7™ qPCR machine and analysis of data on the Viia7™ software (relative quantitation - RQ values, ±minimum and maximum RQ) (ThermoFisher Scientific). (Reaction protocol - 2 min at 50°C, 10 min 95°C then 40 cycles of 15 s at 95°C, 1 min at 60°C).

17. Inhibition of IRE1α-GFP oligomerization in T-Rex293-IRE1-3F6HGFP cells

Oligomerization assays were carried out using T-Rex293-IRE1-3F6HGFP cells which contained a doxycycline inducible IREα construct and were a kind gift from Professor Peter Walker[41]. Cells (6,400/well) were plated into poly-L-lysine coated, dark walled, 96 well plates and induced with 10 nM doxycline for 24 h prior to the assay. On the day of the assay, medium was replaced with TET free medium and cells were pre-treated with 5 drug concentrations for 1 h and then either vehicle treated or stressed with tunicamycin (10 µg/mL) for 4 h. Cells were fixed with formaldehyde, washed with PBS and counterstained with Hoechst 33342. Appropriate positive and negative controls were included. Plates were analysed on an IN Cell Analyzer 1000 using associated software (IN Cell Analyzer Workstation software 3.7.2., GE Healthcare) and 7-12 fields counted per well and the results expressed as Foci/100 cells for each treatment. Data analysis and curve fitting was carried out using PRISM 7 software (Graphpad Prism v7.03).

18. Quantification of total IRE1α and pIRE1α expression in H929 myeloma cells

ProteinSimple capillary electrophoresis immunoassay (ProteinSimple, Santa Clare, CA, USA) was performed according to the ProteinSimple user manual (https://www.proteinsimple.com/wes.html). In brief, whole cell extract samples were mixed at a ratio of 4 parts cell lysates to 1 part 5X Fluorescent Master Mix in a micro-centrifuge tube to give final protein concentrations of 0.3 mg/mL. Samples were denatured at the same time as the biotinylated ladder. All the samples, blocking buffers, primary antibodies (1 in 100 dilutions for pIRE1 and 1 in 50 dilutions for total IRE1) and HRP-conjugated secondary antibodies were loaded into the selected plate wells. Electrophoresis and immunodetection steps within the capillary system took

place automatically under instrument default settings. The digital image was analyzed and quantified with Compass software after normalization to β-actin (loading control) (ProteinSimple Wes, ProteinSimple, Santa Clare, CA, USA).

19. X-ray crystallography of 33-IRE1α

hIRE1α was expressed and purified as previously described[6]. hIRE1 was crystallized by hanging-drop vapor diffusion. A protein-ligand mixture was prepared comprising hIRE1 at 10 mg/mL and compound **33** at 1.4 mM. This was mixed with reservoir solution containing 20% polyethylene glycol 3350, 0.2 M sodium acetate and 0.1 bis-tris propane (pH 6.5) in a 1:1 ratio. Crystallization experiments were conducted at 18°C. Crystals were briefly soaked in reservoir buffer supplemented with 25% ethylene glycol before plunging into liquid nitrogen. X-ray diffraction data were collected at 100 K from a single cryo-cooled crystal using an in-house X-ray system (Rigaku 007-HF, Saturn 944+ CCD detector). Diffraction data were integrated and scaled using CCP4 software[50]. The structure of apo-hIRE1 was solved by molecular replacement using PHASER[S1] with a single protomer from the apo-hIRE1 crystal structure (PDB code 4Z7G[6]). Manual model building was performed in COOT[51] and refinement was performed in PHENIX[S2]. The structure was validated using MolProbity[S3].

S1 McCoy, A. J.; Grosse-Kunstleve, R. W.; Adams, P. D.; Winn, M. D.; Storoni, L. C.; Read, R. J. Phaser crystallographic software. *J. Appl. Crystallogr.* **2007**, *40*, 658-674.

S2 Afonine, P. V.; Grosse-Kunstleve, R. W.; Echols, N.; Headd, J. J.; Moriarty, N. W.; Mustyakimov, M.; Terwilliger, T. C.; Urzhumtsev, A.; Zwart, P. H.; Adams, P. D. Towards automated crystallographic structure refinement with phenix.refine. *Acta Crystallogr. D Biol. Crystallogr*. **2012**, *68*, 352-367.

S3 Davis, I. W.; Leaver-Fay, A.; Chen, V. B.; Block, J. N.; Kapral, G. J.; Wang, X.; Murray, L. W.; Arendall, W. B. 3rd; Snoeyink, J.; Richardson, J. S.; Richardson, D. C. MolProbity: all-atom contacts and structure validation for proteins and nucleic acids. *Nucl. Acids Res.* **2007**, *35*, W375-W383.

20. Table S3: Data collection and refinement statistics for the crystal structures of **2**-IRE1α and **33**-IRE1α.

	2-IRE1α	**33**-IRE1α
PDB code	6hx1	6hv0
Data Collection		
Space group	C 2	C 2
Cell dimensions *a*, *b*, *c* (Å)	144.41, 47.07, 86.37	144.04, 46.05, 86.34
α, β, γ (°)	90.0, 112.1, 90.0	90.00, 112.71, 90.00
Resolution (Å)	2.13 (2.38 - 2.13)[a]	2.73 (2.86 – 2.73)[a]
Unique reflections	28816 (7825)	14150 (1770)
Multiplicity	3.7 (3.6)	3.5 (2.7)
Completeness (%)	94.5 (91.6)	99.2 (94.8)
R_{meas} (%)	8.1 (51.7)	16.7 (74.2)
$CC_{1/2}$	0.998 (0.919)	0.986 (0.584)

Refinement		
Resolution (Å)	80.00 – 2.14	32.97 - 2.73
Number of reflections (working / test)	27136 / 1537	14143 / 1415
R_{cryst} (%)	21.7	21.7
R_{free} (%)	26.8	26.9
Total no. of atoms:		
Protein	3156	3021
Water	122	57
Ligand	24	23
Deviation from ideal geometry:		
Bond lengths (Å)	0.007	0.004
Bond angles (°)	1.25	0.844
All-atom clashscore	0.82	6.88
Ramachandran		
Outliers (%)	0.0	0.54
Allowed (%)	2.9	6.27
Favored (%)	97.1	93.19
Cbeta deviations (%)	0	0
Rotamer outliers (%)	1.40	4.63

[a] Values in parentheses refer to the highest resolution shell.

21. Methods for the synthesis of compound 33.

6-Chloro-3-(*1H*-indazol-5-yl)-*N*-isopropylimidazo[1,2-*b*]pyridazin-8-amine (33): Prepared from isopropylamine, **33** and 5-(4,4,5,5-tetramethyl-1,3,2-dioxaborolan-2-yl)-*1H*-indazole using the methods described for **2** to give **33** (17% over 2 steps). ^{1}H NMR (500 MHz, DMSO-d_6) δ 13.18 (s, 1H), 8.53 – 8.48 (m, 1H), 8.19 (t, *J* = 1.3 Hz, 1H), 7.95 – 7.92 (m, 2H), 7.66 (dd, *J* = 8.7, 1.0 Hz, 1H), 7.61 (d, *J* = 8.6 Hz, 1H), 6.30 (s, 1H), 4.12 – 3.81 (m, 1H), 1.27 (d, *J* = 6.4 Hz, 6H); ^{13}C NMR (126 MHz, DMSO-d_6) δ 147.6, 142.8, 139.1, 134.1, 132.8, 128.9, 125.5, 122.9, 120.8, 118.4, 110.4, 99.5, 90.7, 43.7, 21.7 (2C); LCMS (2 min) t_R = 1.70 min, *m/z* (ESI$^+$) 327 (M+H$^+$); HRMS *m/z* calcd. for $C_{16}H_{16}N_6{}^{35}Cl$ (M + H) 327.1119, found 327.1116.

22. Copies of ^{1}H and ^{13}C NMR data for test compounds 2, 5 – 12, 19 – 33.

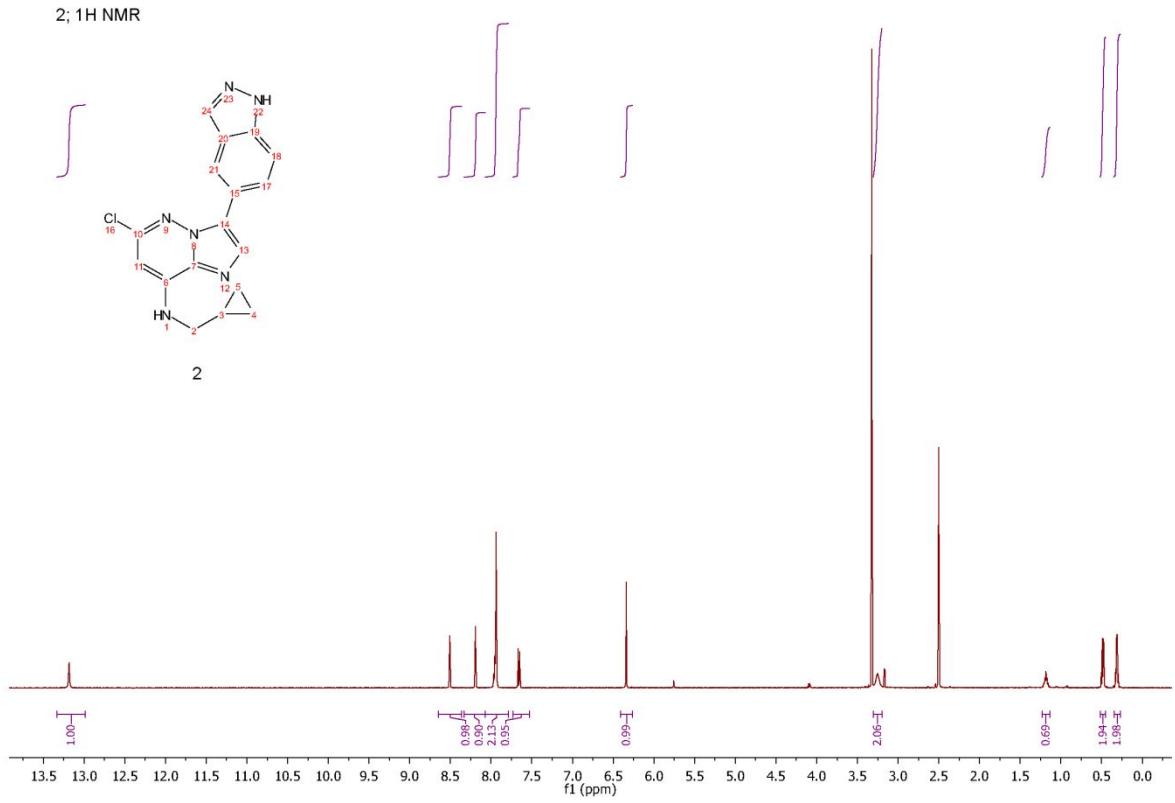

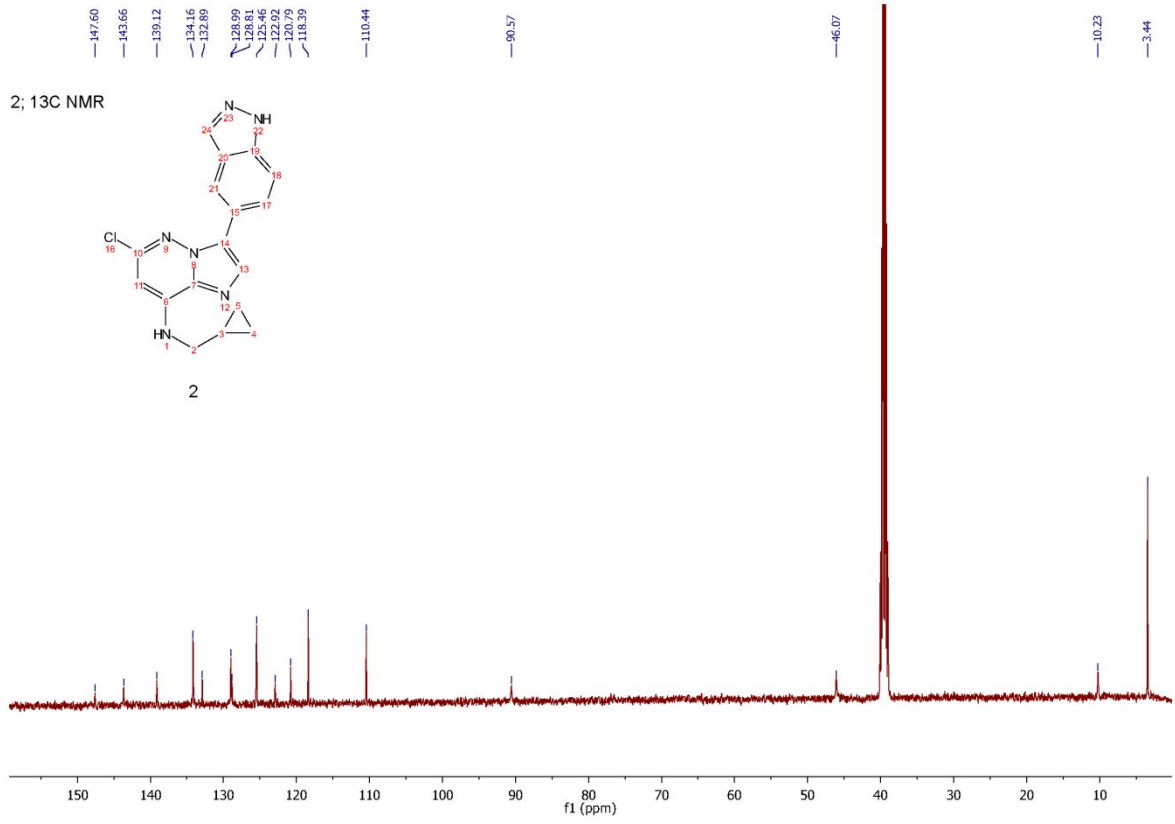

5; 1H NMR

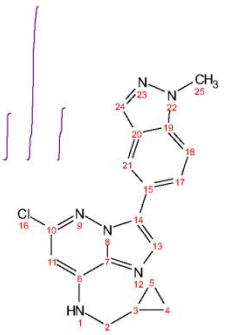

5

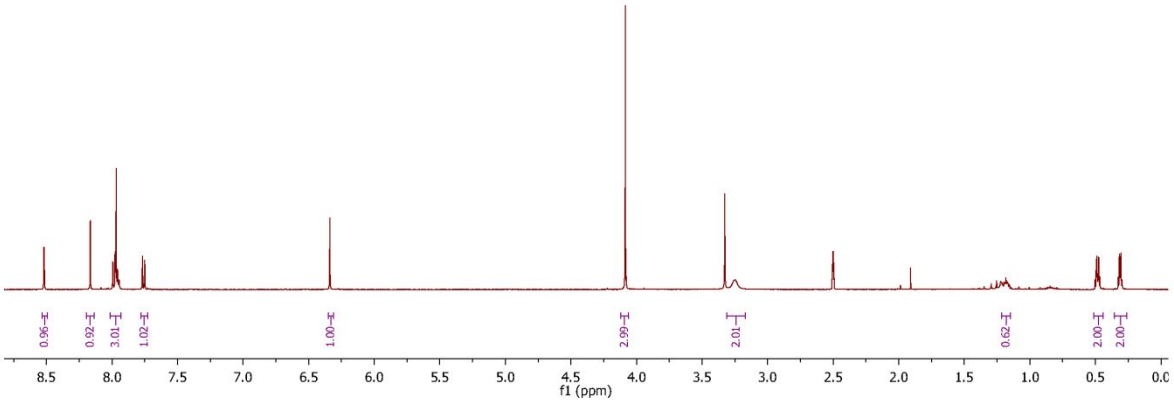

5; 13C NMR

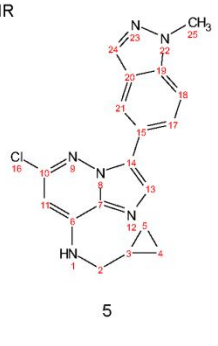

5

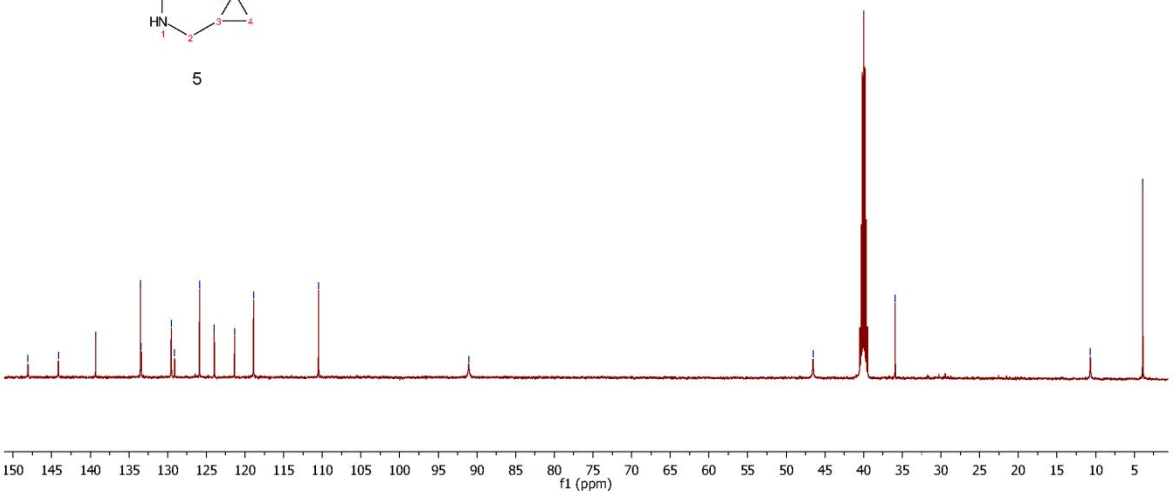

6; 1H NMR

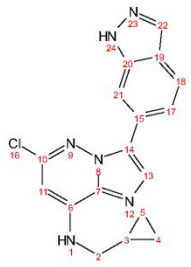

6

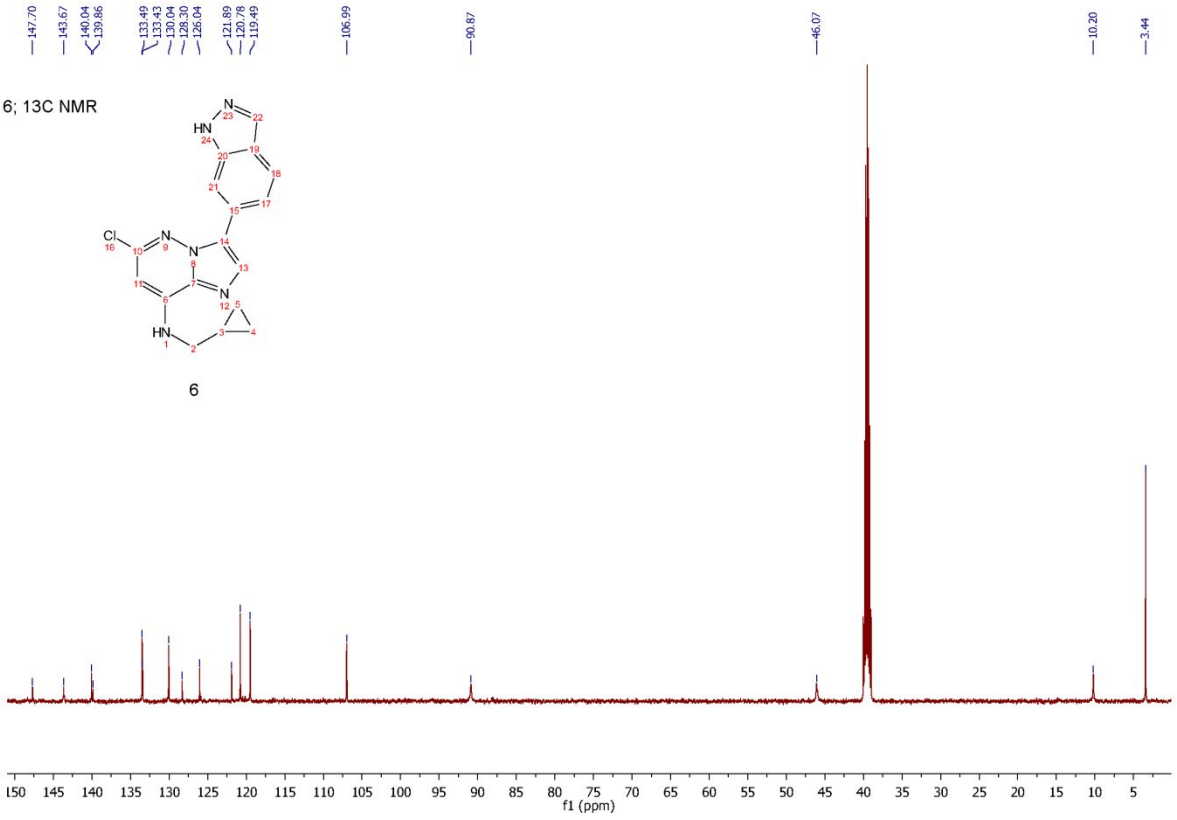

6; 13C NMR

6

7; 1H NMR

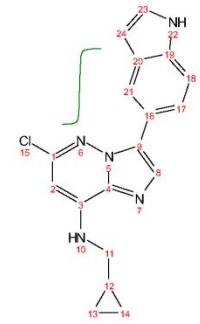

7

7; 13C NMR

7

8; 1H NMR

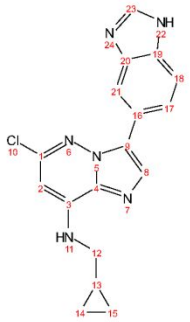

8

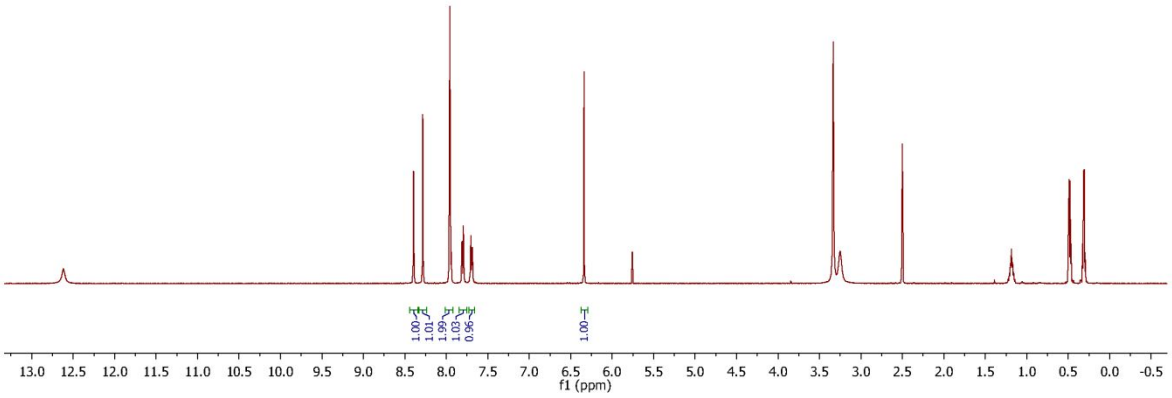

8; 13C NMR

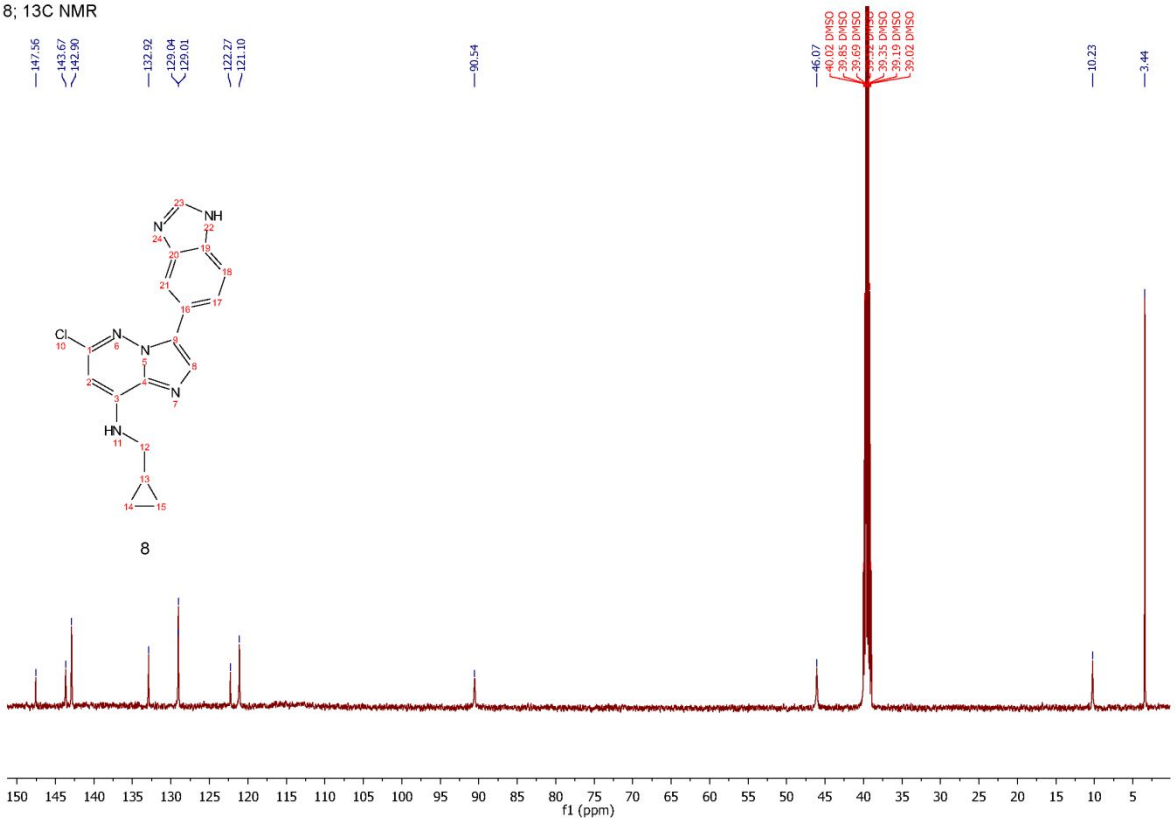

8

9; 1H NMR

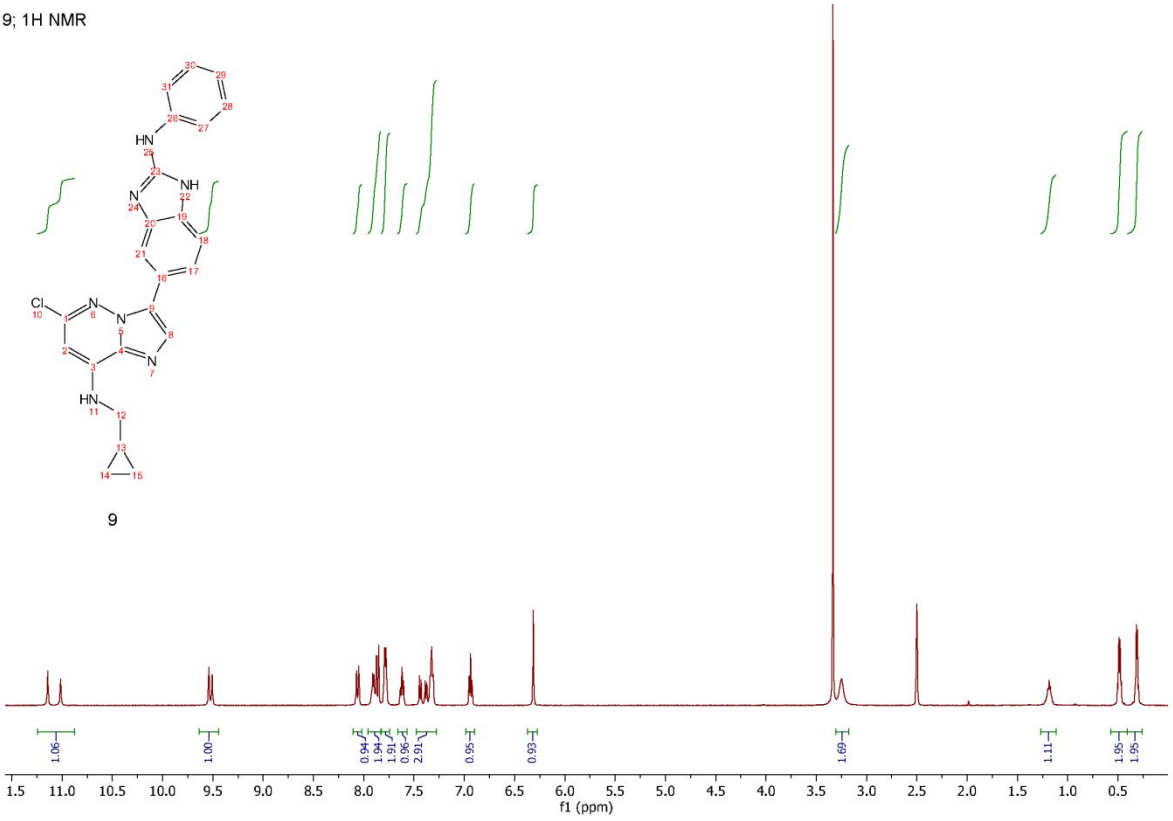

9

9; 13 C NMR

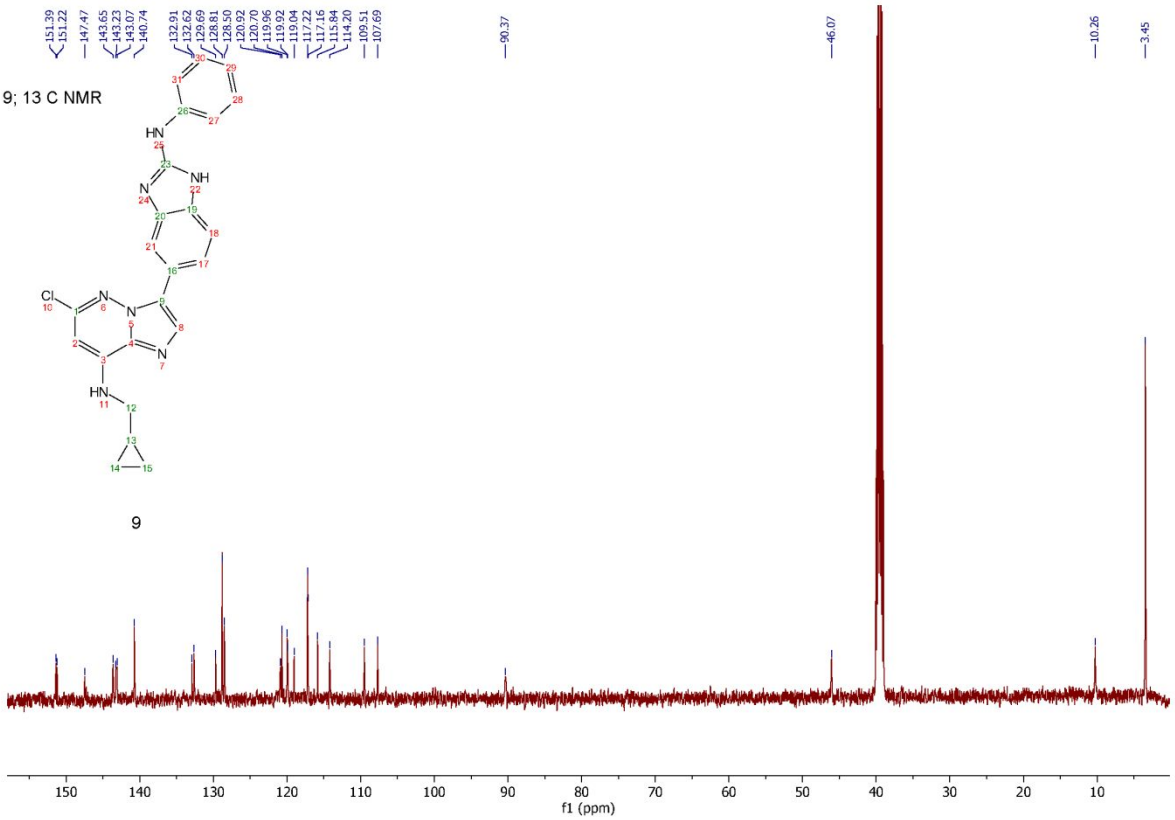

9

10; 1H NMR

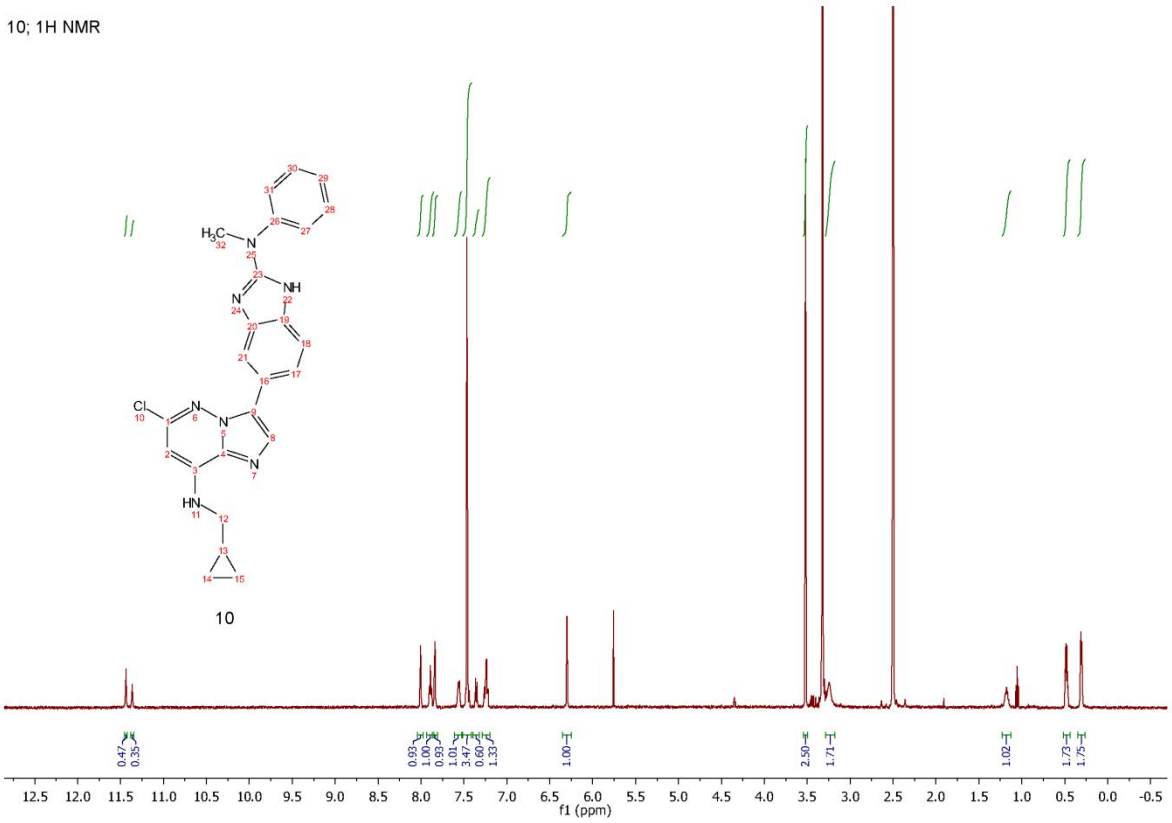

10; 13C NMR

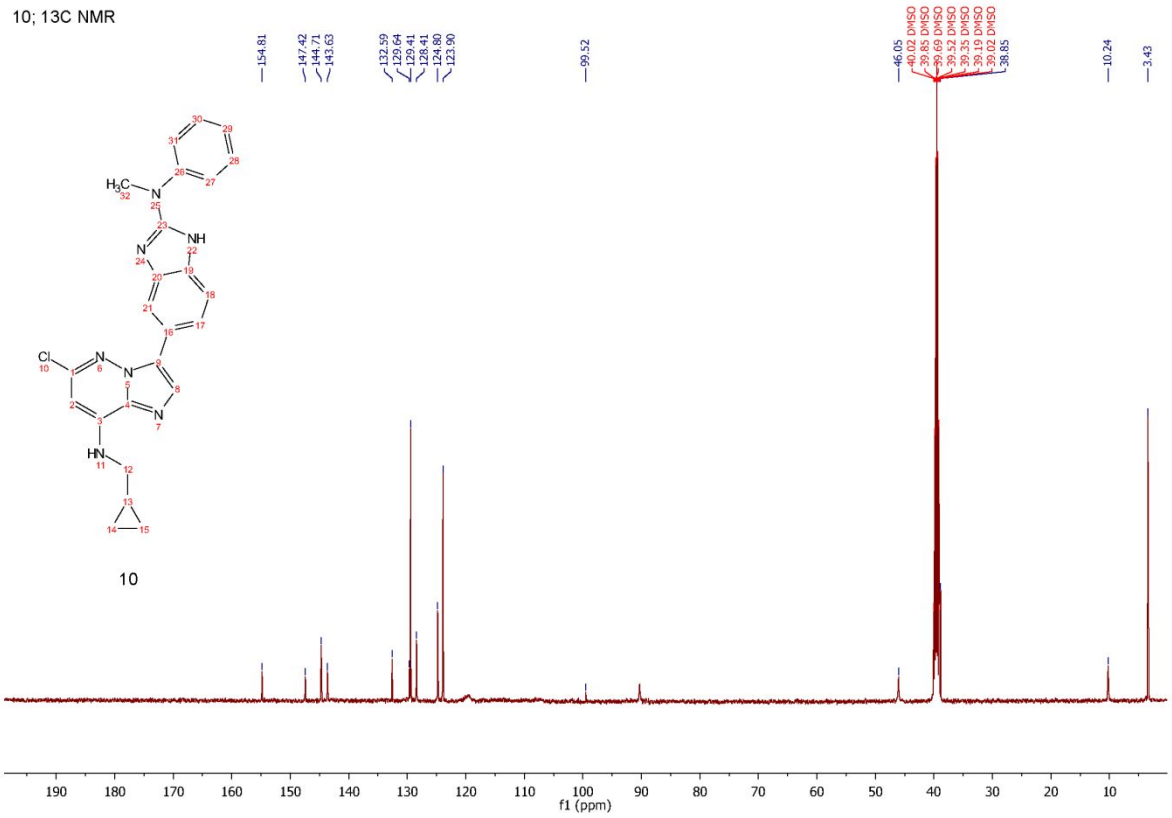

11; 1H NMR

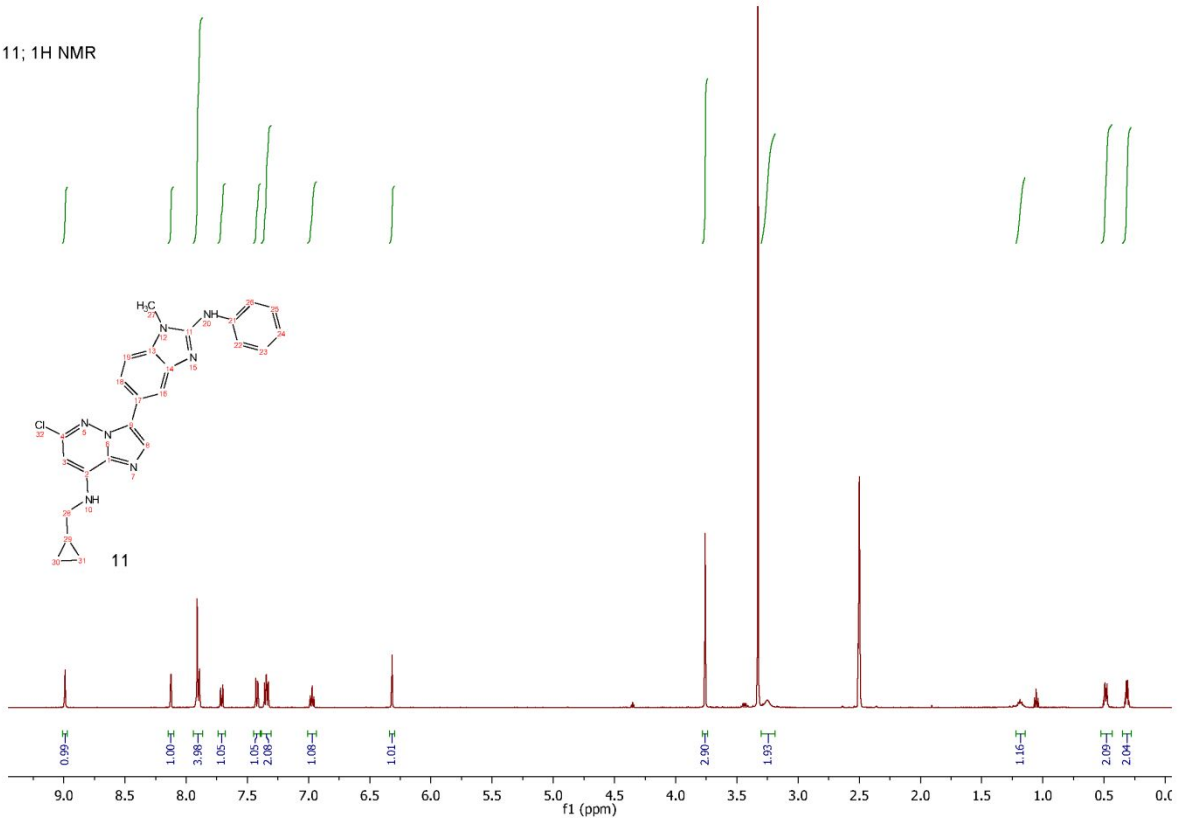

11

11; 13C NMR

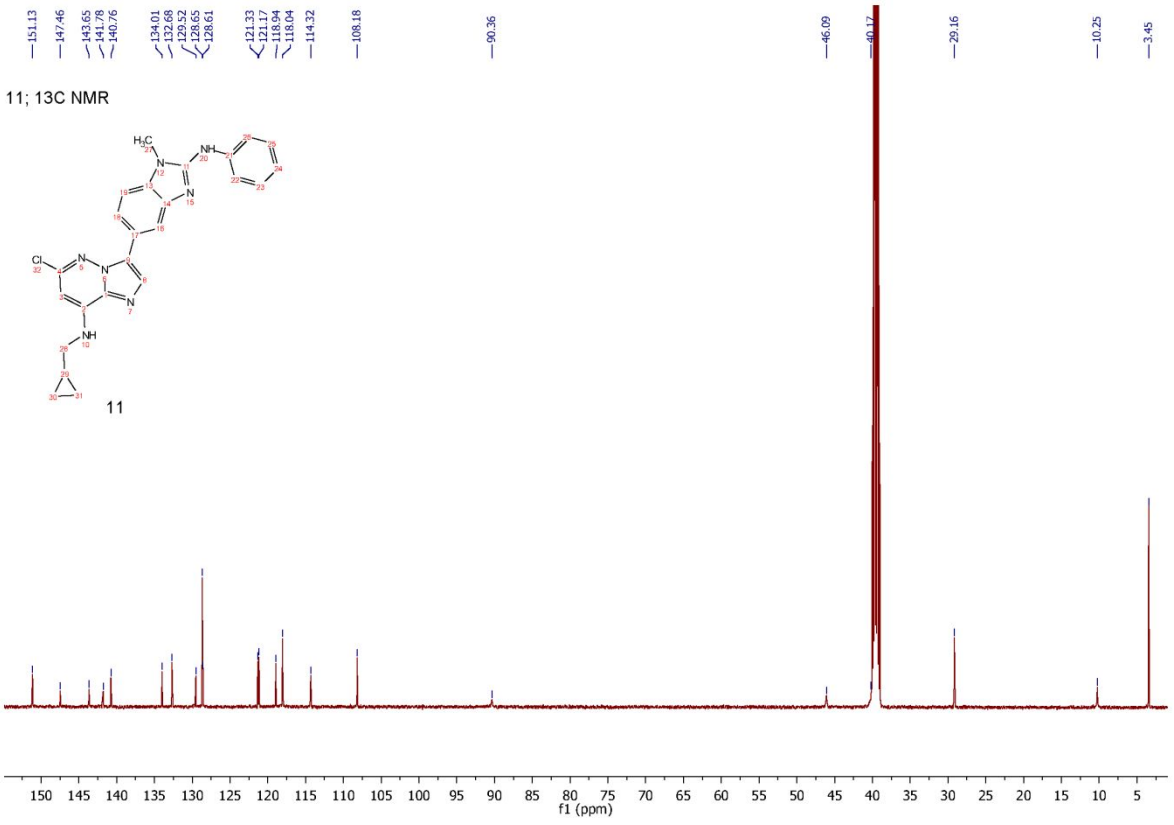

11

12; 1H NMR

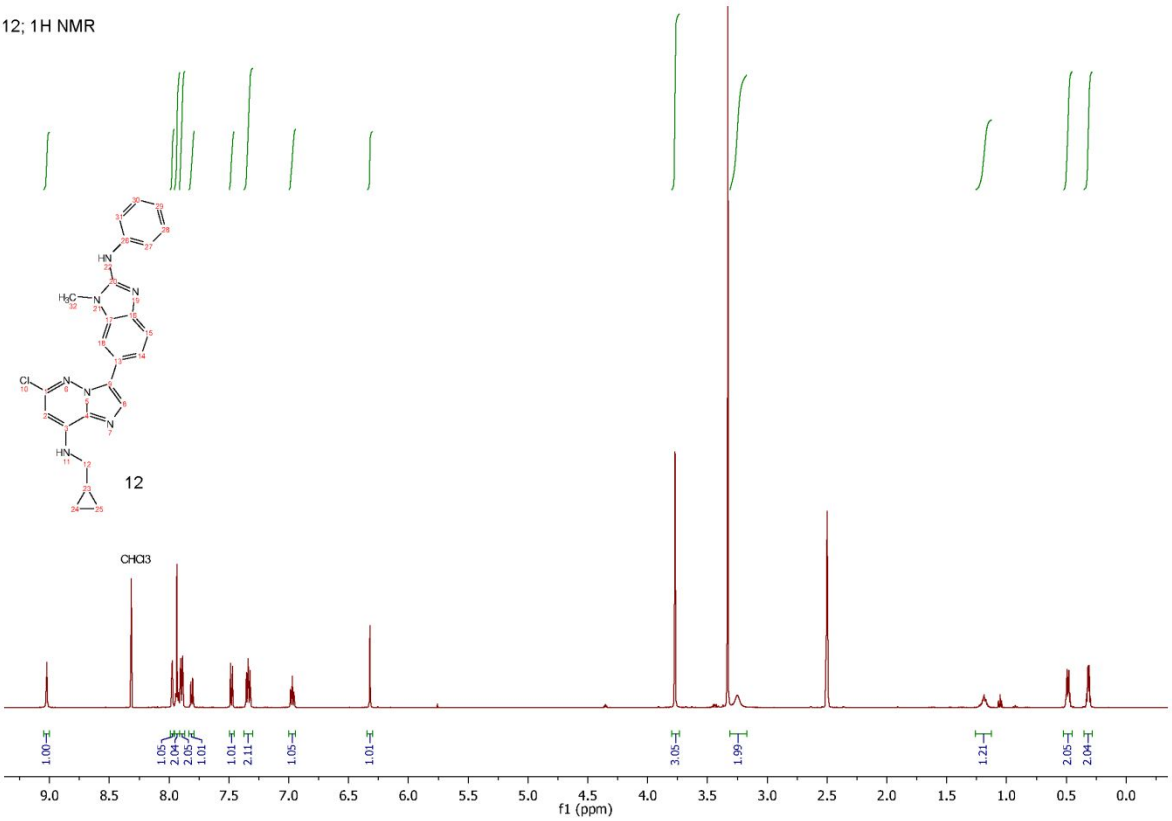

12; 13C NMR

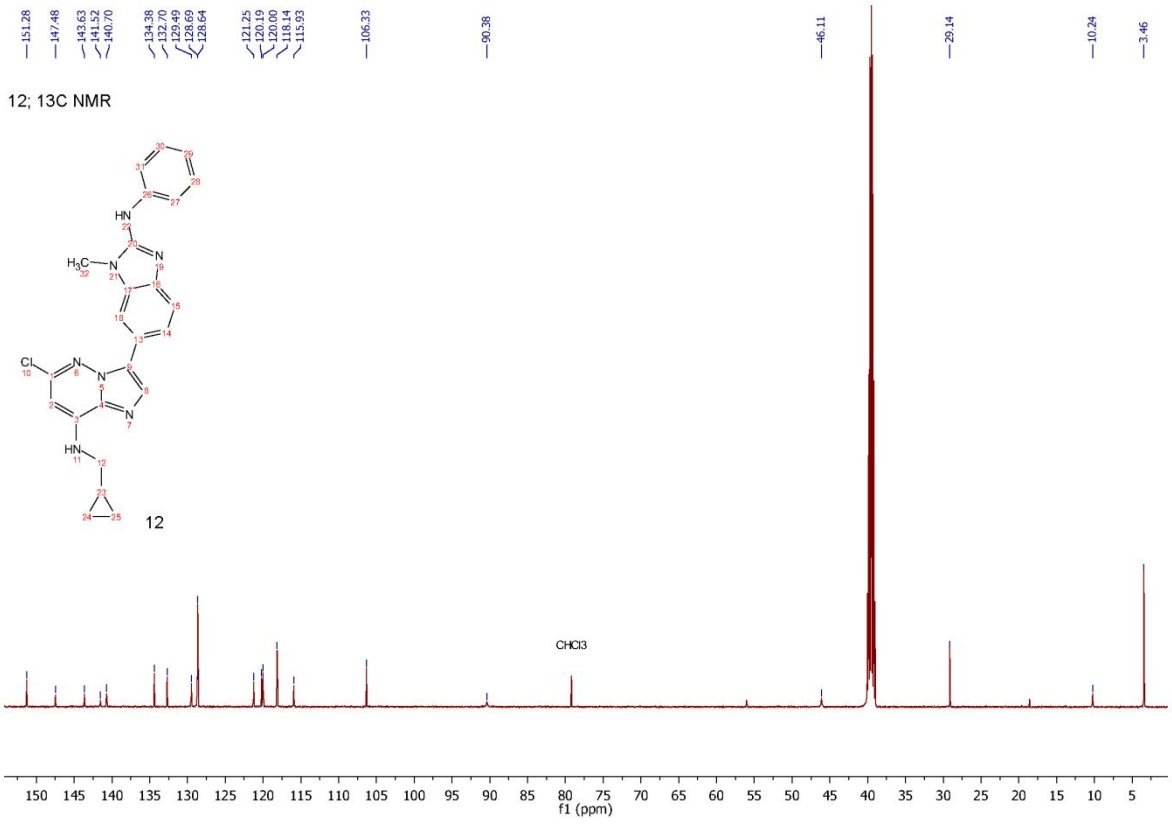

19; 1H NMR

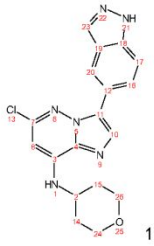

19

19; 13C NMR

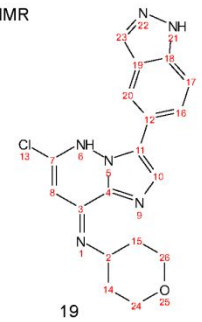

19

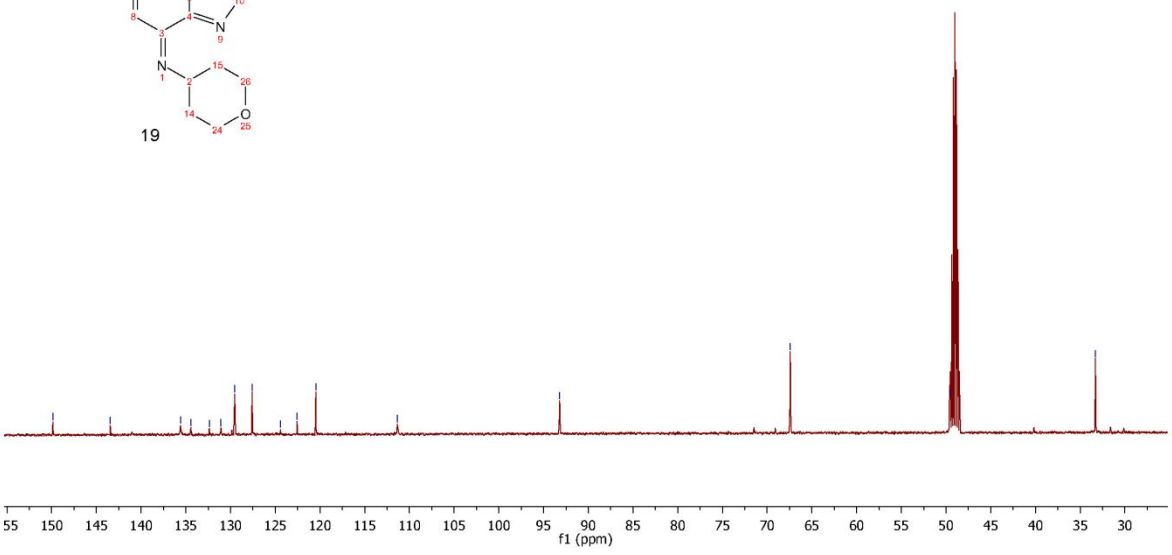

20; 1H NMR

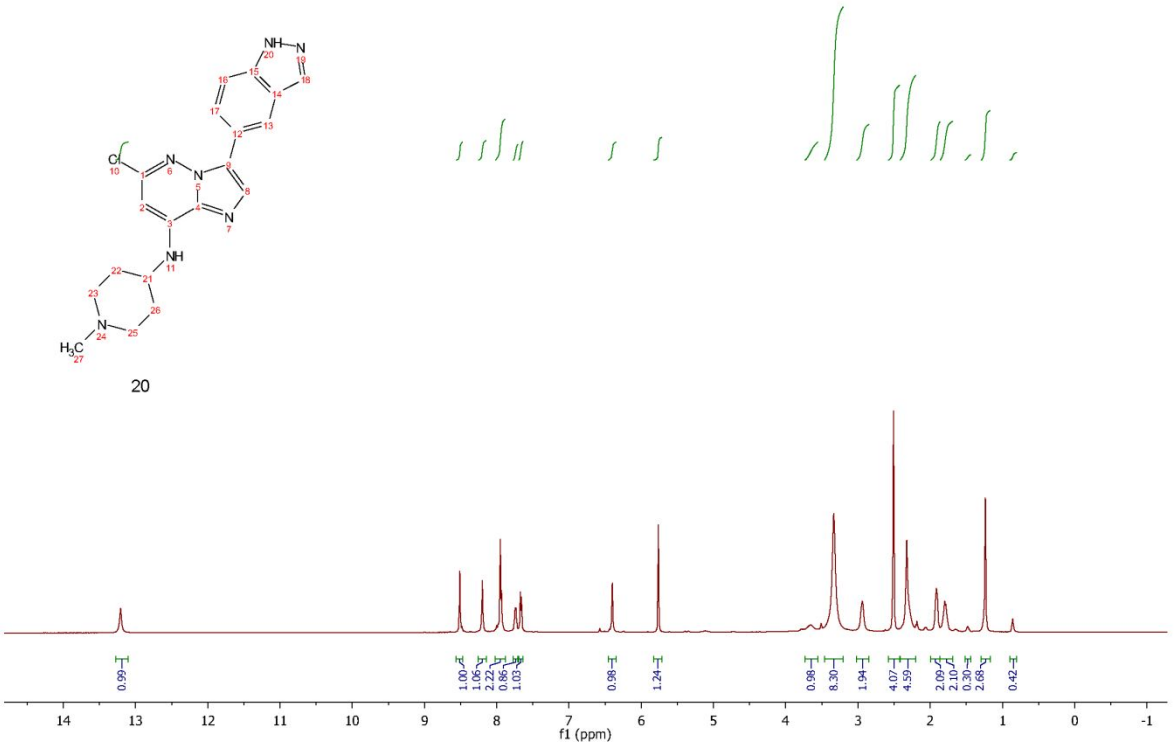

20; 13C NMR

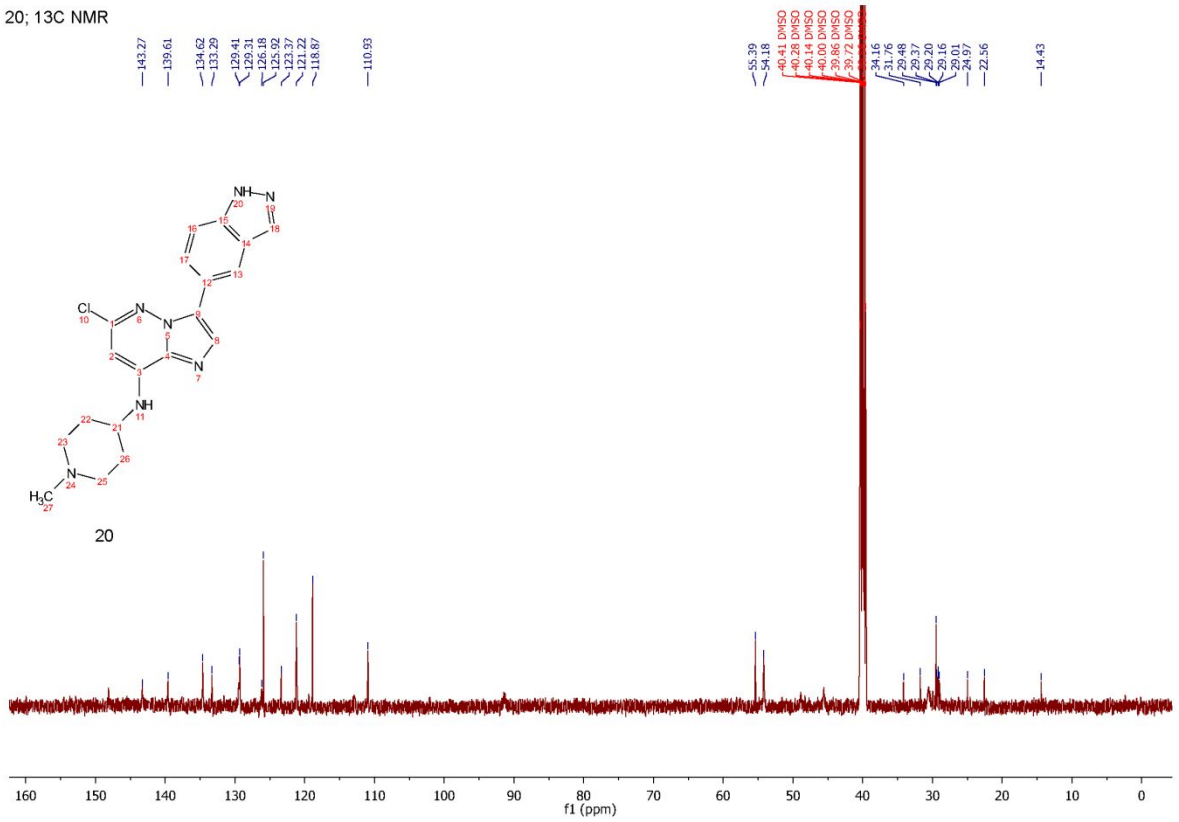

21; 1H NMR

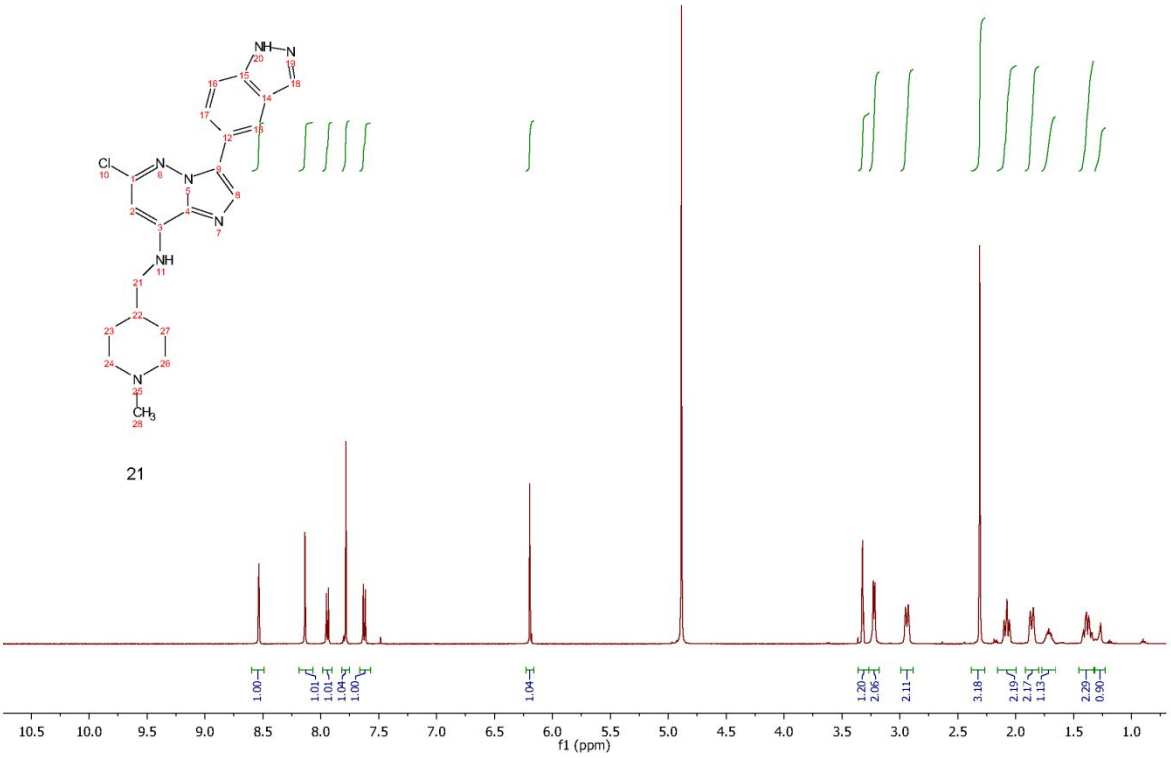

21; 13C NMR

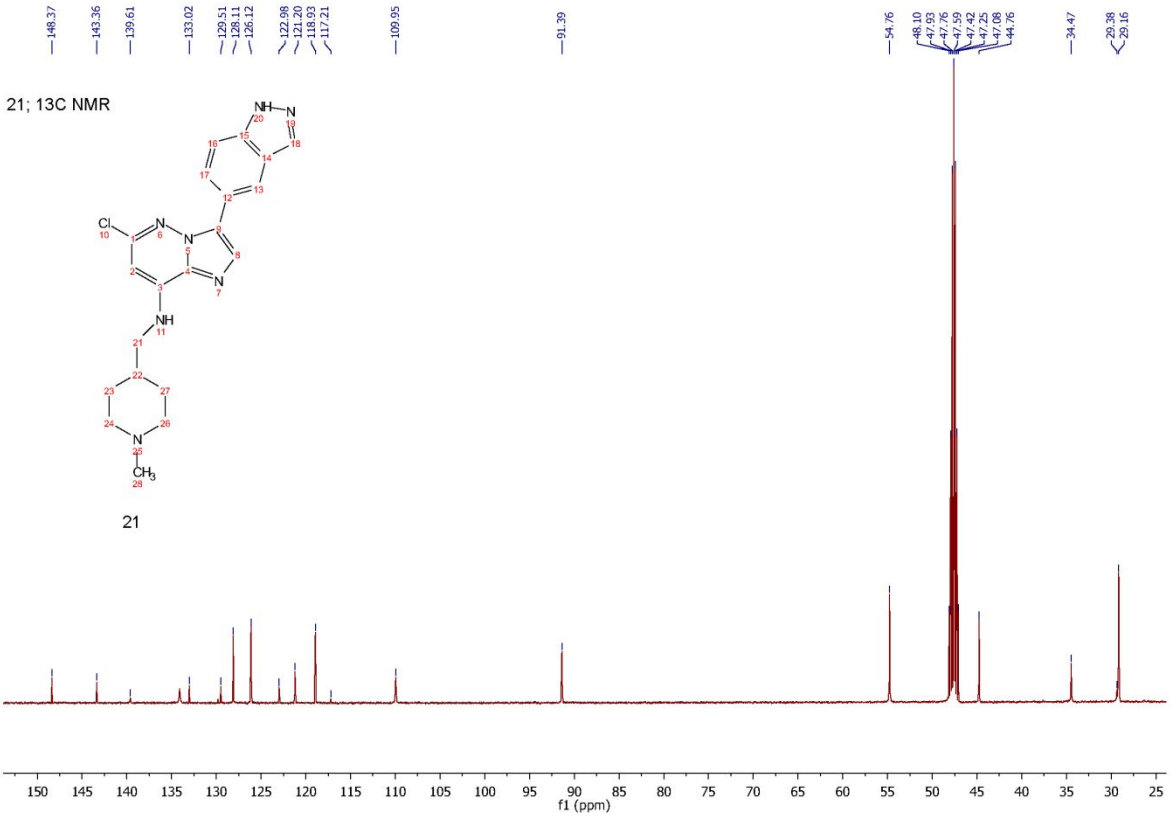

22; 1H NMR

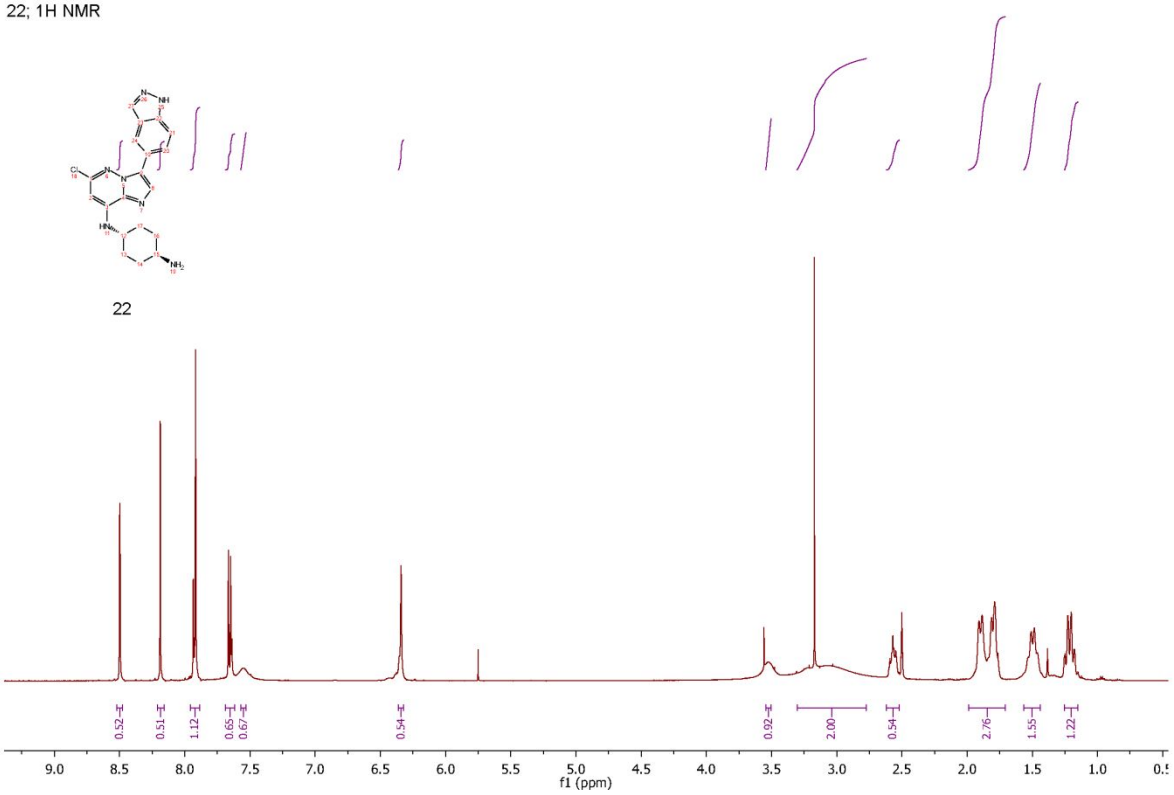

22; 13C NMR

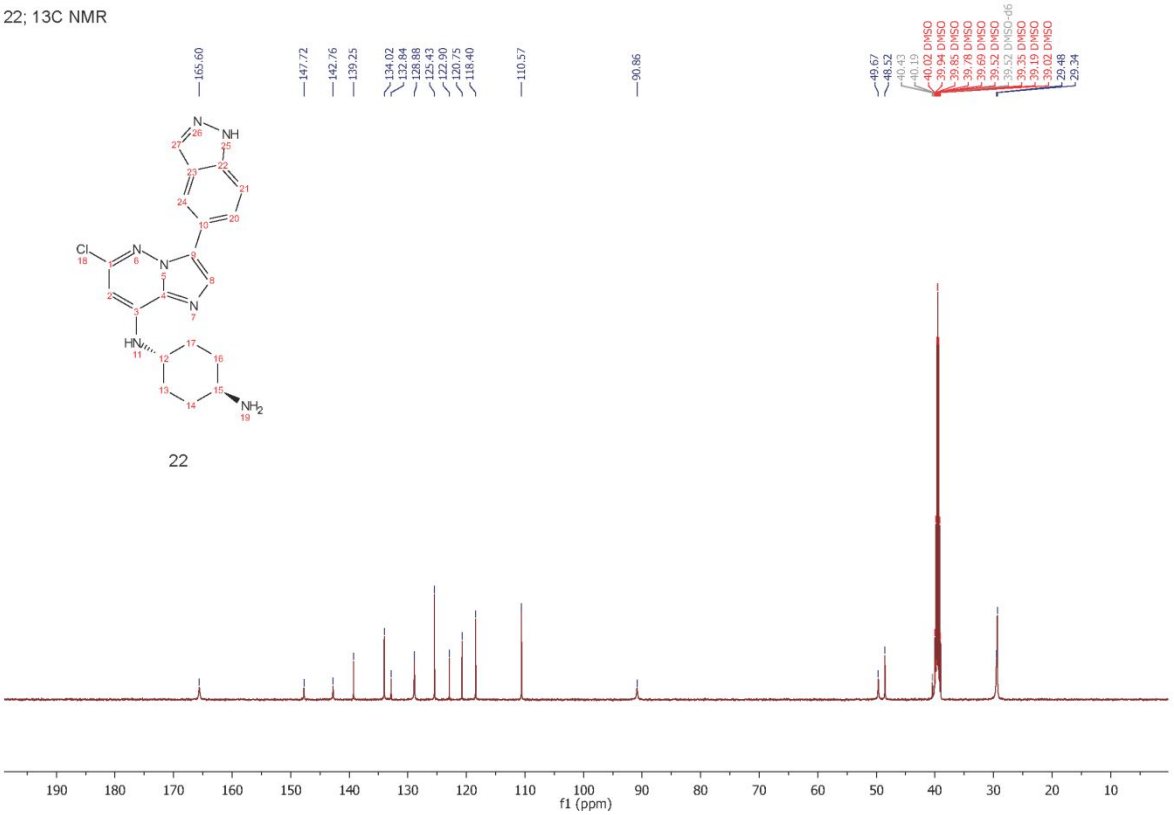

23; 1H NMR

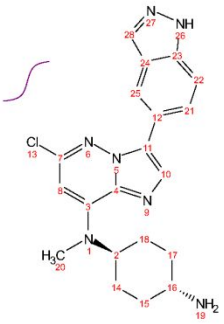

23

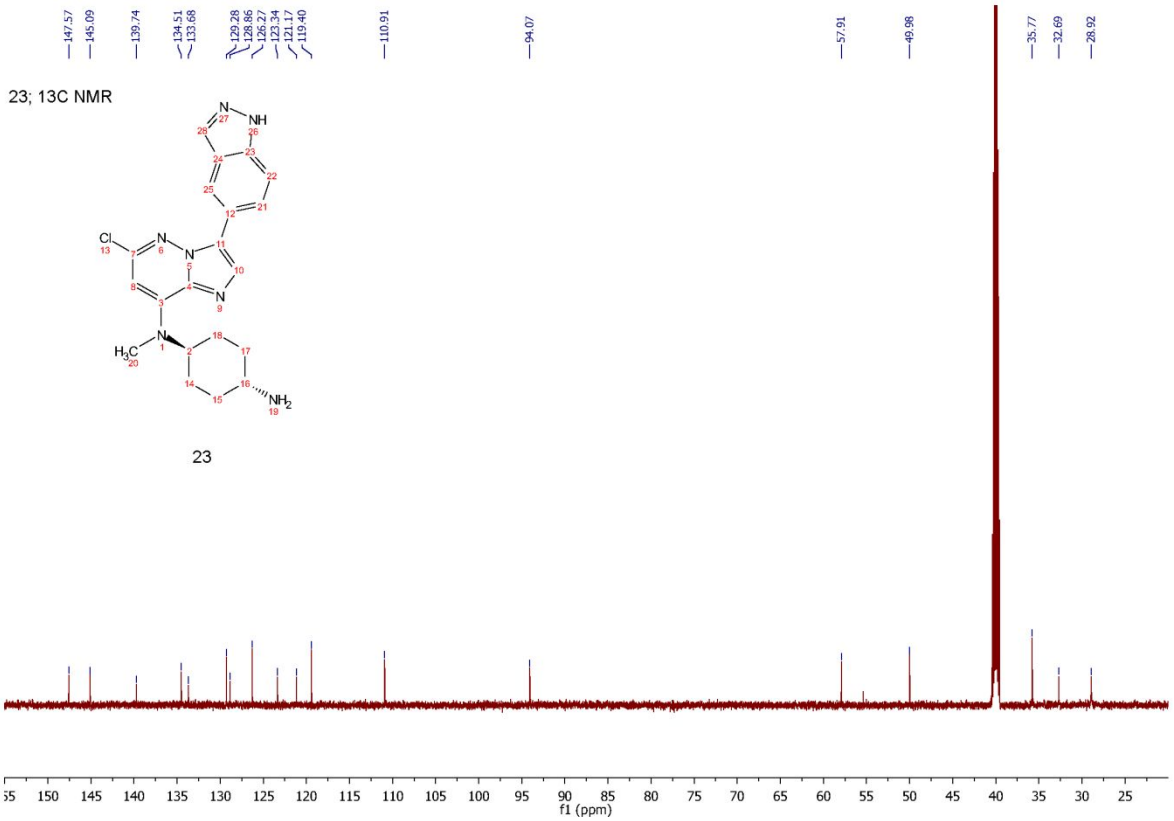

23; 13C NMR

23

24; 1H NMR

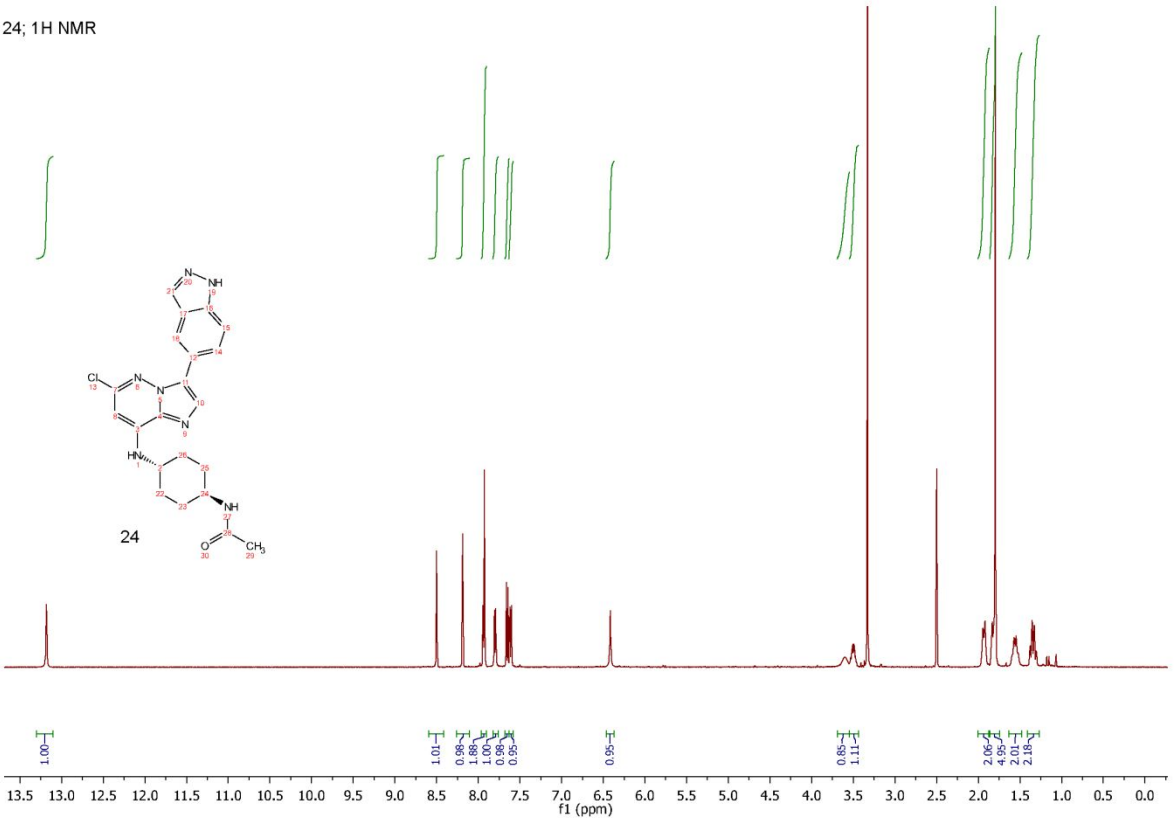

24; 13C NMR

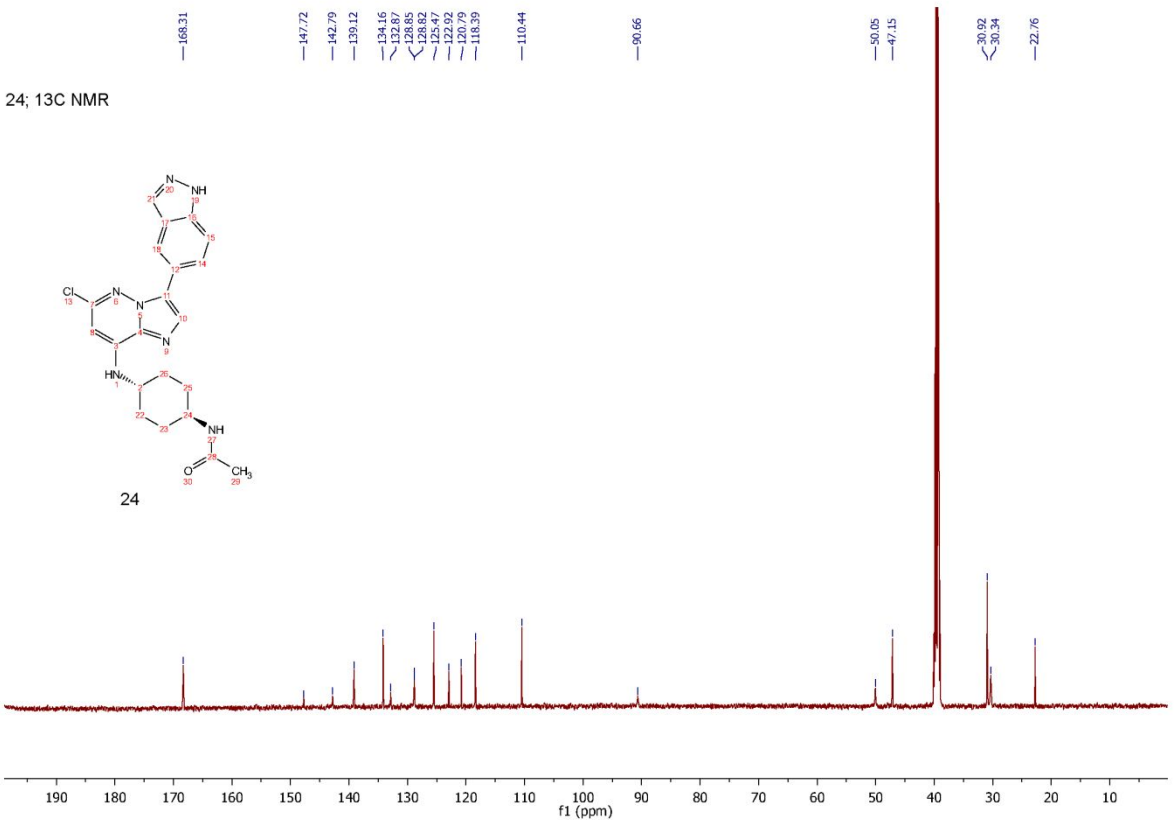

25; 1H NMR

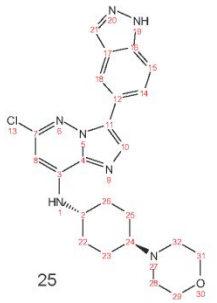

25

25; 13C NMR

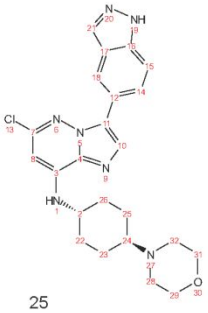

25

26; 1H NMR

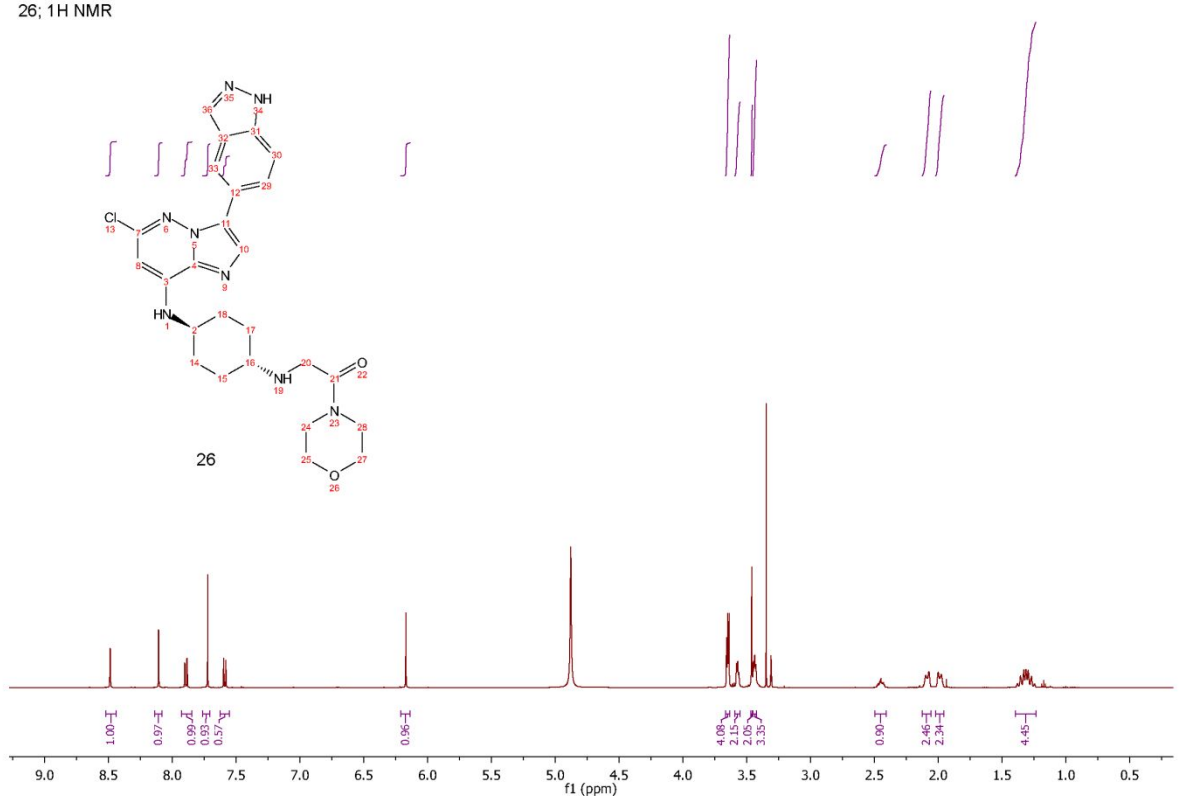

26; 13C NMR

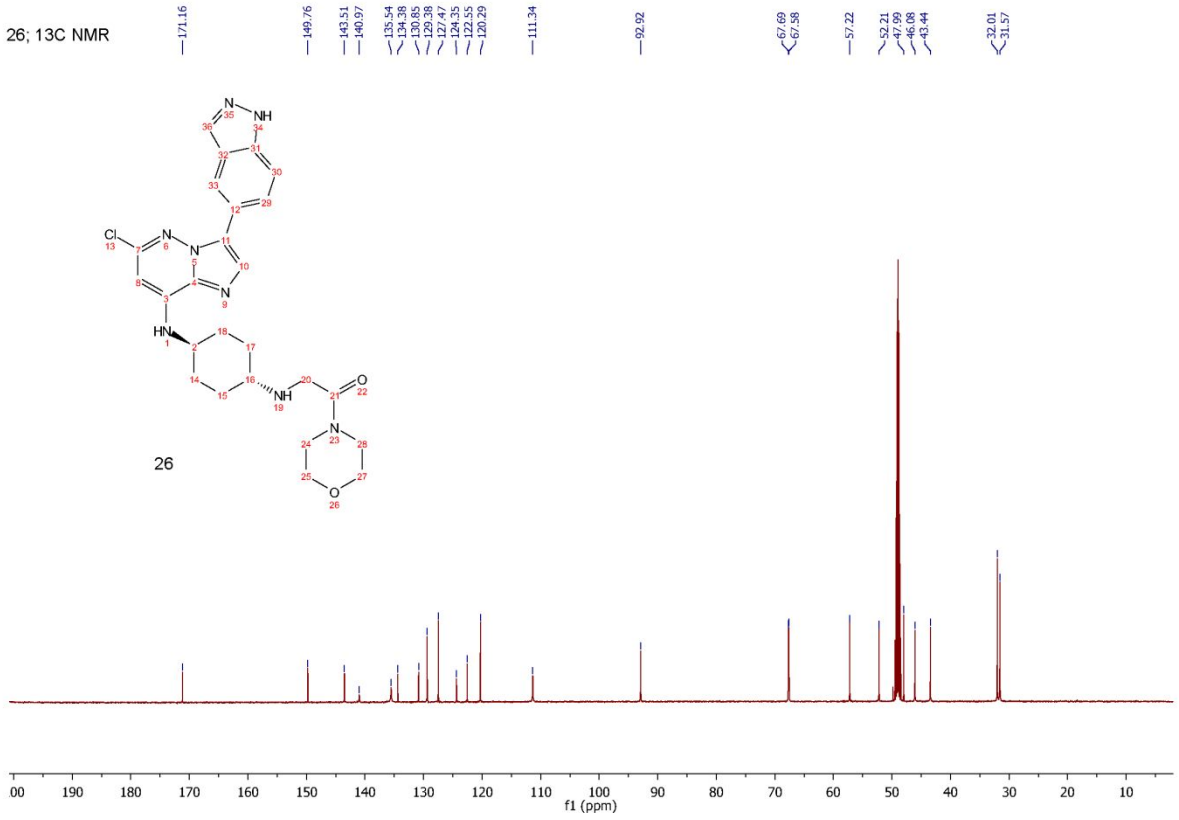

27; 1H NMR

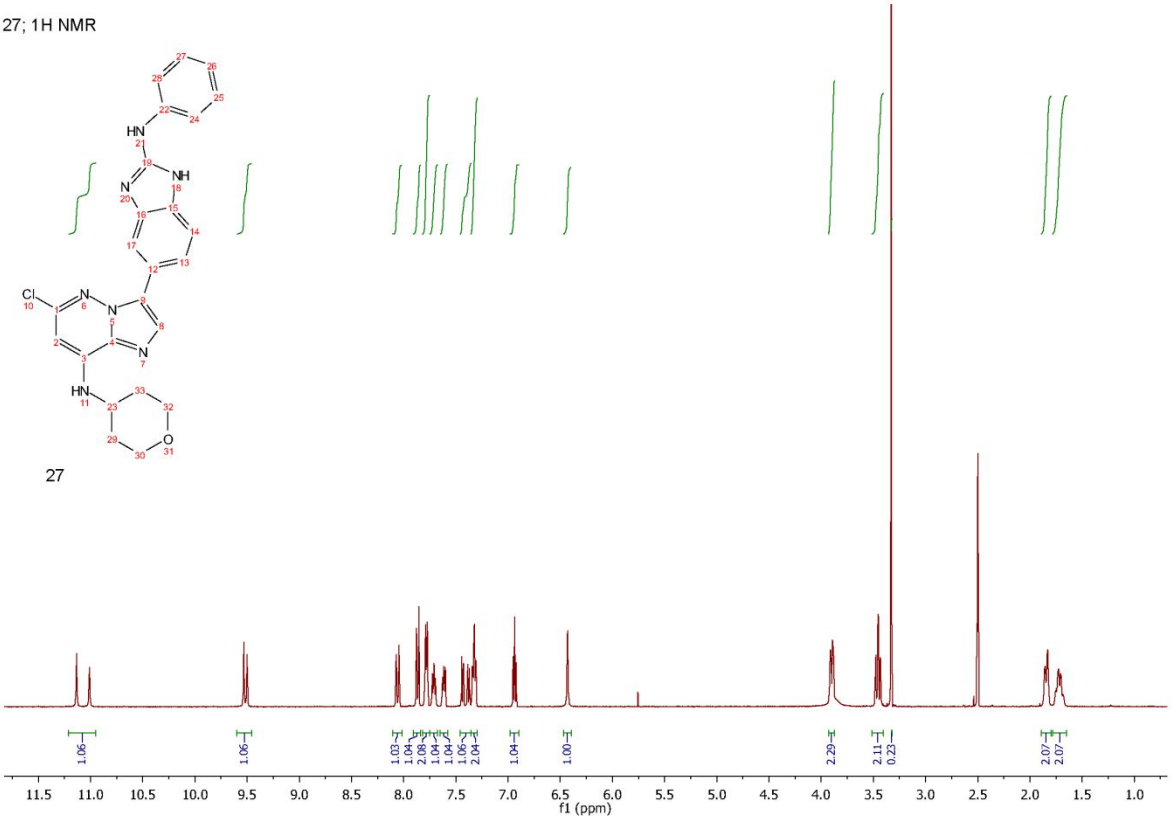

27; 13C NMR

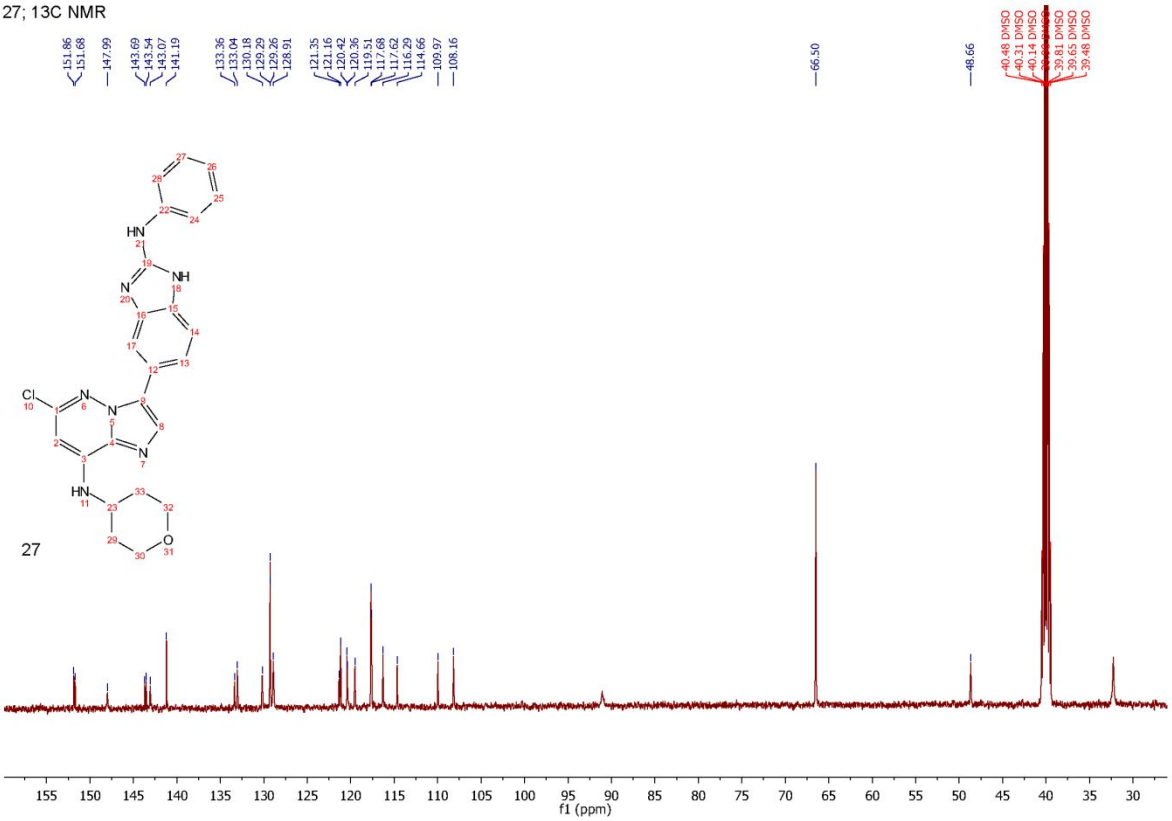

28; 1H NMR

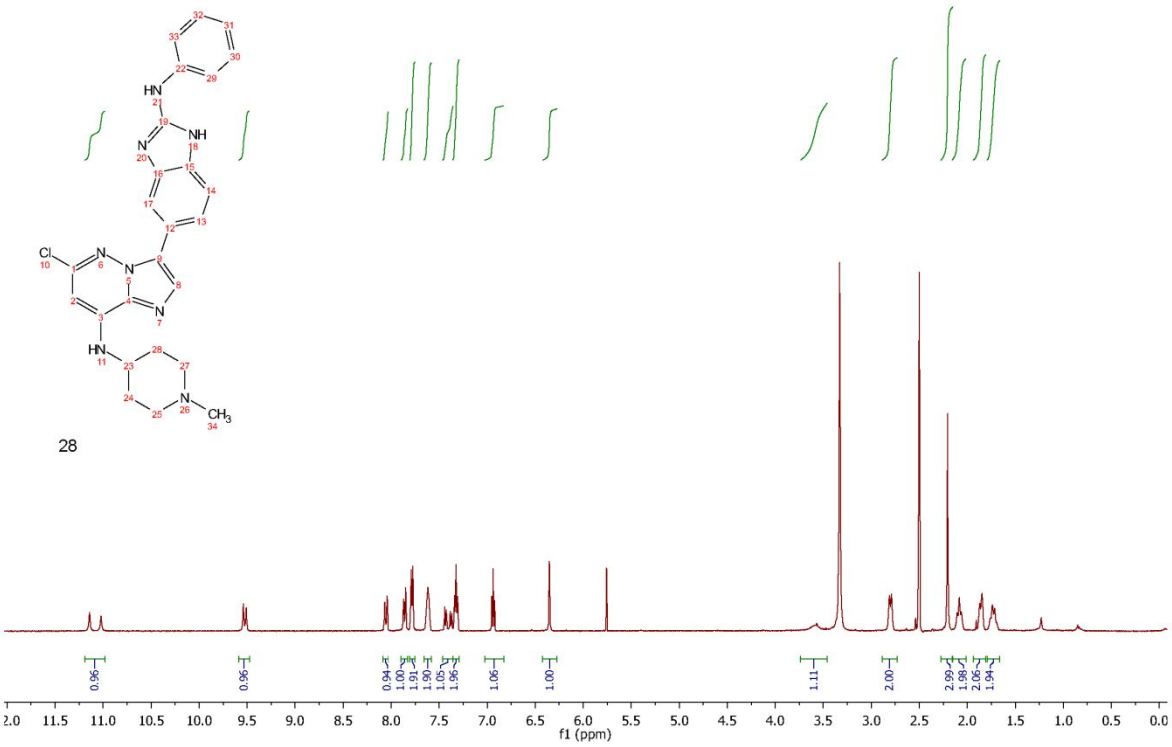

28; 13C NMR

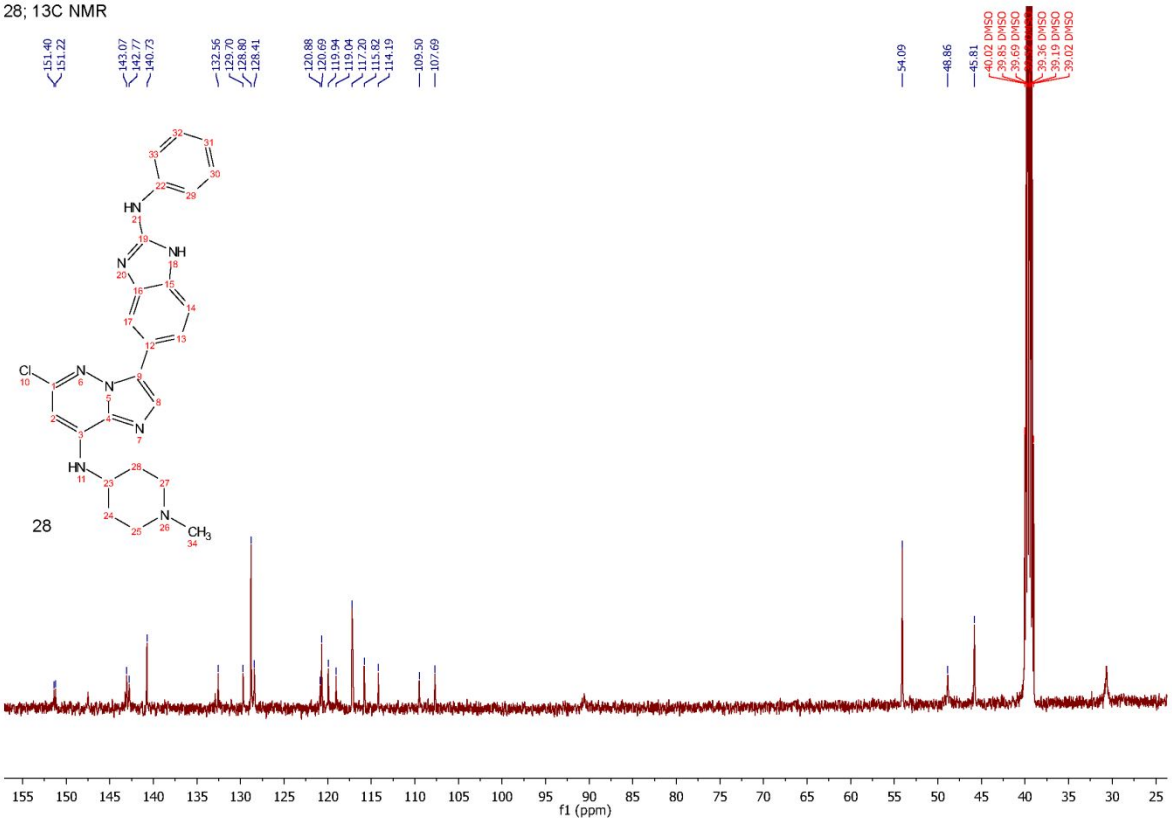

29; 1H NMR

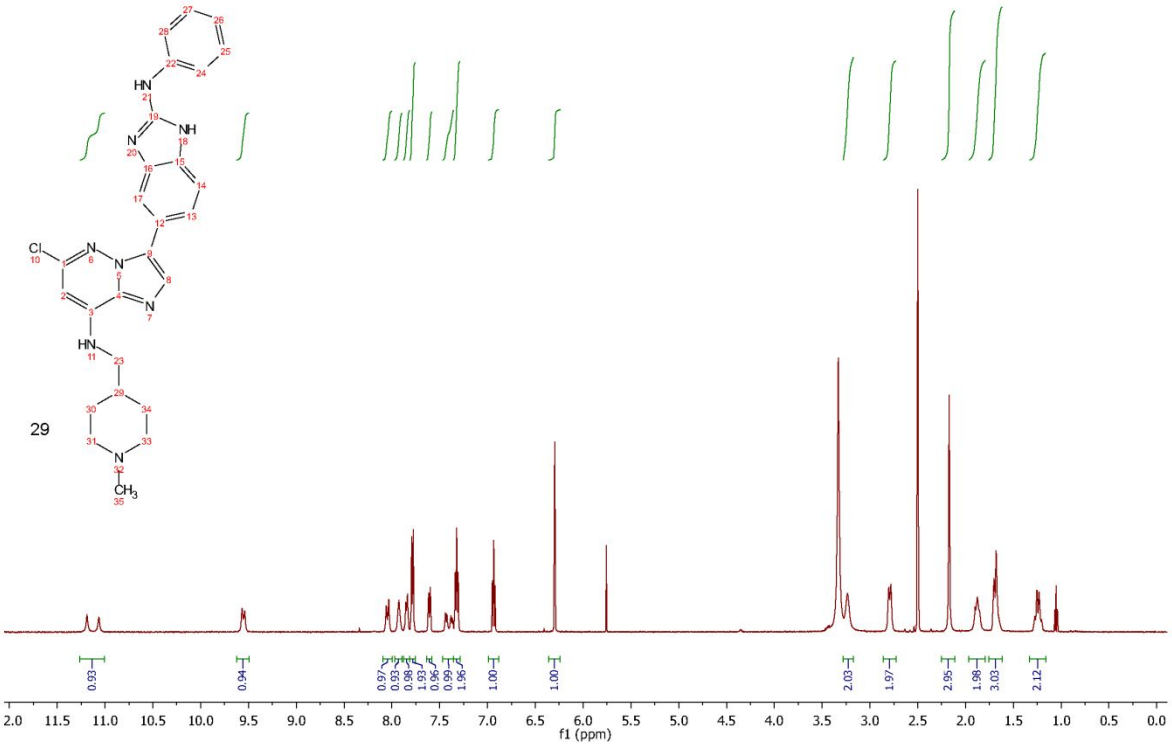

29; 13C NMR

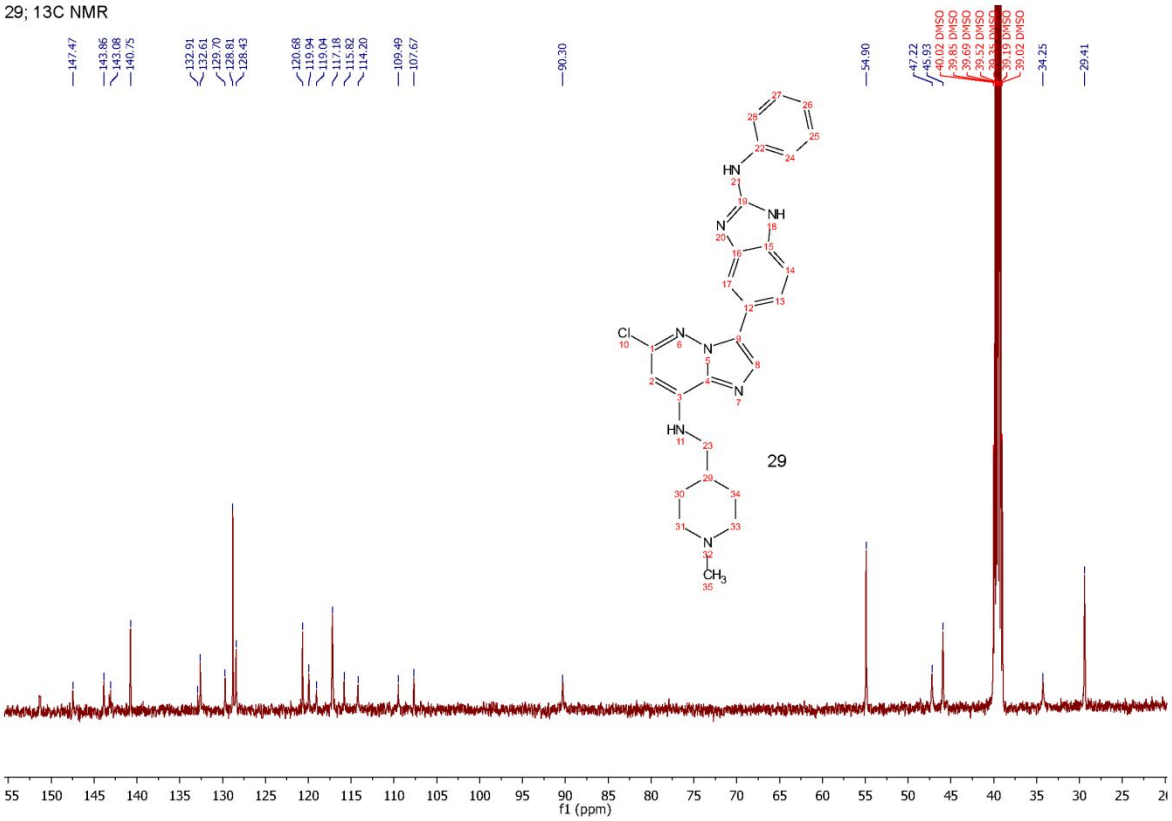

30; 1H NMR

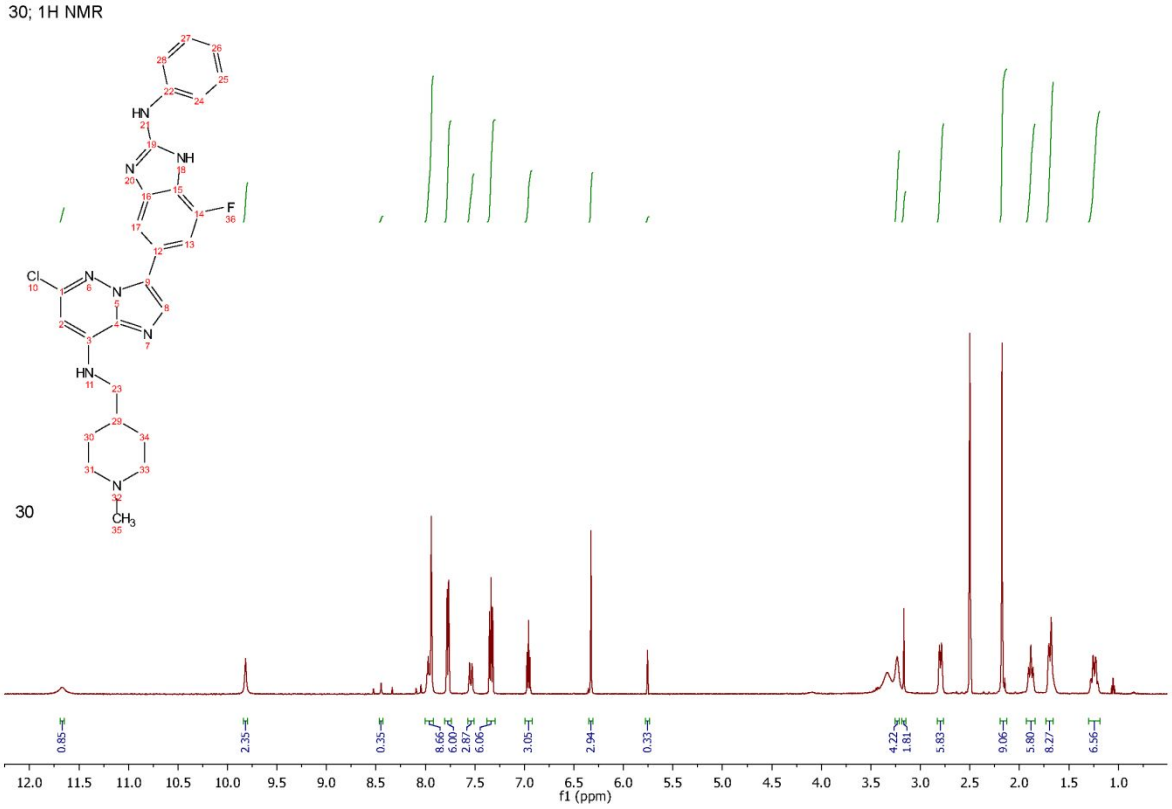

30; 13C NMR

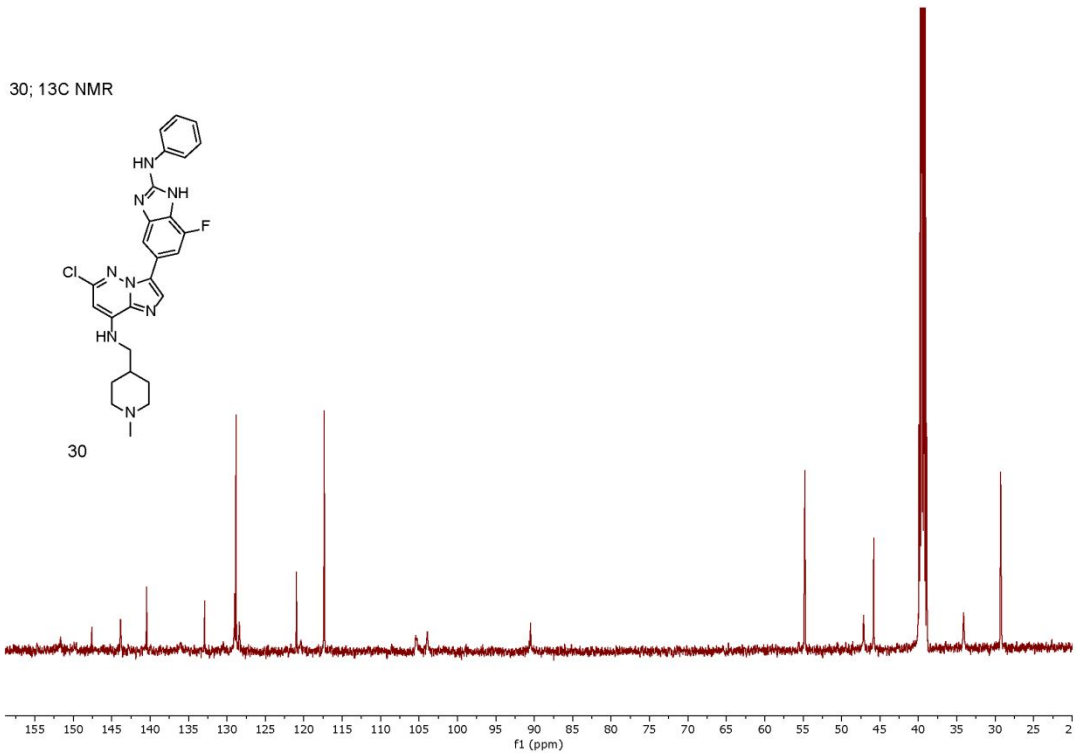

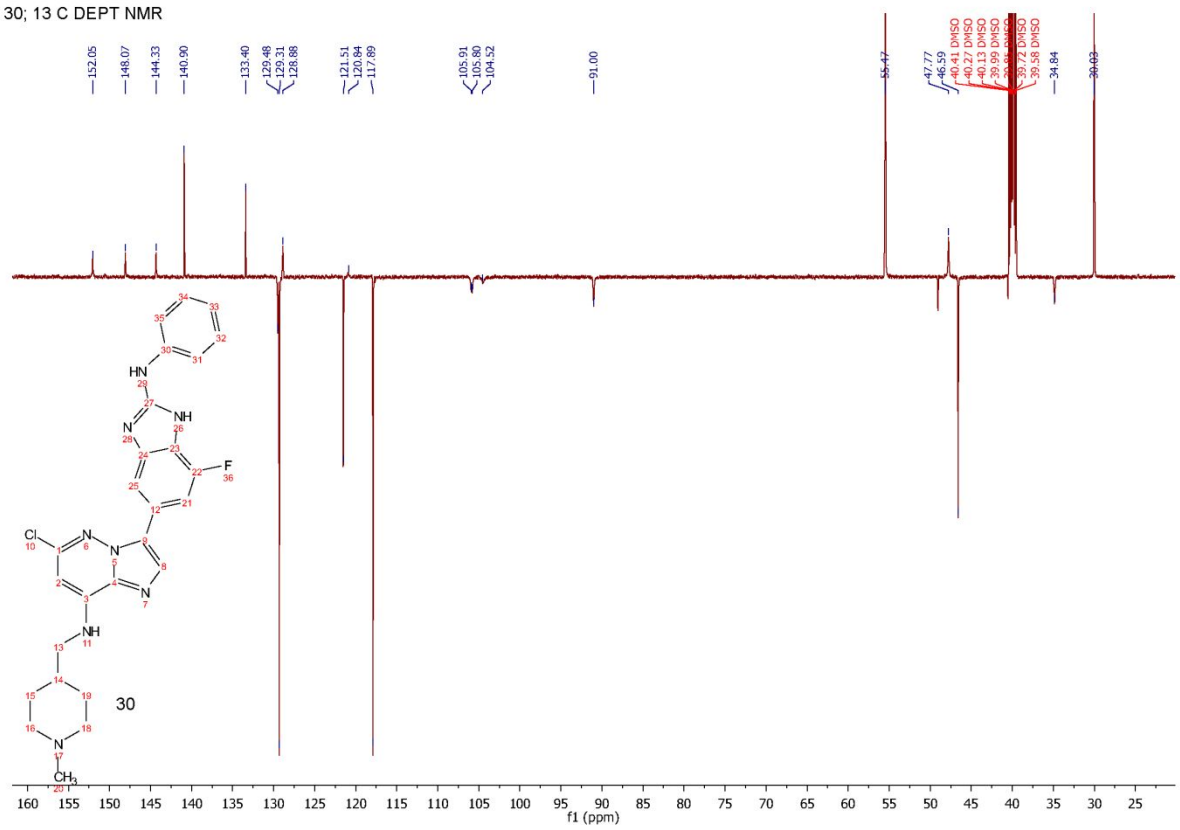
30; 13 C DEPT NMR
152.05
148.07
144.33
140.90
133.40
129.48
129.31
128.88
121.51
120.84
117.89
105.91
105.80
104.52
91.00
55.47
47.77
46.59
40.41 DMSO
40.27 DMSO
40.13 DMSO
39.99 DMSO
39.72 DMSO
39.58 DMSO
34.84
30.03
30
f1 (ppm)

31; 1H NMR

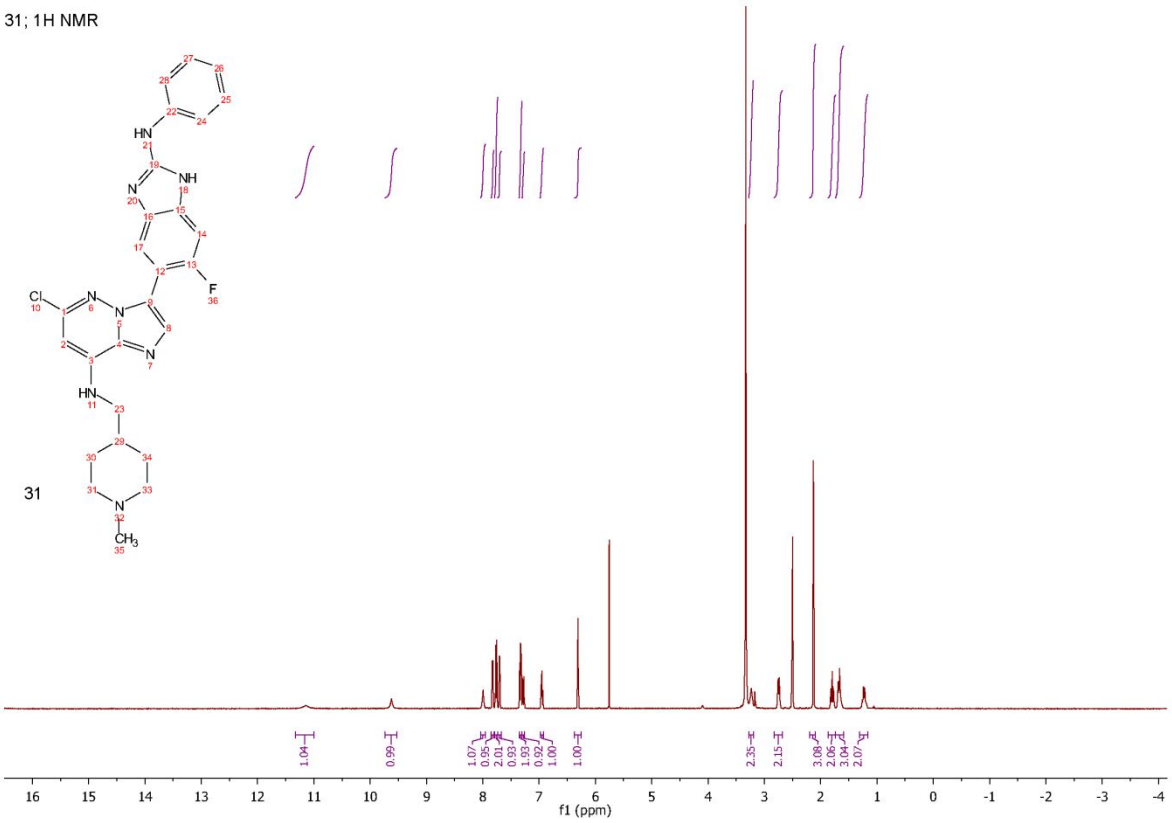

31; 13C NMR

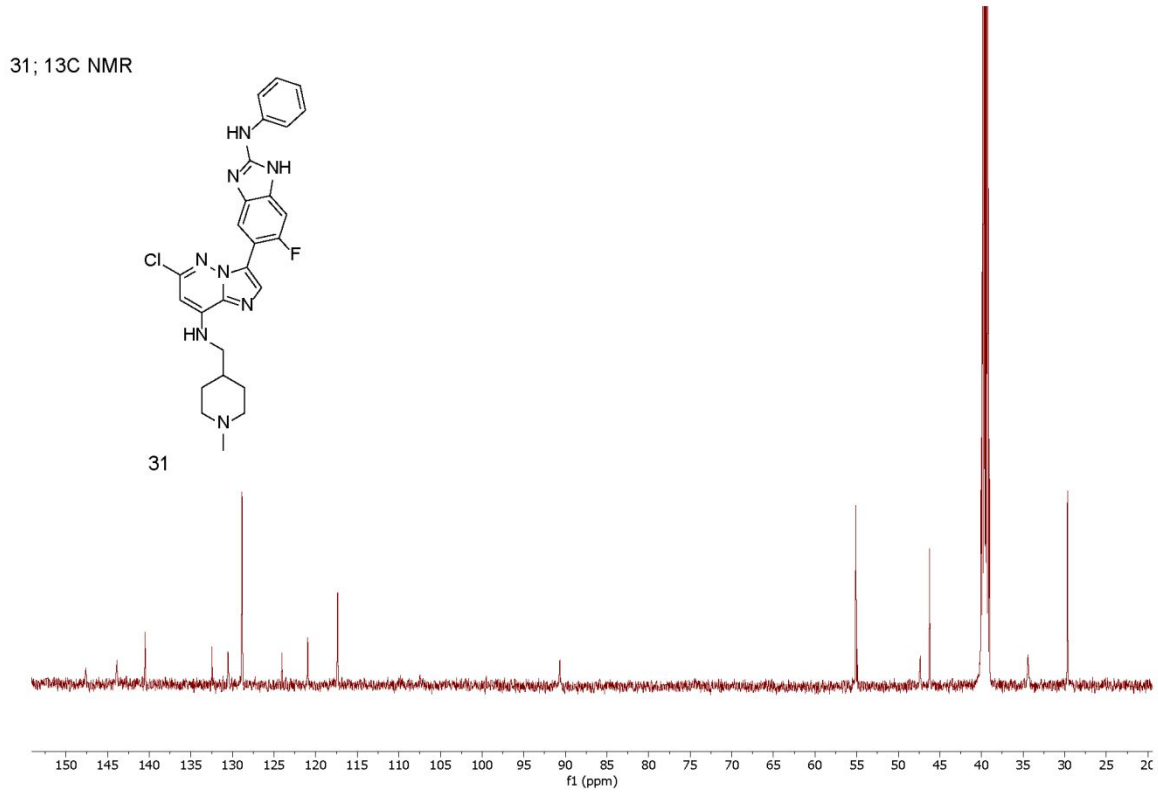

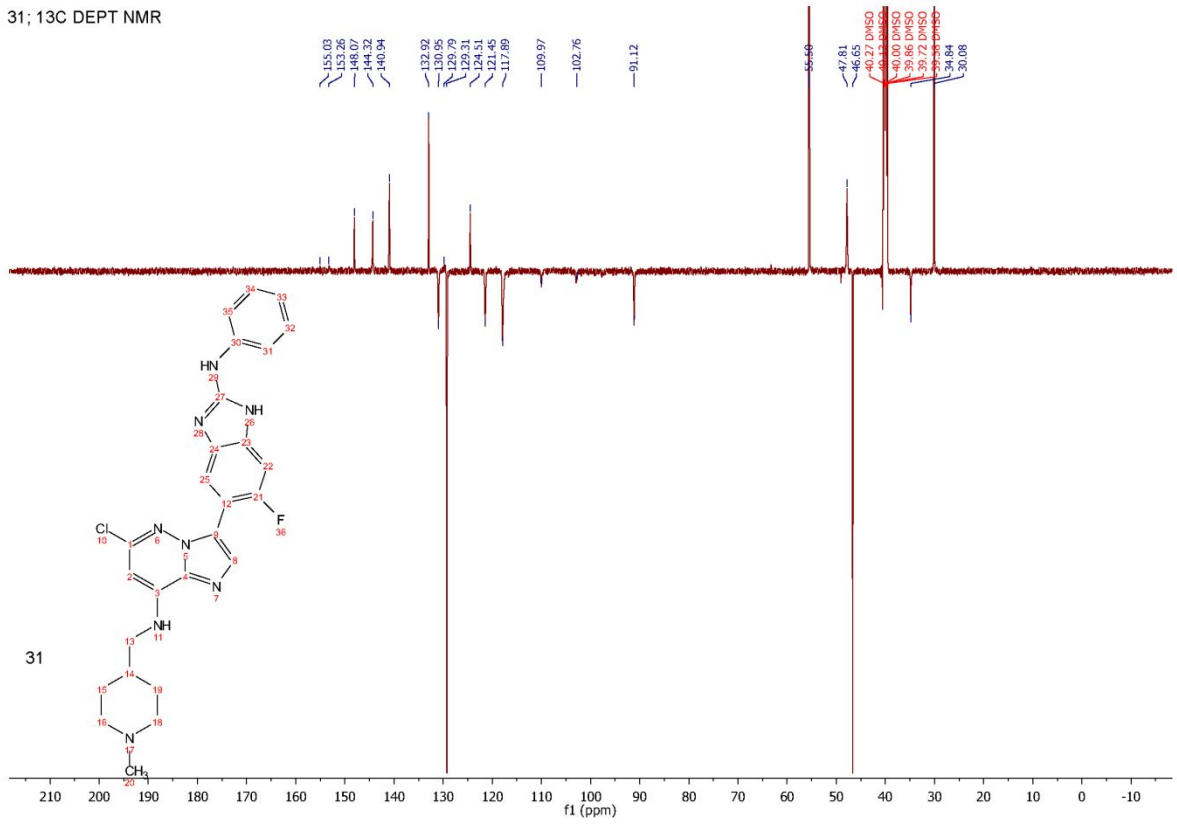
31; 13C DEPT NMR
155.03
153.26
148.07
144.32
140.94
132.92
130.95
129.79
129.31
124.51
121.45
117.89
109.97
102.76
91.12
55.60
47.81
46.65
40.27 DMSO
40.13 DMSO
40.00 DMSO
39.86 DMSO
39.72 DMSO
39.58 DMSO
34.84
30.08
31
f1 (ppm)

32; 1H NMR

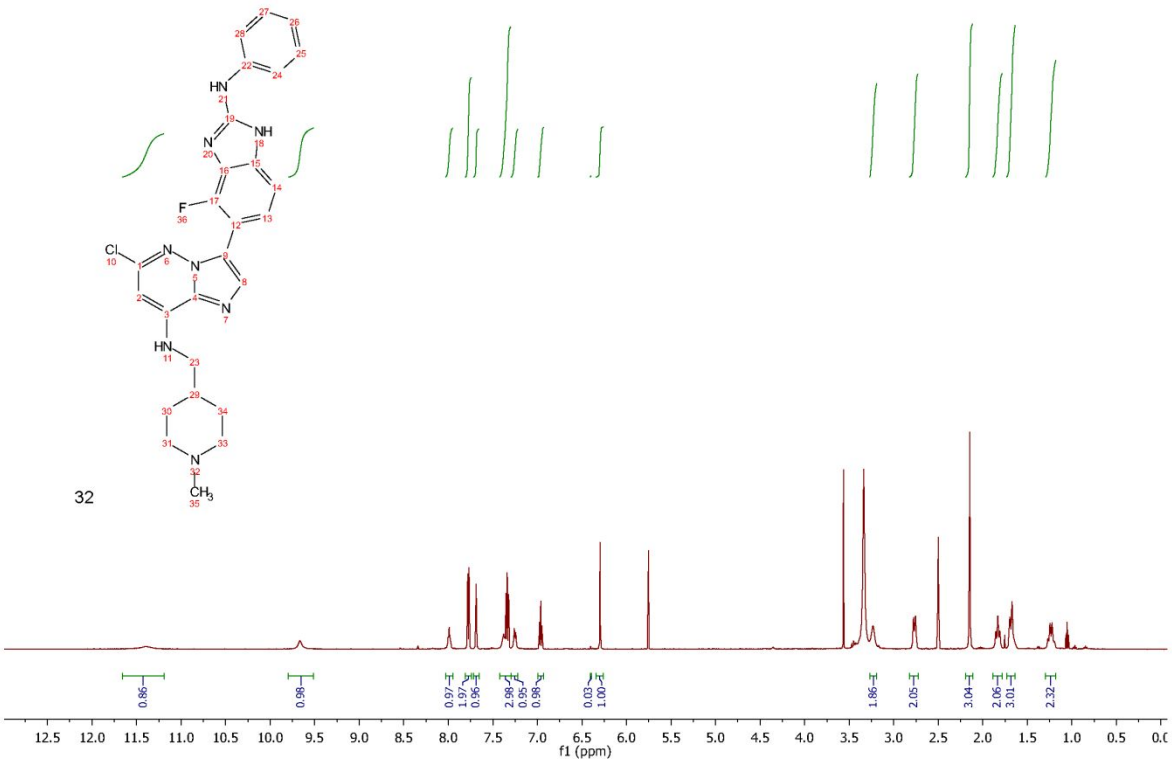

32; 13C NMR

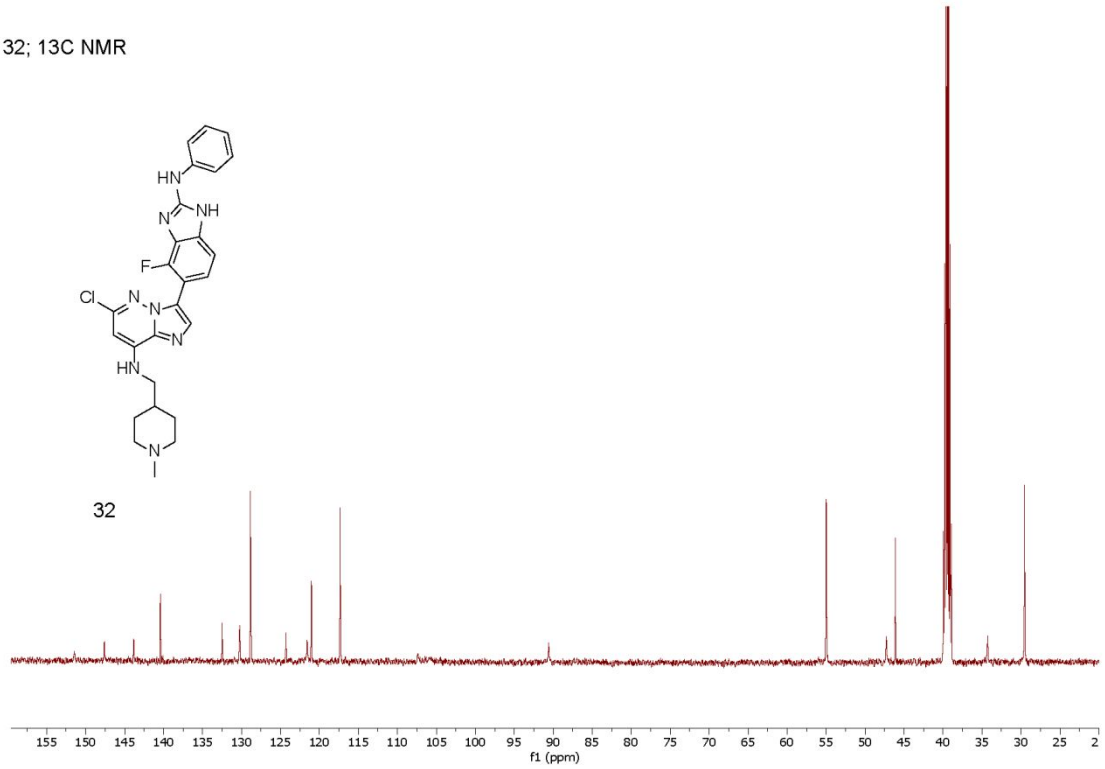

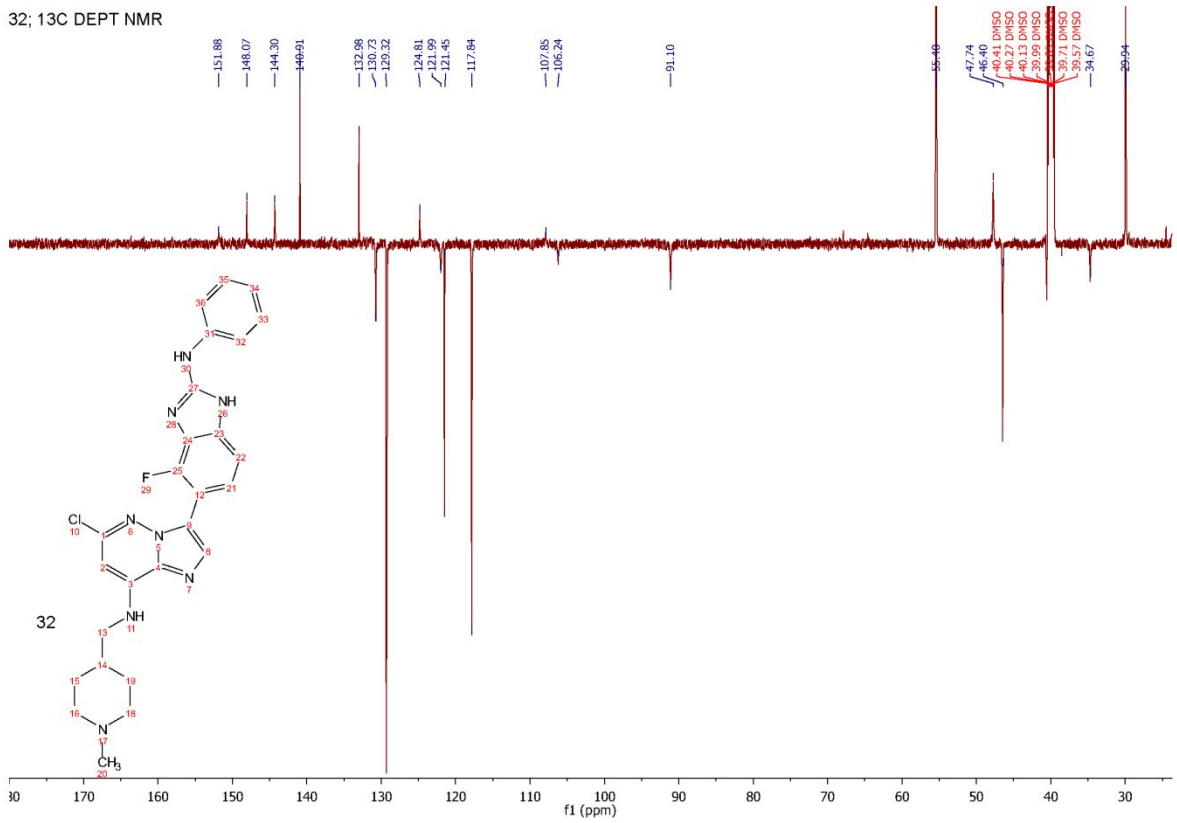
32; 13C DEPT NMR
151.88
148.07
144.30
140.91
132.98
130.73
129.32
124.81
121.99
121.45
117.84
107.85
106.24
91.10
55.48
47.74
46.40
40.41 DMSO
40.27 DMSO
40.13 DMSO
39.99 DMSO
39.71 DMSO
39.57 DMSO
34.67
29.94
32
f1 (ppm)

33; 1H NMR

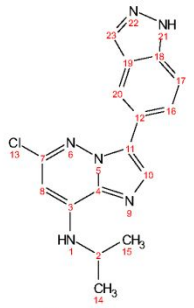

33

33; 13C NMR

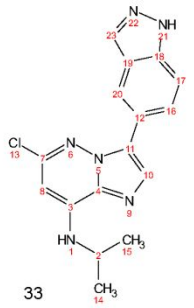

33

24. Copies of HPLC traces for test compounds **2**, **5** – **12**, **19** – **33.**

Compound **2**

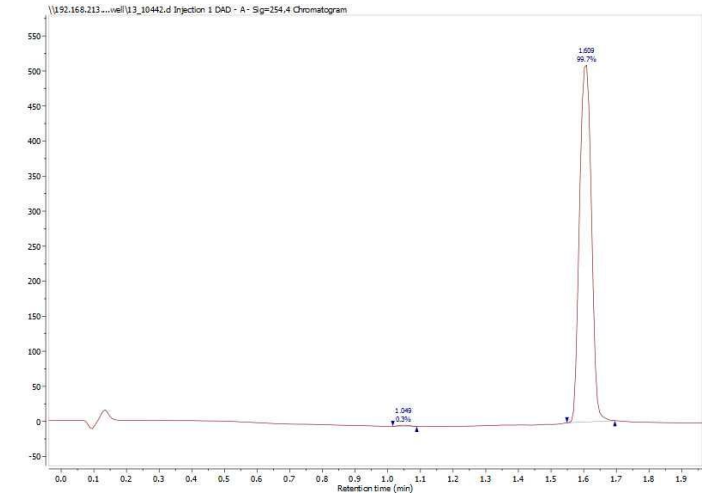

Compound **5**

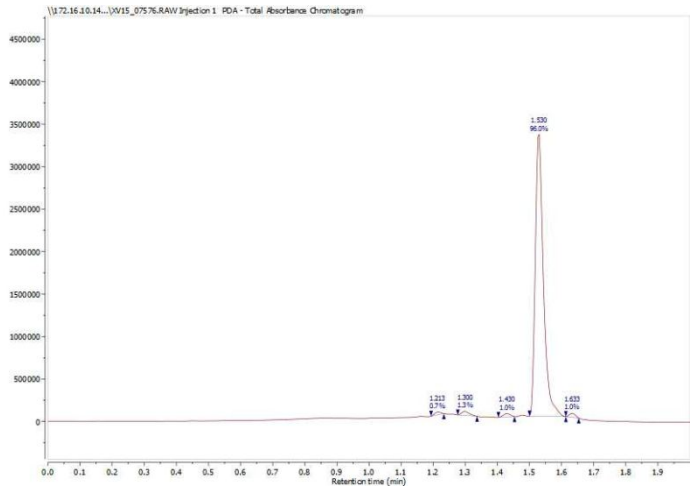

Compound **6**

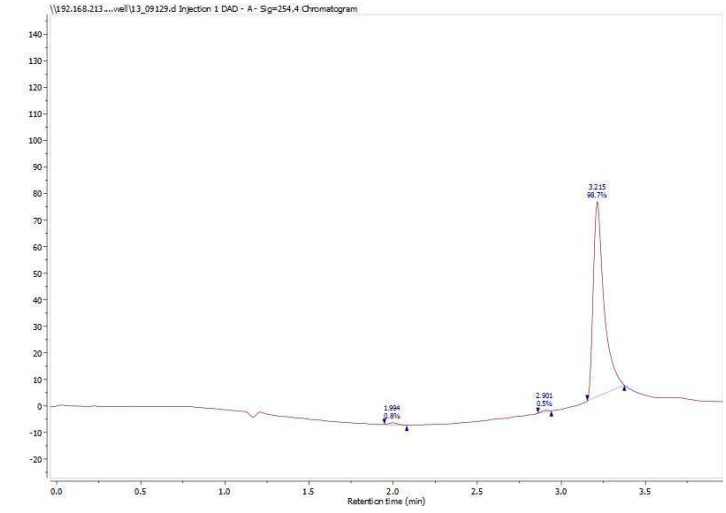

Compound **7**

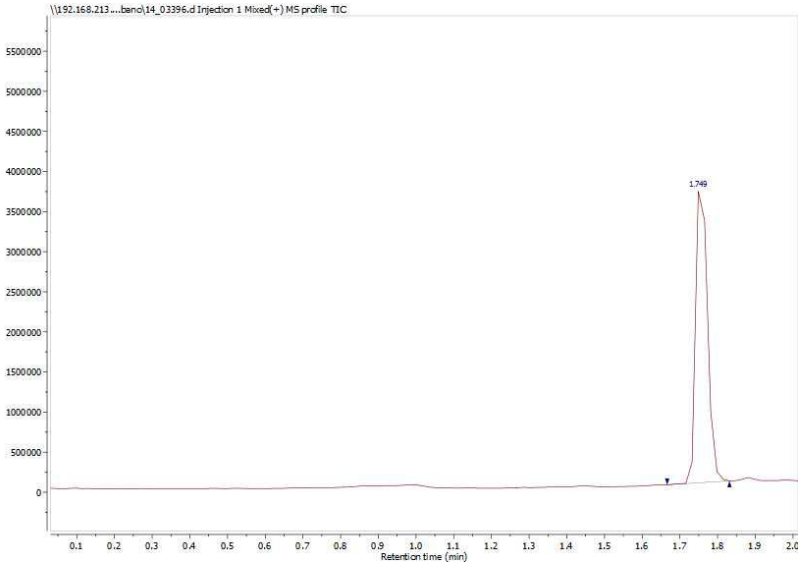

Compound **8**

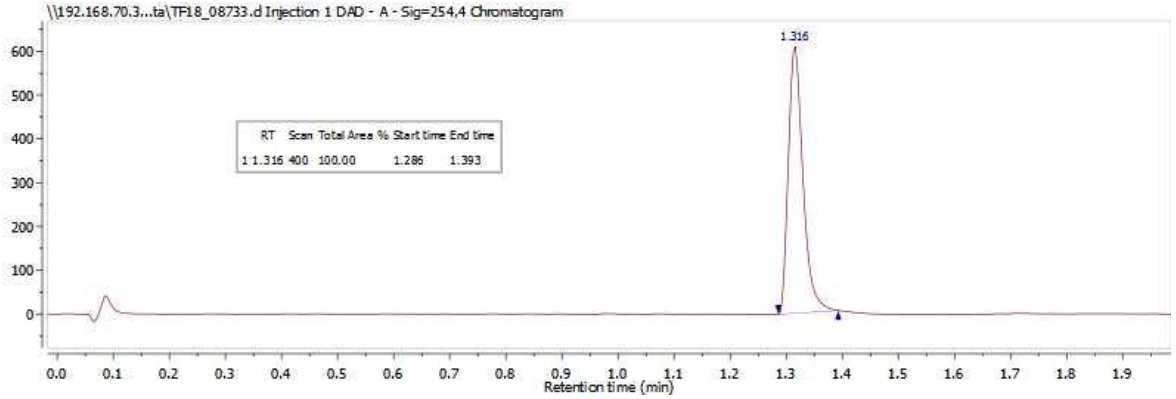

Compound **9**

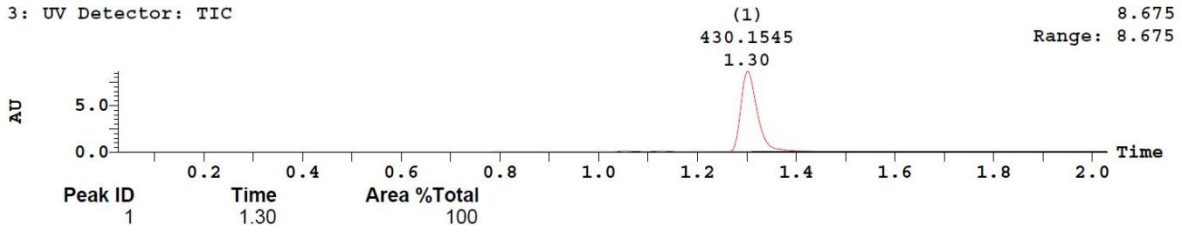

Compound **10**

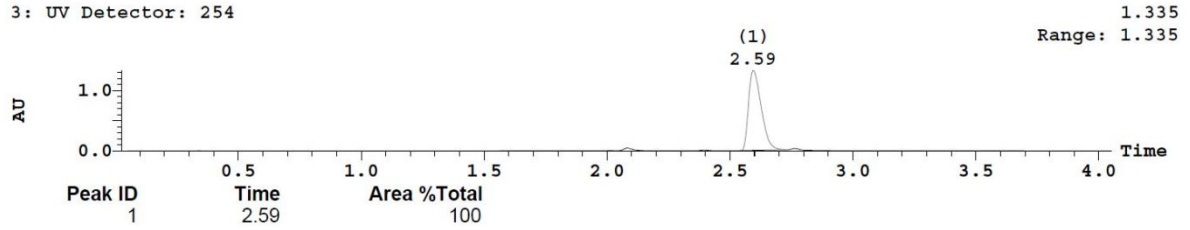

Compound **11**

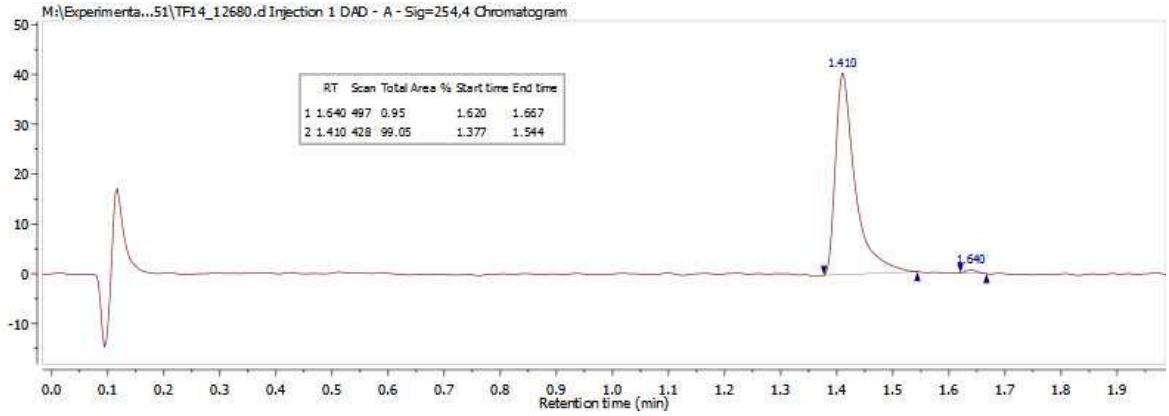

Compound **12**

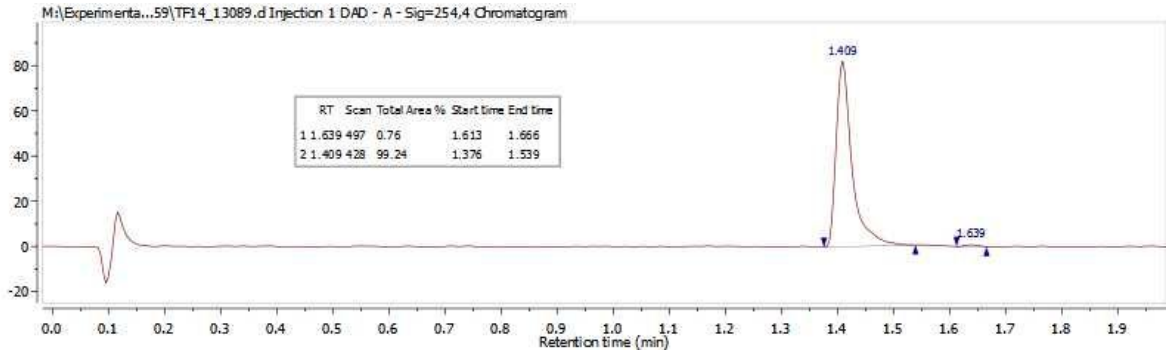

Compound **19**

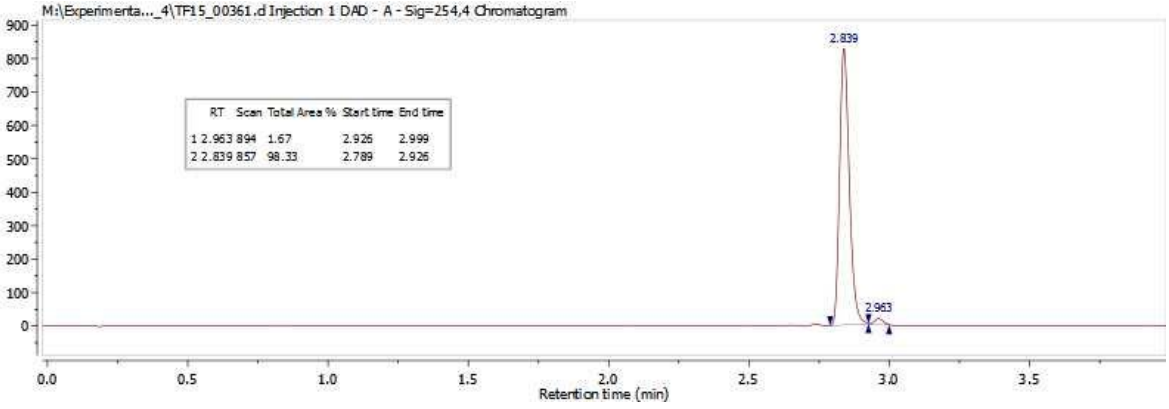

Compound **20**

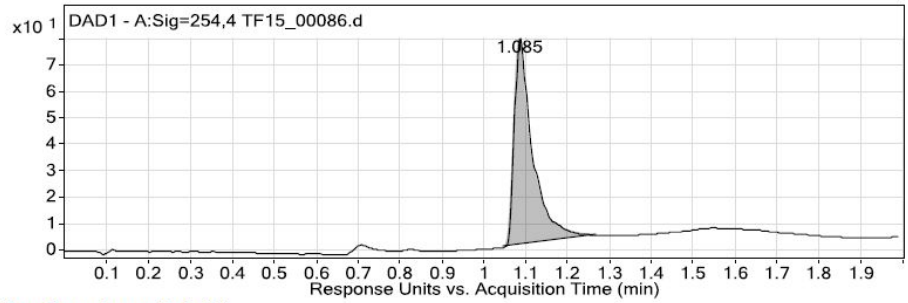

User Chromatogram Peak List

Peak #	RT (mins)	Area	Area Sum %
1	1.085	241.69	100

Compound **21**

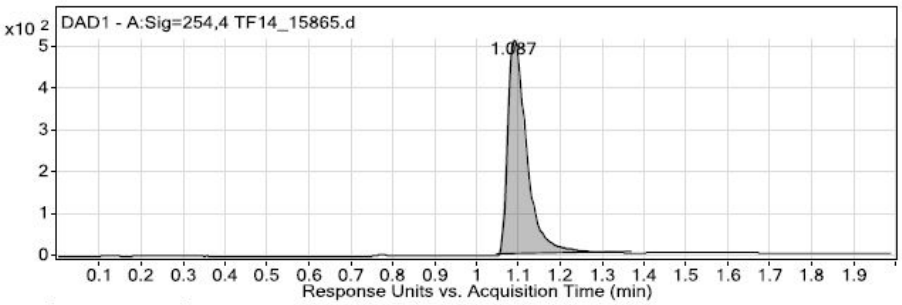

User Chromatogram Peak List

Peak #	RT (mins)	Area	Area Sum %
1	1.087	1644.09	100

Compound **22**

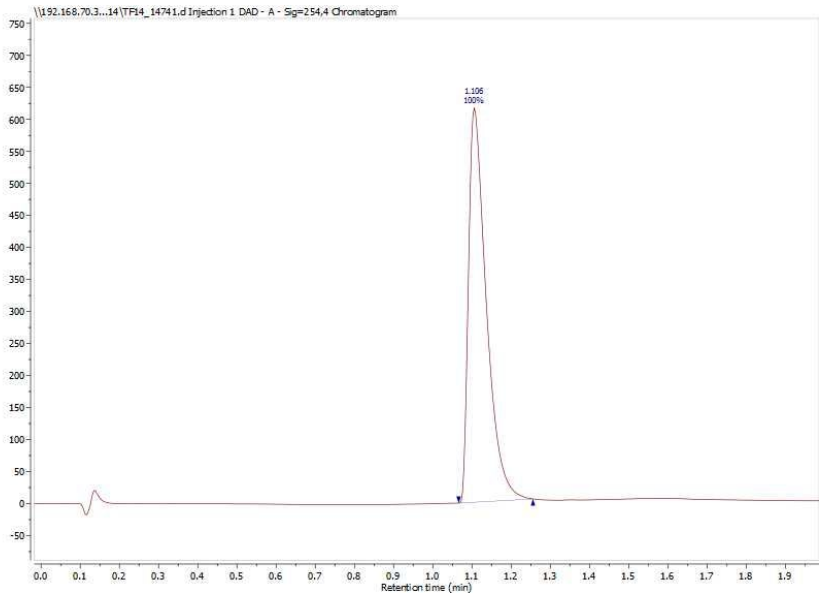

Compound **23**

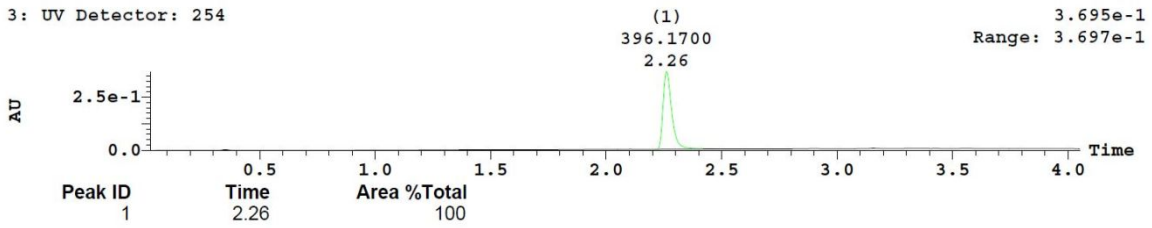

Compound **24**

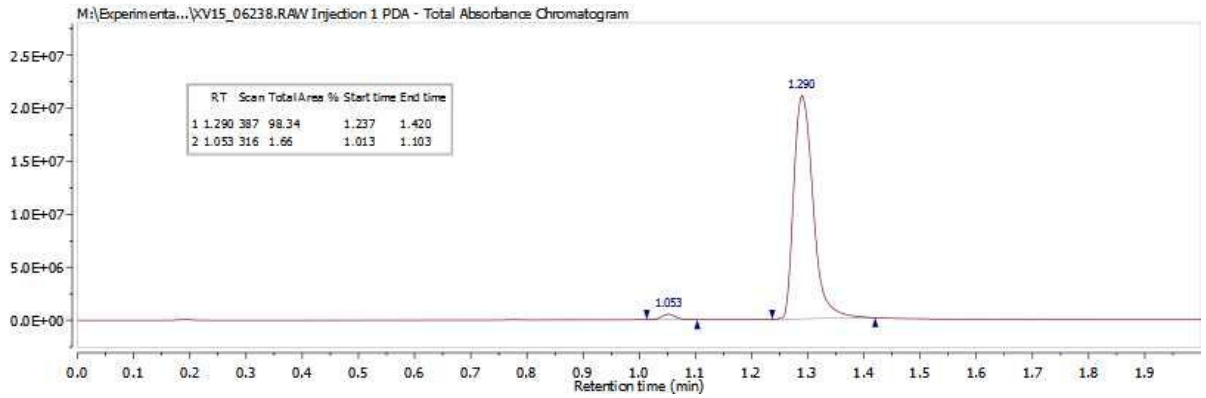

Compound **25**

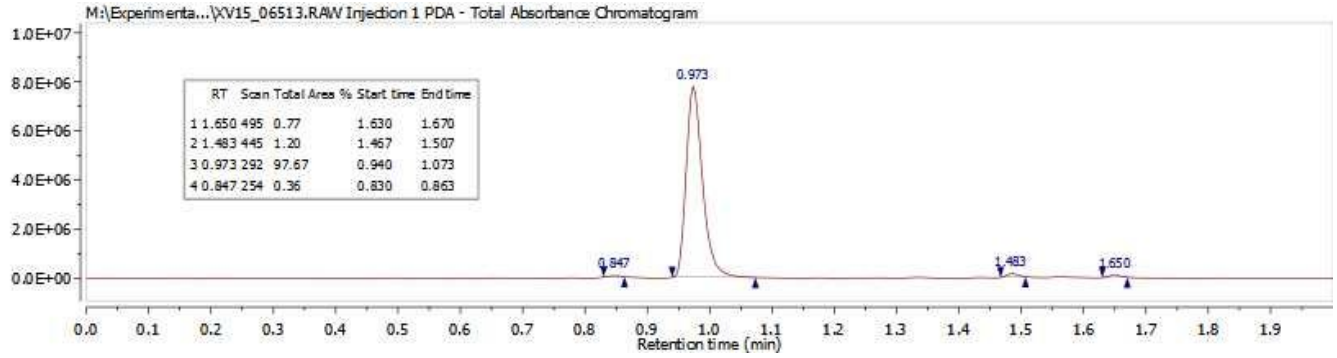

Compound **26**

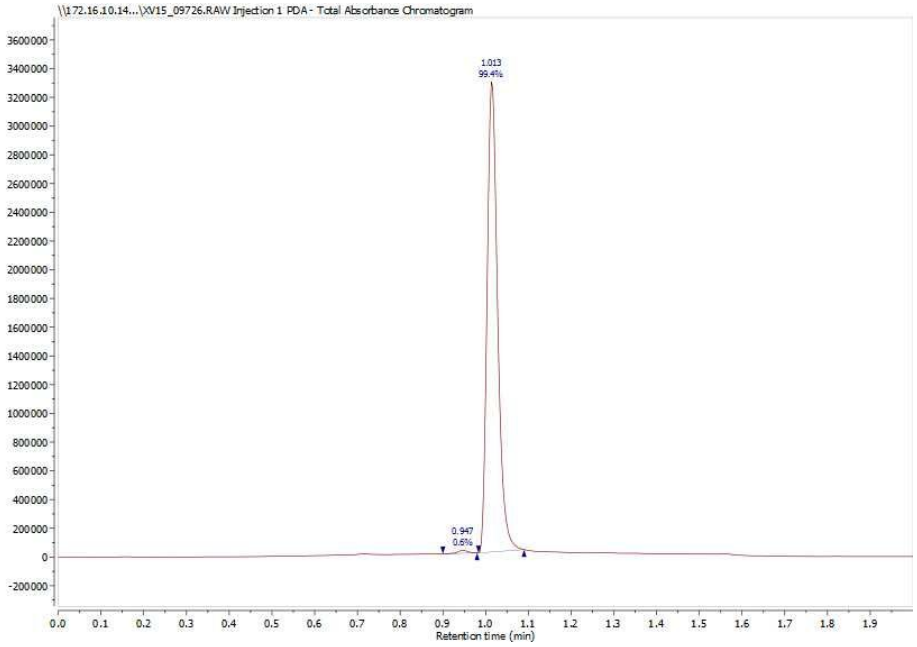

Compound **27**

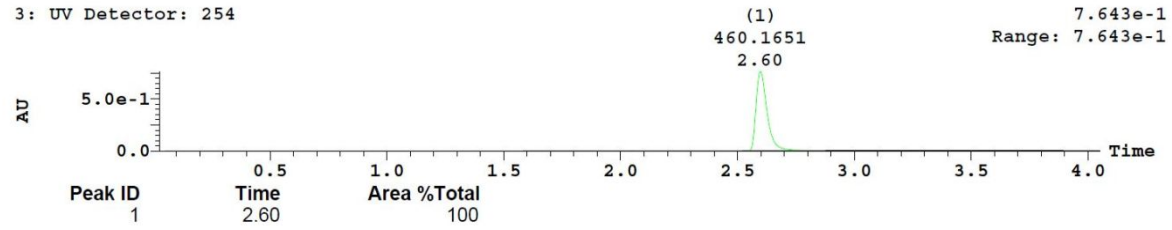

Compound **28**

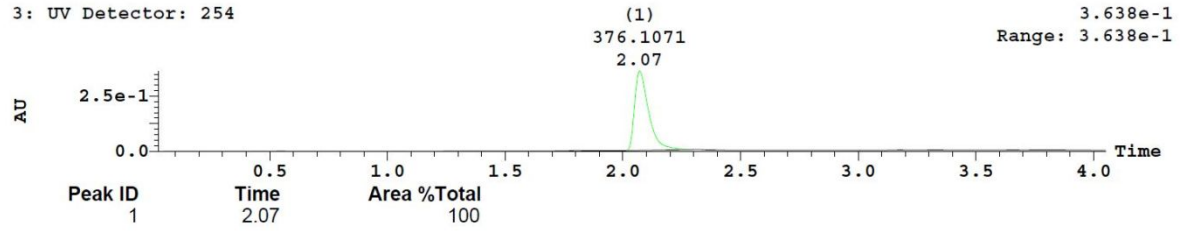

Compound **29**

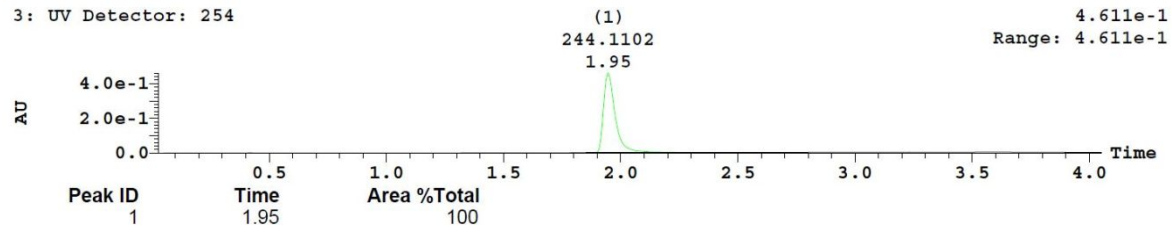

Compound **30**

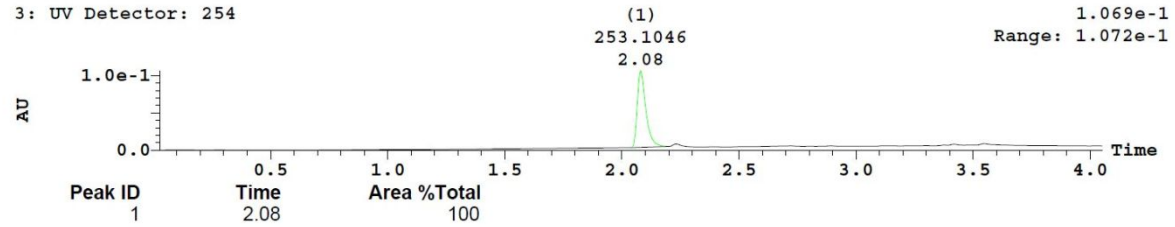

Compound **31**

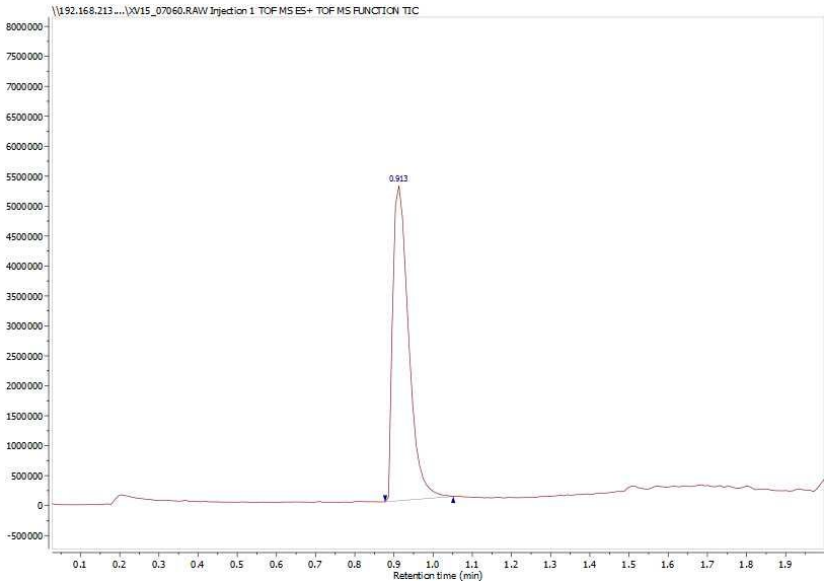

Compound **32**

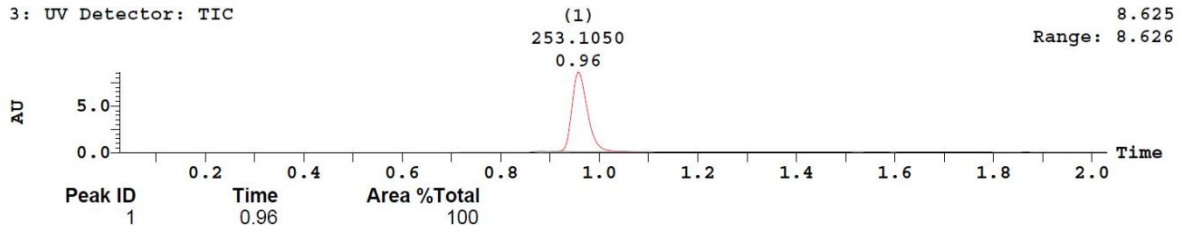

Compound **33**

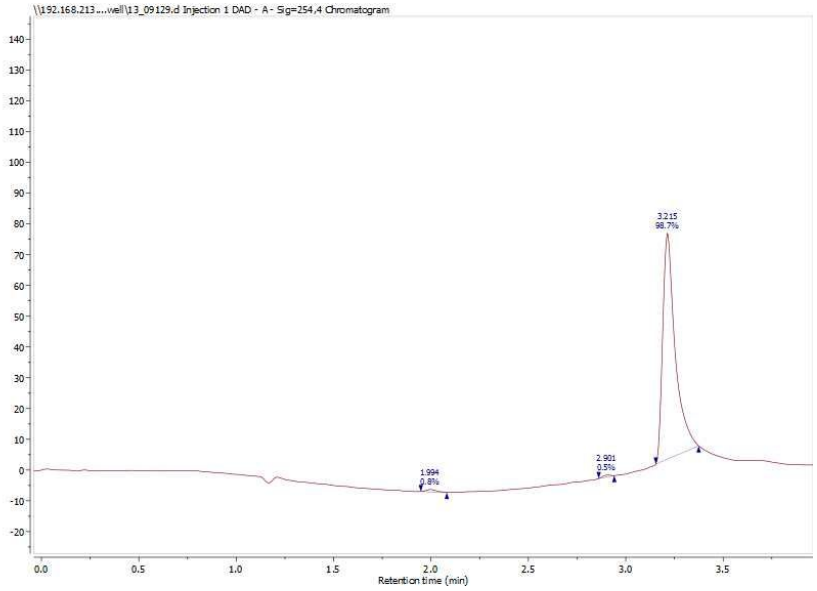
\\192.168.213....well\13_09129.d Injection 1 DAD - A - Sig=254,4 Chromatogram
140
130
120
110
100
90
80
70
60
50
40
30
20
10
0
-10
-20
3.215
98.7%
2.901
0.5%
1.994
0.8%
0.0
0.5
1.0
1.5
2.0
2.5
3.0
3.5
Retention time (min)